Spatial and temporal variation of selected physical and chemical properties of soil

Bogusław Usowicz, Jerzy Bogdan Usowicz

EDITED BY
BOGUSŁAW USOWICZ, RYSZARD T. WALCZAK

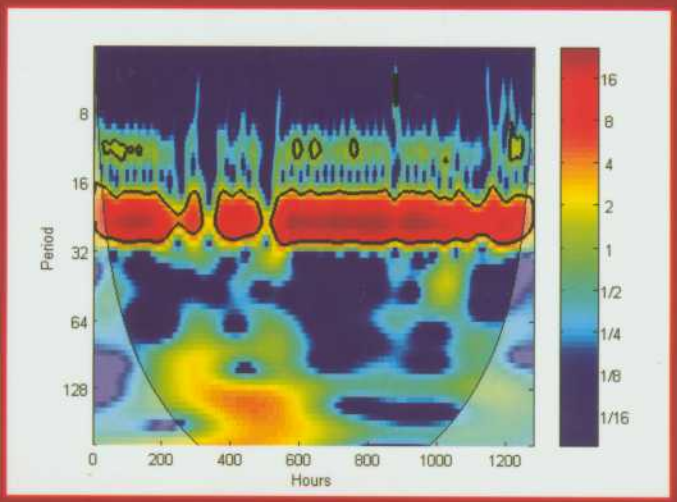

Centre of Excellence for Applied Physics in Sustainable Agriculture AGROPHYSICS

Institute of Agrophysics Polish Academy of Sciences

EU 5th Framework Program QLAM-2001-00428

Spatial and temporal variation of selected physical and chemical properties of soil

B. Usowicz, J.B. Usowicz

EDITED BY
B. USOWICZ, R. T. WALCZAK

Lublin 2004

Centre of EC Excellence AGROPHYSICS
Centre of Excellence for Applied Physics
in Sustainable Agriculture QLAM-2001-00428

Reviewed by: Assist. prof. dr hab. Cezary Sławiński

ISBN 83-87385-96-4

Edition: 250 copies

Project of cover and computer edition: Boguslaw Usowicz

Printed by: ALF-GRAF, ul. Kościuszki 4, 20-006 Lublin, Poland

CONTENTS

1. INTRODUCTION

Spatial and temporal variability of the natural environment is its inherent and unavoidable feature. Every element of the environment is characterized by its own variability, and at the same time each element affects one or more other elements of the environment. In recent years, special attention has been turned to environmental variation as a phenomenon that comprises processes leading to given physical, chemical or biological conditions [1-4,7,27,28,38,39,86-101,201-232,329-365]. One of the kinds of variability in the natural environment is the variability of the soil environment [9-13,20,35,44,118-141,272,286-321,338]. The variability is related to the spatial and temporal variation of soil-forming factors and to human activity. At the same time, the natural and the anthropogenic components of the spatial and temporal variability of soil are not sufficiently identified, and – so far – the least known. To the latter we should assign, among other things, excessive compaction of soil within the arable layer and beneath it, resulting – as a side effect – from the application of agricultural machinery, which has a significant effect on the hydro-physical, thermal and air relations in soil [64, 105,170,253,289,388,403,416,442]. Likewise with the chemical properties of soil, including its reaction (pH) and cation-exchange capacity [399]. Consequences of the failure to consider the spatial variability of the soil environment, and therefore the conditions of growth and development of plants, may include irrational tillage (not adapted to the existing conditions), plant development below optimum, meaningful losses in crop yields, excessive costs of fertilization and liming of soil, long-term retention of chemical components in the soil and their release in the form of gases or salts etc., as shown by studies conducted, among others, in the USA, Sweden, Great Britain, Australia, and also in Poland [6,8,34,116,117, 124,150, 154,156,171,207,229, 247, 286,393-398,411,418,426].

To acquire better and deeper knowledge and understanding of the temporal and spatial variability of the physical, chemical and biological features of the soil environment, we should determine the causes that induce a given variability. The primary causes of the natural variability may be sought in the geomorphological form of the terrain (mountains, uplands, flat lands, valleys, faults, terraces, detrital fans, dunes, etc.), among the soil-formation factors, i.e. the climatic, hydrological or biological factors and their interactions, and in the differences in the lithology of the parent rock from which he soil was formed. The intensity of erosion, sedimentation and weathering processes may also affect the temporal and spatial variation of soil properties [222,311,355-360].

It should be emphasized that the study of the spatial variability of the physical and chemical properties of soil provides the very foundations for precision agriculture that is now being promoted and implemented in the most economically developed countries [212,246,251,444].

Types of soils (including their genesis and primary features) are documented on the national, regional or administrative unit scale by means of soil maps with various degrees of generalization [21,83-85,186,252,362,365,384,419], and – though to a lesser extent – with the help of data banks [113,131,172,381,382, 452]. These provide a basis for the formulation of conclusions concerning the greater or lesser variability of soils within a given area [209,214,222,392-399,416-419,446]. The variability of soil properties within an arable field, even though it exists [11,12,18,19,392], is often underestimated not only by farmers, but also by science. As a rule, the soil in a field is considered to be homogeneous, which permits the study of its physical and chemical parameters to be restricted to a single measurement point, and at the same time suggests the unification of all the applied tillage and other agricultural measures. This kind of approach causes that in the field of studies on the spatial variability of soil properties, conducted so far in Poland, there have been no significant research publications. The least known is the spatial variability of the properties of soil environment in the sense of mathematical-physical description and, moreover, the natural and anthropogenic components of the spatial variability of soils are not sufficiently distinguished [166,282,400,425].

Among the features of soil we can distinguish those relatively stable (little changing with time) and those of a more dynamic character which change with the occurrence of certain external factors (soil tillage, meteorological conditions). Relatively stable features of soil include its texture and mineral composition; examples of those variables in time are the soil pH or organic matter content; an example of a feature with strong dynamics is the soil moisture content.

1.1. Objective

The objective of this work was to investigate and describe the spatial and temporal variability of selected physical and chemical properties of soil, determination of the extent of the variability and its significance in the soil environment using geostatistical methods and time series analysis.

2. GEOSTATISTICAL METHODS

2.1.Introduction

The processes of mass and energy exchange taking place in soil are dynamic processes. This is affected primarily by the soil itself – a dispersive and multi-phase medium – as well as by plants and the meteorological conditions. Actual soil objects studied under natural conditions are conveniently treated as systems connected to the environment that can be described by means of suitable functions of time or as systems being functions of time and spatial coordinates. With the physical structure of the systems studied not fully known (usually), their responses and contacts with the environment (inputs, outputs) can be analyzed in terms of static random processes, or treated as a form of interrelationship of random fields [36-75,127-137,145-185,199,236-285,404]. Statistical methods extensively used for the description of soil objects pre-assume that observations are independent from one another, which hinders their accurate description and analysis. In environmental studies we deal with observations which, by their very nature, are dependent on one another. The dependence is interesting as such (from the cognitive point of view) [17-22,142,144,204,213,288,319,364,368,369-384,389,405-457]. In such a case, the chosen methods of random field analysis which, among other things, constitute the foundations for the mathematical apparatus of geostatistics, have a fundamental importance for the study of variation of soil parameters. As we are aware, our knowledge on a phenomenon or on the features studied with respect to a medium is fragmentary, as it relates to areas or, rather, points that have been sampled [9,24-85,322-379]. What we do not know is what actually happens in between the measurement points. The need to acquire knowledge on those areas resulted in the emergence of a new branch of science – geostatistics.

Most of the features of the natural environment show continuity. The study of the physical properties of soil can be conducted with the help of classical statistics, using for the purpose the distribution function and the relevant statistical moments, or with the help of the autocorrelation function on which geostatistics is based. However, when we use classical statistics, we leave out information concerning the space from which data have been collected, and the data is irretrievably lost. On the other hand, basing on classical statistics we can solve the problem of sample population required for the determination of a given feature with specific accuracy. Geostatistics, which bases on observations that are similar within a certain proximity, indicates that they have to be mutually

correlated [315,345]. It represents a methodology that permits the spatial or temporal analysis of correlated data. Its basic tool is variogram analysis which involves the study of the variogram function of a specific variable physical value or of a soil property under study. The variogram function, with its specific parameters (nugget value, threshold and correlation range), presents the behaviour of the variable under study, called the "regionalized variable" [75,136,137,225, 426], and thus permits the formulation of conclusions concerning areas that are not represented by any measurement data [46, 53,57,62,63,70,126,159,179,190, 205, 214,377].

The concept of mathematical description of natural structures characterized by geometric heterogeneity of linearity or surface may be conducted with the help of the fractal theory [6,8,10,14-16,346-352]. The fundamental concept in this theory is the concept of the fractal dimension *D* [29,42,43,161,167,176,220,221] which expresses the effective geometric dimension of linearity, surface or volume of a structure under study. According to the fractal theories, the value of *D* is a global value and therefore characterizes the whole object studied [275-278,291-297, 383, 396]. The value may assume values within the range of $1 \leq D \leq 2$ for linear sections and $2 \leq D \leq 3$ for surfaces, and can be interpreted in terms of spatial organisation of the feature or process under study, i.e. it provides information on how far the feature/process is determined or has a random character.

Comprehensive study of the dynamics and correlation of many physical properties of soil and the close-to-ground layer of atmosphere combined is now possible thanks to the existence of suitable methods of measurement, availability of automatic data acquisition and analysis systems, and the adaptation of geostatistical methods and the fractal theory to the temporal and spatial analysis of data variability.

2.2. Regionalized Variable

A basic concept in geostatistics is the regionalized variable introduced by G. Matheron [225]. The variable, distributed in space, forms a certain random field and is used for the description of phenomena occurring within a specific zone. The duality of the regionalized variable is manifest in two aspects – deterministic (structured) and random (erratic) after Pannatier [280,281]:

"- The structured aspect is related to the overall distribution of the natural phenomenon,

- The erratic aspect is related to the local behavior of the natural phenomenon.

The formulation of a natural phenomenon must take this double aspect of randomness and structure into account. A consistent and operational formulation is the probabilistic representation provided by Random Functions.

A Random Function is a set of Random Variables {$Z(x)$ | location x belongs to the area investigated} whose dependence on each other is specified by some probabilistic mechanism. It expresses the random and structured aspect of a natural phenomenon in the following way :

- Locally, the point value $z(x)$ is considered as a Random Variable.

- This point value $z(x)$ is also a Random Function in the sense that for each pair of points x_i and $x_i + h$, the corresponding Random Variables $Z(x_i)$ and $Z(x_i + h)$ are not independent but are related by a correlation expressing the spatial structure of the phenomenon."

2.3.Semivariogram

As has been mentioned earlier, in studies on the soil environment we deal with observations that are mutually correlated [2,47,48,60,61,66,126,129,138,140]. Statistical methods assume that observations are independent from one another, which hinders the accurate description and analysis. We know that our knowledge on the processes studies is fragmentary as it relates to areas, or rather to points that have been observed. We do not know what happens within the areas in between the observations [70,90,94,96-120,248-268,315,325,387,436-450]. Acquisition of knowledge about those areas is in the focus of interest of numerous branches of science, including agrophysics [392-400,419]. The probability, confirmed by numerous observations, that next to a point with a specific value of a certain variable there are points with similar values of that variable indicate that the values must be mutually correlated. The basis for the calculation of data so correlated is the method of variogram function analysis, and more specifically a half of the expected value of differences of the value $Z(x)$ of the variable in point x and value $Z(x+h)$ in a point removed by the vector h. The semivariogram presents therefore the spatial or temporal behaviour of a given variable which is also called the "regionalized" variable. The variable has its random aspect which accounts for local irregularities, and its structural aspect which reflects the overall tendency or trend of the phenomenon (trend) [122]. Analysis of such a variable consists in the identification of the structure of variability. Three stages can be identified in the analysis: preliminary examination of collected data and evaluation of basic statistics, calculation of empirical variogram of the regionalized variable under analysis, and fitting a mathematical model to the

course of the empirical variogram. This requires the knowledge of the first two statistical moments of the random functions ascribed to a given phenomenon: the first moment (the mean) [281],

$$E[Z(x)] = m(x) \tag{1}$$

and the second (variance, covariance, semivariogram – semivariance)

$$Var\{Z(x)\} = E\left\{[Z(x) - m(x)]^2\right\}. \tag{2}$$

If the random variables of $Z(x_1)$, $Z(x_2)$ have variance, they also have covariance which is a function of position x_1, x_2:

$$C(x_1, x_2) = E\{[Z(x_1) - m(x_1)] \cdot [Z(x_2) - m(x_2)]\} = E\{Z(x_1) \cdot Z(x_2)\} - m(x_1) \cdot m(x_2) \tag{3}$$

Semivariogram $\gamma(x_1,x_2)$ is defined as a half of the variance from the difference of random variables $\{Z(x_1) - Z(x_2)\}$ [281,424,425]:

$$\gamma(x_1, x_2) = \frac{1}{2} Var\{Z(x_1) - Z(x_2)\}. \tag{4}$$

It is also required that the process under study be stationary, i.e. does not change its properties with a change in the beginning of the temporal or spatial scale. In the stationarity condition is met, the random function $Z(x)$ is defined as a stationary function of the second order. Moreover, it is expected that [188, 189, 281]:

- the expected value exists and does not depend on the position of x

$$E[Z(x)] = m, \qquad \forall x \tag{5}$$

- for each pair of random variables $\{Z(x), Z(x+h)\}$ there exists covariance dependent only on the separation vector h

$$C(h) = E\{Z(x+h) \cdot Z(x)\} - m^2, \qquad \forall x \tag{6}$$

- the stationarity of covariance implicates the stationarity of variance and semivariogram

$$Var\{Z(x)\} = E\left\{[Z(x) - m]^2\right\} = C(0), \qquad \forall x. \tag{7}$$

It can be shown that there is a correlation between covariance and the semivariogram [281]:

$$\begin{aligned} &2C(h) = 2E\{Z(x+h\cdot Z(x))\} - 2m^2 = \left[E\left\{Z(x+h)^2\right\} - m^2\right] + \left[E\left\{Z(x)^2\right\} - m^2\right] \\ &- \left[E\left\{Z(x+h)^2\right\} - 2E\{Z(x+h)\cdot Z(x)\} + E\left\{Z(x)^2\right\}\right] \\ &2C(h) = 2C(0) - 2\gamma(h) \\ &C(h) = C(0) - \gamma(h) \end{aligned} \tag{8}$$

- for all the values of vector h the difference $\{Z(x+h) - Z(x)\}$ has finite variance and does not depend on x

$$\gamma(h) = \frac{1}{2} Var\{Z(x+h) - Z(x)\} = \frac{1}{2} E\left\{[Z(x+h) - Z(x)]^2\right\}, \qquad \forall x. \tag{9}$$

When the value of vector h equals zero, the value of semivariance is also equal to zero. The semivariogram is symmetrical with relation to h:

$$\gamma(h) = \gamma(-h). \tag{10}$$

The experimental semivariogram $\gamma(h)$ for the distance h is calculated from the equation [124,191,267,281,323,380, 402,424]:

$$\gamma(h) = \frac{1}{2N(h)} \sum_{i=1}^{N(h)} [z(x_i) - z(x_i + h)]^2 \tag{11}$$

where: $N(h)$ is the number of pairs of points distant for each other by h. The equation illustrates the differentiation of deviations of the value of a given feature or physical value z from the equation of trend with relation to the distance between the measurement points. Three characteristic parameters are distinguished for the semivariogram: the nugget effect, the threshold, and the range.

If the semivariogram is an increasing function beginning not from zero but from a certain value, the value is called the nugget effect. It expresses the variability of the physical value under study with a scale smaller than the sampling interval (it can also result from low accuracy of measurement). The value, reached by the semivariogram function, from which no further increase of the function is observed, (approximately equal to the sample variance) is called

the threshold or sill, while the interval from zero to the point where the semivariogram reaches 95% of the constant value is called the range. The last parameter expresses the greatest distance at which the values samples are still correlated.

To semvariograms determined empirically, the following mathematical models are fitted [91, 280,281]:

- The linear isotropic model describes a straight line variogram. Note that there is no sill in this model; the range A_0 is defined arbitrarily to be the distance interval for the last lag class in the variogram. The formula used is [109]:

$$\gamma(h) = C_0 + \left[h\left(C \big/ A_0 \right) \right] \tag{12}$$

- The spherical isotropic model is a modified quadratic function for which at some distance A_0, pairs of points will no longer be autocorrelated and the semivariogram reaches an asymptote. The formula used for this model is:

$$\gamma(h) = \begin{cases} C_0 + C \cdot \left[1.5\frac{|h|}{A_0} - 0.5\left(\frac{|h|}{A_0} \right)^3 \right] & |h| \le A_0 \\ C_0 + C & h > A_0 \end{cases}, \tag{13}$$

- The exponential isotropic model is similar to the spherical in that it approaches the sill gradually, but different from the spherical in the rate at which the sill is approached and in the fact that the model and the sill never actually converge. The formula used for this model is:

$$\gamma(h) = C_0 + C \cdot \left[1 - e^{-\frac{|h|}{A_0}} \right] \qquad |h| > 0 \tag{14}$$

- The Gaussian or hyperbolic isotropic model is similar to the exponential model but assumes a gradual rise for the y-intercept. The formula used for this model is:

$$\gamma(h) = C_0 + C \cdot \left[1 - e^{-\frac{|h|^2}{A_0^2}} \right] \qquad |h| > 0 \tag{15}$$

where: $\gamma(h)$ semivariance for internal distance class h, h – lag interval, C_0 – nugget variance ≥ 0, C – structural variance $\geq C_0$, A_0 – range parameter. In the case of linear model there is no effective range A – is set initially to the separation

distance (h) for last lag class graphed in the variogram. In the case of the spherical model the effective range $A = A_0$. In the case of the exponential model the effective range $A = 3A_0$ which is the distance at which the sill ($C + C_0$) is within 5% of the asymptote. In the case of the Gaussian model, the effective range $A = 3^{0.5}A_0$ which is the distance at which the sill ($C + C_0$) is within 5% of the asymptote.

When fitting a model to empirical semivariograms, the least squares method is most frequently used.

2.4. Trend

In the regionalized variable we can distinguish the random or erratic component – $\varepsilon(x)$, which covers local irregularities, and the structural component – $m(x)$, which reflects the overall tendencies of the phenomenon (trends). The components are closely related to each other through the decomposition equation [71,122,424]:

$$z(x) = \varepsilon(x) + m(x) \tag{16}$$

Like above, analysis of such a variable consists in the identification of the structure of variability through examination of the collected data and evaluation of the basic statistics, calculation of the empirical semivariogram of the regionalized variable under consideration, and fitting a mathematical model to the course of the empirical semivariogram. It is also required for the process under study to be stationary, i.e. not to change its properties with a change in the beginning of a spatial or temporal scale. The existence of trends in a data set causes a change in the properties of the feature together with scale change. In such a case fulfilling the stationarity condition requires the removal of the trend – $m(x)$ from the data set [114]:

$$\varepsilon(x) = z(x) - m(x). \tag{17}$$

For a linear run of values the trend equations are as follows:

$$\begin{aligned} m(x) &= a_0 \\ m(x) &= a_0 + a_1 x \\ m(x) &= a_0 + a_1 x + a_2 x^2 \end{aligned} \tag{18}$$

When we have a surface trend with *x*, *y* coordinates, the trend equations are as follows:

$$\begin{aligned} m(x,y) &= a_0 \\ m(x,y) &= ax + by + c \\ m(x,y) &= ax^2 + by^2 + cxy + dx + ey + f \end{aligned} \tag{19}$$

where: a, a_0, a_1, a_2, b, c, d, e, f – parameters.

After the elimination of the trend from the data set, the resultant random or erratic component should be characterized by the mean value of zero and by finite variance.

The empirical semivariogram – $\gamma(h)$ for the distance h is calculated from the equation:

$$\gamma(h) = \frac{1}{2N(h)} \sum_{i=1}^{N(h)} [\varepsilon(x_i) - \varepsilon(x_i + h)]^2 \tag{20}$$

where:: $N(h)$ is the number of pairs of points distant by h. The equation illustrates the differentiation of deviations of the values of a given features or physical value $\varepsilon(x_i)$ from the trend equation depending on the distance between the measurement points.

2.5. Standardized semivariogram

Semivariance values calculated from the classical equation are sometimes so scattered that it is difficult to them a semivariogram model. Better model fit can be achieved through the standardization of the semivariogram γ_s [281]:

$$\gamma_s = \frac{\gamma(h)}{\sigma_{h=0} \cdot \sigma_h} \ . \tag{21}$$

In such a case we must additionally calculate the standard deviation of the random variable at the origin of vector h ($\sigma_{h=0}$) and the standard deviation of the value of the random variable for a point distant by h (σ_h).

2.6. Cross-semivariogram

Regionalized variables are assigned to various physical properties of the soil medium. The variables are usually correlated with one another, to a lesser or greater degree. Assuming that the condition of stationarity of the second order is met, and that the values of variables z_1 and z_2 have cross-covariance defined as [123,193,230,407,434]:

$$C_{12}(h) = E\{Z_1(x) \cdot Z_2(x+h)\} - m_1 m_2 \tag{22}$$

and

$$C_{21}(h) = E\{Z_2(x) \cdot Z_1(x+h)\} - m_1 m_2 \tag{23}$$

and cross-semivariogram as:

$$\gamma_{12}(h) = \gamma_{21}(h) = \frac{1}{2} E\{[Z_1(x+h) - Z_1(x)] \cdot [Z_2(x+h) - Z_2(x)]\}, \quad \forall x\,. \tag{24}$$

When m_1 and m_2 are the expected values $E\{Z_1(x)\}$ and $E\{Z_2(x)\}$ then, taking the above relations we can write the cross-semivariogram as:

$$2\gamma_{12}(h) = 2\gamma_{21}(h) = 2C_{12}(0) - C_{12}(h) - C_{21}(h) \tag{25}$$

The empirical cross-semivariogram – $\gamma(h)$ for the distance h is calculated from the equation:

$$\gamma_{12}(h) = \frac{1}{2N(h)} \sum_{i=1}^{N(h)} [z_1(x_i) - z_1(x_i + h)] \cdot [z_2(x_i) - z_2(x_i + h)] \tag{26}$$

where $N(h)$ is the number of pairs of points with values of $[z_1(x_i), z_1(x_i+h)]$, $[z_2(x_i), z_2(x_i+h)]$, distant by h. When calculating the cross-semivariogram, the number of z_1 and z_2 values need not be even. Like in the semivariogram, in the cross-semivariogram three basic parameters are distinguished: the nugget, the sill, and the correlation range. Also, mathematical functions are fitted into empirically determined cross-semivariograms.

The obtained mathematical functions of semivariograms and cross-semivariograms can be used for the spatial (temporal) analysis of autocorrelation or for the visualization, through estimation, of the physical value under

consideration in space with the kriging or cokriging methods [30-33,91,127-129, 200,281].

2.7. Kriging

Estimation of values in places where no samples have been taken can be conducted with the help of an estimation method called the kriging method [40,41,55,58,77,80,164,223,270,320,363,412-415,420-432]. The method yields the best non-biased estimation of point or block values of the regionalized variable under consideration $Z(x)$. With this method we also obtain the minimum variance in the process of estimation. Kriging variance values depend on the situation of samples with reference to the location under estimation, on the weight assigned to the samples, and on the parameters of the semivariogram model.

The estimator of kriging is a linear equation expressed by the formula [30-33, 424]:

$$z^*(x_o) = \sum_{i=1}^{N} \lambda_i \, z(x_i) \tag{27}$$

where: N is the number of measurements, $z(x_i)$ – value measured at point x_i, $z^*(x_o)$ – estimated value at the point of estimation x_o, λ_i – weights. If $z(x_i)$ is the realization of the random function $Z(x_i)$, the estimator of the random function can be written as:

$$Z^*(x_o) = \sum_{i=1}^{N} \lambda_i \, Z(x_i). \tag{28}$$

The weights assigned to samples are called the kriging coefficients. Their values change with the changing sampling situation and with spatial changes expressed by the variable under estimation. The weights assigned to samples as selected so as to achieve the minimal mean-square error. The error is called the kriging variance σ_k^2 and can be calculated for every sampling situation and estimation area configuration. The fundamental problem in the determination of the random variable is the finding of the weight λ_i. The weights are determined from a system of equations after inclusion of the condition of estimator non-bias [269,424]:

$$E\{Z^*(x_o) - Z(x_o)\} = 0 \tag{29}$$

and its effectiveness:

$$\sigma_k^2(x_o) = Var\left\{Z^*(x_o) - Z(x_o)\right\} = \min . \tag{30}$$

After substituting the estimator of the weighted mean to the expected value we get:

$$E\left\{Z^*(x_o) - Z(x_o)\right\} = \sum_i \lambda_i E\{Z(x_i)\} - E\{Z(x_o)\} = m\sum_i \lambda_i - m = 0 . \tag{31}$$

As can be seen from the above equation, the expected value equals zero when:

$$\sum_{i=1}^{N} \lambda_i = 1 . \tag{32}$$

while substituting to the variance the random variable estimator we can show that [424]:

$$\sigma_k^2(x_o) = \sum_i \sum_j \lambda_i \lambda_j C(x_i, x_j) + C(0) - 2\sum_i \lambda_i C(x_i, x_o) \tag{33}$$

or (through semivariance):

$$\sigma_k^2(x_o) = -\sum_i \sum_j \lambda_i \lambda_j \gamma(x_i, x_j) + 2\sum_i \lambda_i \gamma(x_i, x_o) . \tag{34}$$

Minimization of variance can be achieved by means of the Lagrangin technique, where *N* equations of partial differentials are equal to zero [424]:

$$\frac{\partial\left[\sigma_k^2(x_o) - 2\mu\sum_i \lambda_i\right]}{\partial \lambda_i} = 0 , \tag{35}$$

where: μ is the Lagrangin factor. After the differentiation and reduction of the equation we can arrive at the solution:

$$-2\sum_j \lambda_j \gamma(x_i, x_j) + 2\gamma(x_i, x_o) - 2\mu = 0 . \tag{36}$$

Including the condition for sum of kriging weights, we obtain the system of equations:

$$\begin{cases} \sum_{j=1}^{N} \lambda_j \gamma(x_i, x_j) + \mu = \gamma(x_i, x_o) \qquad i = 1 \cdots N \\ \sum_{i=1}^{N} \lambda_i = 1 \end{cases} \tag{37}$$

Solving the above system of equations we determine the kriging weights – λ_i. The weights permit also for the determination of the estimated random function Z^* and its variance from the formula:

$$\sigma_k^2(x_o) = \mu + \sum_{i=1}^{N} \lambda_i \gamma(x_i, x_o). \tag{38}$$

2.8.Cokriging

Cokriging is a specific method for the analysis of random fields. It consists in the determination of covariance and reciprocal covariance as well as the cross-semivariogram function for specific soil parameters Z_1 and Z_2. The main advantage of the method described is the possibility of indirect reconstruction of the spatial variability of soil features, the measurement of which is difficult and expensive, through field analysis of other soil parameters, easier to determine with standard measuring equipment, or of improving the estimation of one of the variables under consideration on the basis of another variable.

Estimation of values at sites where no samples have been taken, $x_{o,}$ can be made with the help of the estimation method known as the cokriging method. The mathematical basis for cokriging is the theorem on the linear relationship of the unknown estimator $Z_2^*(x_o)$ expressed by the formula [265, 283, 407, 424]:

$$Z_2^*(x_o) = \sum_{i=1}^{N_1} \lambda_{1i} Z_1(x_{1i}) + \sum_{j=1}^{N_2} \lambda_{2j} Z_2(x_{2j}), \tag{39}$$

where: λ_{1i} and λ_{2j} are weights associated with Z_1 and Z_2. N_1 and N_2 are numbers of neighbours of Z_1 and Z_2 included in the estimation at point x_o. Cokriging weights are determined from a system of equations with the inclusion of the condition of estimator non-bias [407]:

$$E\{Z_2^*(x_o) - Z_2(x_o)\} = 0 \tag{40}$$

and its effectiveness:

$$\sigma_k^2(x_o) = Var\left\{Z_2^*(x_o) - Z_2(x_o)\right\} = \min . \tag{41}$$

After the substitution of the estimator of weighted mean to the expected value we obtain:

$$\begin{aligned} E\left\{Z_2^*(x_o) - Z_2(x_o)\right\} &= \sum_{i=1}^{N_1} \lambda_{1i} E\left\{Z_1(x_{1i})\right\} + \sum_{j=1}^{N_2} \lambda_{2i} E\left\{Z_2\left(x_{2ij}\right)\right\} - E\left\{Z_2(x_o)\right\} \\ &= m_1 \sum_i \lambda_{1i} + m_2 \sum_j \lambda_{2j} - m_2 = 0 \end{aligned} . \tag{42}$$

As can be seen from the above equation, the expected value equals zero when:

$$\sum_{i=1}^{N_1} \lambda_{1i} = 0 \quad \text{and} \qquad \sum_{j=1}^{N_2} \lambda_{2j} = 1 \tag{43}$$

After substitution of the estimator to the variance we obtain:

$$\sigma_{ck}^2(x_o) = E\left\{Z_2^{*2}(x_o)\right\} + E\left\{Z_2^2(x_o)\right\} - 2E\left\{Z_2^*(x_o) Z_2(x_o)\right\} \tag{44}$$

Substituting to the variance the estimator of random function we can show that [411]:

$$\begin{aligned} \sigma_{ck}^2(x_o) &= \sum_i \sum_k \lambda_{1i}\lambda_{1k} C_{11}(x_{1i}, x_{1k}) + \sum_i \sum_l \lambda_{1i}\lambda_{2l} C_{12}(x_{1i}, x_{2l}) \\ &+ \sum_j \sum_k \lambda_{2j}\lambda_{1k} C_{21}(x_{2j}, x_{1k}) + \sum_j \sum_l \lambda_{2j}\lambda_{2l} C_{22}(x_{2j}, x_{2l}) \\ &- 2\sum_k \lambda_{1k} C_{21}(x_o, x_{1k}) - 2\sum_l \lambda_{2l} C_{22}(x_o, x_{2l}) + C_{22}(0) \end{aligned} \tag{45}$$

Minimization of variance can be achieved according to the Lagrangin technique in which N_1 and N_2 of equations of partial differentials are equal zero [407]:

$$\frac{\partial\left[\sigma_{ck}^2(x_o) - 2\mu_2 \sum_l \lambda_{2l}\right]}{\partial \lambda_{2l}} = 0, \tag{46}$$

and

$$\frac{\partial\left[\sigma_{ck}^2(x_o)-2\mu_1\sum_k\lambda_{1k}\right]}{\partial\lambda_{1k}}=0, \tag{47}$$

where: μ_1 i μ_2 are Lagrangin factors. After the differentiation and reduction of the equation, and taking into account the condition for the sum of cokriging weights, we obtain the system of equations:

$$\begin{cases}\sum_{i=1}^{N_1}\lambda_{1i}C_{11}(x_{1i},x_{1k})+\sum_{j=1}^{N_2}\lambda_{2j}C_{12}(x_{1k},x_{2j})-\mu_1=C_{21}(x_o,x_{1k}) & k=1,N_1\\ \sum_{i=1}^{N_1}\lambda_{1i}C_{21}(x_{2l},x_{1i})+\sum_{j=1}^{N_2}\lambda_{2j}C_{22}(x_{2j},x_{2l})-\mu_2=C_{22}(x_o,x_{2l}) & l=1,N_2\\ \sum_{i=1}^{N_1}\lambda_{1i}=0 & \\ \sum_{j=1}^{N_2}\lambda_{2j}=1 & \end{cases} \tag{48}$$

Solving the above system we determine the cokriging weights – λ_i. The weights permit also the determination of the estimated random function Z_2* and its variance from the formula [407]:

$$\sigma_{ck}^2(x_o)=C_{22}(0)+\mu-\sum_{i=1}^{N_1}\lambda_{1i}C_{21}(x_o,x_{1i})-\sum_{j=1}^{N_2}\lambda_{2j}C_{22}(x_{2j},x_o). \tag{49}$$

2.9. Fractal dimension

Temporal or spatial runs obtained in the course of agrophysical measurements are manifested in the form of irregular shapes. Such irregularity (chaos) can be treated in two ways: as a deviation from an ideal condition – the classical statistical approach, or secondly, as a disordered run bound with intrinsically inseparable features. It can be assumed that the study of such a disordered run will yield useful information not only on the run itself, but also about the object from which it originated. Irrespective of the scale of measurement, runs of this type

can be analyzed with the help of semivariograms. This statement results directly from the assumptions of geostatistics. Another useful tool that can be employed in the analysis of irregularities is the fractal theory which, by definition, deals with just such objects [67,68,72,98,112,158,168,308,312-314,324,385,386].

Studies performed so far indicate that there are no direct methods for the determination or estimation of the fractality of actual objects [173-175, 208,209,303]. Therefore, such properties of objects are sought that can incorporate in their structure the features of natural fractals, or features that can be related to the definition of fractals.

In recent years, fractal analysis has been used not only for the description of the geometry of materials, but also for the study of spatial variability of the properties of a porous medium, including – among other things – the texture of the medium, its electric conductivity, penetrometric resistance, density, content of different salts in soil, or the effect of the colloidal fraction on soil erosion [5, 23,26]. The fractal dimension was determined through the slope index of a semivariogram plotted in the logarithmic system of coordinates.

In this study, the fractal dimension D was determined basing on the semivariogram from the formula [43]:

$$D = 2 - \frac{H}{2}, \tag{50}$$

where: H is the slope of the semivariogram line, plotted in the logarithmic system of coordinates.

3. METHODS AND OBJECTS OF THE STUDY

Measurements of soil moisture and density were conducted with the help of the gravimetric method. Soil moisture was also measured with the help of a moisture meter operating on the reflectometric principle of measuring the dielectric constant of a porous medium (TDR). Thermal properties of soil were determined through the application of the statistical-physical model of thermal conductivity and of the empirical formulae for thermal capacity and diffusivity.

3.1. Reflectometric method for soil moisture measurement

The principle of operation of the TDR meter is based on measurement of the propagation velocity of electromagnetic waves within the medium under study (soils) at steady transmission line parameters [216,217,218,342,343,417]. The propagation velocity is expressed by the ratio of the velocity of light in vacuum to

the square root of the dielectric constant of the medium studied. The dielectric constant of a given soil depends primarily on the content of water in a unit of soil volume and can be described, with sufficient accuracy, with a third order polynomial.

In practice, soil moisture measurement with the TDR method is reduced to measurement of the time necessary for electromagnetic wave to penetrate the medium, from the moment of entering the medium (where the first reflection occurs), along the needle probe to its end (where the wave gets reflected for the second time). With help of a certain set of equations, the measured time of wave propagation is converted to the water content in a volumetric unit of the soil.

The TDR meter [216,217,218,342,343,417] is made up of a microprocessor controlled meter with a matrix graphic display, battery supplied, and a probe connected to the meter. Probes of various lengths of stem made of PCV (2 cm in outer diameter) are tipped with steel pins 10 cm long and with 1.6 cm spacing. The instrument measures moisture within water content range of 0%-100% with the accuracy of ±2% and a resolution of 0.1%. The duration of a single measurement is under 10 seconds.

3.2. Determination of thermal properties of soil

Under steady state conditions and in uniform and isotropic medium heat flux density q (Wm^{-2}) is proportional to temperature gradient $\partial T/\partial z$ (Km^{-1}) measured along the direction of heat flow:

$$q = -\lambda \frac{\partial T}{\partial z}. \tag{51}$$

The proportionality coefficient λ ($W\ m^{-1}\ K^{-1}$) called thermal conductivity is a characteristic of thermal conductivity of the given medium. Determination of the thermal conductivity and its spatial distribution in the soil is very difficult since it is a porous medium. Therefore, the methods for determination of the thermal conductivity based on other and easily measured properties are useful.

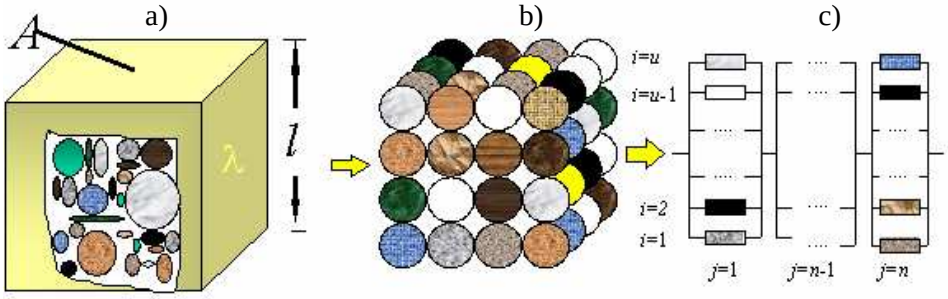

Fig. 1. Schematic diagram of the statistical model construction, a) unit volume of soil, b) the system of spheres that form overlapping layers, c) parallel connection of resistors in the layers and series between layers.

In our study we used the statistical-physical model of soil thermal conductivity [390]. This model is based on the terms of heat resistance (Ohm's law and Fourier's law), two laws of Kirchhoff and polynomial distribution [88]. The volumetric unit of soil in the model (Fig. 1a) consists of solid particles, water and air, is treated as a system made up of the elementary geometric figures, in this case spheres, that form overlapping layers (Fig. 1b).

It is assumed that connections between layers of the spheres and the layer between neighbouring spheres will be represented by the serial and parallel connections of thermal resistors, respectively (Fig. 1c). Comparison of resultant resistance of the system, with consideration of all possible configurations of particle connections together with the mean thermal resistance of given unit volume of soil, allows the estimation of thermal conductivity of soil λ (W m^{-1} K^{-1}) according to the equation [390]:

$$\lambda = \frac{4\pi}{u\sum_{j=1}^{L}\frac{P(x_{1j},...,x_{kj})}{x_{1j}\lambda_1(T)r_1 + ... + x_{kj}\lambda_k(T)r_k}} \tag{52}$$

where: u is the number of parallel connections of soil particles treated as thermal resistors, L is the number of all possible combinations of particle configuration, x_1, x_2 ,..., x_k – the number of particles of individual particles of a soil with thermal conductivity λ_1, λ_2 ,..., λ_k and particle radii r_1, r_2 ,..., r_k, where $\sum_{i=1}^{k} x_{ij} = u$, $j=1,2,...,L$, $P(x_{ij})$ – probability of occurrence of a given soil particle configuration calculated from the polynomial distribution:

$$P(x_{1j},...,x_{kj}) = \frac{u!}{x_{1j}^{!}...x_{kj}^{!}} f_1^{x_{1j}} ... f_k^{x_{kj}} . \quad (53)$$

The condition: $\sum_{j=1}^{L} P\left(X = x_j\right) = 1$ must also be fulfilled. The probability of selecting a given soil constituent (particle) f_i, $i = s, c, g$, in a single trial was determined based on fundamental physical soil properties. In this case f_s, f_c, and f_g are the content of individual minerals and organic matter – $f_s = 1 - \phi$, liquid – $f_c = \theta_v$ and air – $f_g = \phi - \theta_v$ in a unit of volume, ϕ – soil porosity.

So far, investigations showed that to calculate soil thermal conductivity the conductivities of main soil components can be used [390]. They are: quartz, other minerals, organic matter, water and air. Their values of thermal conductivity and relations to temperature are presented in Table 1.

Table 1. Values and expressions for parameters used in calculating the thermal conductivity of soils (T in ^{o}C).

Source [a]	Parameters [b] (W m^{-1} K^{-1})	Expression, value [b]
	λ_q,	9.103 - 0.028 T
2	λ_{mi},	2.93
2	λ_o,	0.251
1	λ_w,	$0.552 + 2.34 \cdot 10^{-3} T - 1.1 \cdot 10^{-5} T^2$
1	λ_a,	0.0237 + 0.000064 T

[a] 1. [162]; 2. [78], [b] thermal conductivity of: quartz λ_q, other minerals, λ_{mi}, organic matter, λ_o water or solution, λ_w air, λ_a.

Parameters of the model were defined earlier on the basis of empirical data [390,391].

The agreement between predicted and measured results was determined with a mean square error (σ_b) and relative maximum error (η_b):

$$\sigma_b = \sqrt{\frac{\sum_{i=1}^{n} \left(f_{mi} - f_{ci}\right)^2}{k}} , \quad (54)$$

where: f_{mi} is the measured value, f_{ci} is the calculated value, $k = n - 1$ if $n < 30$ and $k = n$ $n > 30$, n – number of data.

The relative maximum error was calculated using the following equation:

$$\eta_b = \max_{i=1,2,\cdots,n} \left\{ \left| \frac{f_{mi} - f_{ci}}{f_{mi}} \right| \cdot 100\% \right\}. \quad (55)$$

Also regression equations of the thermal conductivity and determination coefficient R^2 were developed.

Predicted thermal conductivity values were compared with measured data on the Fairbanks sand, Healy clay, Felin silty loam, Fairbanks peat and loam [78,390,391]. Regression coefficients were close to unity, however permanent factors in the equation were close to zero. Determination coefficients of the linear regression were high and ranged from 0.948 to 0.994. Mean square errors σ(W m^{-1} K^{-1}) and relative maximum errors η(%) ranged from 0.057 to 0.123 (W m^{-1} K^{-1}) and from 12 to 38.3%. These data indicate good performance of the model in predicting the thermal conductivity.

Volumetric heat capacity C_v (MJ m^{-3} K^{-1}) was calculated using empirical formulae proposed by de Vries [78]:

$$C_v = \left(2.0x_s + 2.51x_o + 4.19x_w\right) \cdot 10^6 \quad (56)$$

where: x_s , x_o , x_w (m^3 m^{-3}) – are volumetric contributions of mineral and organic components and water, respectively.

Thermal diffusivity α was calculated from the quotient of the thermal conductivity and volumetric heat capacity:

$$\alpha = \frac{\lambda}{C_v}. \quad (57)$$

4. TEMPORAL VARIATIONS IN THE AGRO-METEOROLOGICAL DATA

In this chapter we present some preliminary results for the analysis of temporal variations of agro-meteorological data. The novelty of our approach consists in the utilization of the following modern methods:

- Wavelet transform (WT)
- Empirical Mode Decomposition (EMD)
- Multitaper Method (MTM)

4.1.The data

The analyzed data were recorded by the automatic agro-meteostation manufactured by Eijkelkamp Company (http://www.eijkelkamp.com/). The station is shown in Fig. 2.

Fig. 2. The automatic agro-meteostation of the type 16.98.

The following parameters are measured by the station: wind speed and wind direction, global radiation, air temperature, air humidity, soil temperature and precipitation. The wind data were not used in our analysis. The radiation sensor operates in a measuring range of 305-2800 nm with accuracy of 2.5%. The air temperature and relative humidity sensor with radiation shield measures temperature between –40°C and +60°C with accuracy of +/- 0.2°C, humidity between 0 to 100 % with accuracy better than 2%. The soil temperature sensor operates in a measuring range of –40°C and +60°C, accuracy 0.1°C at 0-50°C and 0.2°C at –40°C till +60°C. The last one, the rain gauge of UV-resistant plastic, aerodynamic design, and with a tipping bucket has a resolution of 0.2 mm precipitation and a surface area of 507 cm^2.

The data covering the period of May-June 2003 are shown in Fig.3. Here we focus ourselves on the variation of soil temperature since it influences strongly crop development and plant growth. It is well known that soil temperature depends on both the soil surface energy balance and on the thermal properties of the soil [37,79,89,160]. As it is seen in Fig. 3 the daily soil temperature variations follow closely the air temperature and solar radiation. However, the bad weather and heavy precipitations can destroy this synchrony and we observe the intermittent behavior in these parameters. Such an intermittency is the main obstacle in using classical methods for the analysis of that kind of data. In addition, seasonal variations in the data can not be extracted easily. These are perhaps more important than daily variations. Due to the above reasons we have to resort to the afore-mentioned more advanced methods of data analysis.

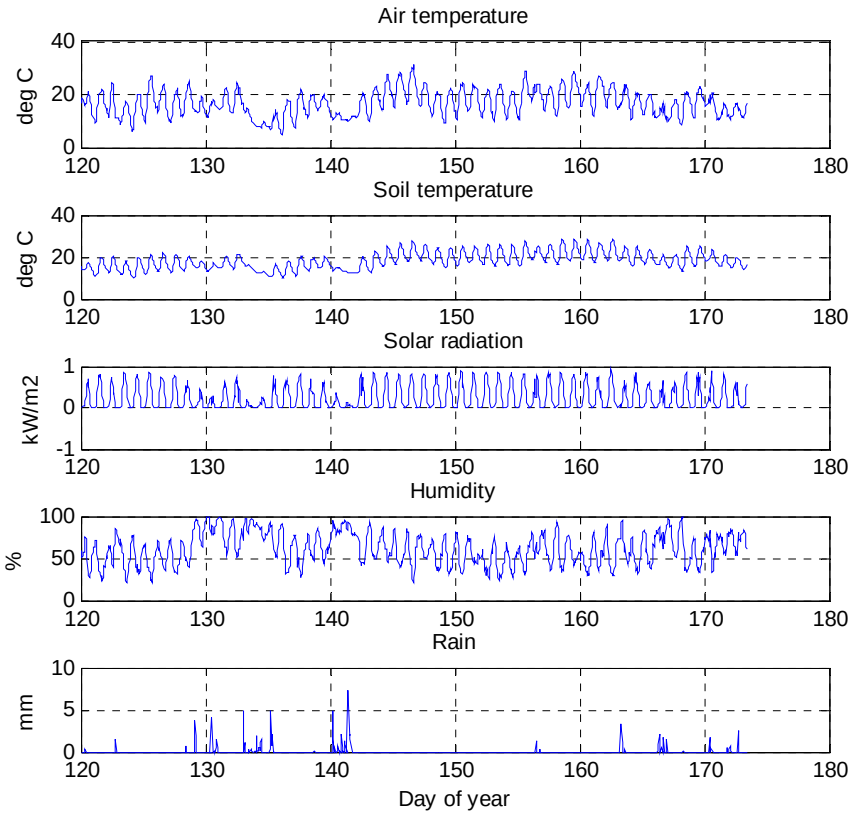

Fig. 3. The data set recorded by the agro-meteostation during May-June 2003.

4.2.Wavelet transform

Wavelet transform is a method that allows studying time series simultaneously at time-scale or equivalently in time-frequency domain. It means that WT due to its local nature is able to analyze properly any localized variations in the data. This aspect makes the WT very useful in the analysis of nonlinear and non-stationary time series. Most of the time or spatial series encountered in soil science belong to this category.

Until now, the WT has not been widely used in the analysis of data in soil science. However, Lark with co-workers have shown in a series of papers that the WT should be considered as a standard tool in the analysis of various soil data. In a paper [187] the authors have shown how the wavelet transform can be used to analyze complex spatial variations of soil properties sampled regularly on transects. The paper can be treated as an introduction of wavelets to soil science. In another paper [192] they have studied variation and covariation in small data sets from soil survey. The data sets comprise measurements of pH and the contents of clay and calcium carbonate on a 3-km transect in Central England. In that paper they have used a variant of the WT, called the maximal overlap discrete wavelet transform (MODWT) developed in statistical community. Electrical conductivity of soil was analyzed using wavelets in a third paper [194]. Recently Lark's group has widely studied an intermittent variation of nitrous oxide emissions from soils using wavelets [195,196,197,454]. In their most recent [198] the authors have successfully extended wavelet analysis to two dimensions. Every soil scientist seriously interested in using wavelets for the analysis of soil data should consult their paper.

First we study the temporal variations in the data using Continuous Wavelet Transform (CWT).

One of the most popular approaches in practice is the CWT based on the Morlet mother wavelet [374]. The popularity of this approach comes from the conceptual similarities to the Fourier orthogonal analyzing functions $e^{-i\omega t}$.

The Morlet wavelet (Fig. 4) is defined as follows:

$$\psi_0(\eta) = \pi^{-1/4} e^{i\omega_0 \eta} e^{-\eta^2/2}, \tag{58}$$

where ω_0 is dimensionless frequency and η is dimensionless time. To achieve the optimal localization in time and frequency usually $\omega_0=6$ is usually adopted. This choice also satisfies the admissibility condition. The Gaussian envelope $exp(-\eta^2/2)$ localizes the wavelet in time. Fourier frequency f and wavelet scale s

are not directly related. One has to rescale the result of wavelet analysis with a factor depending on the mother wavelet. For the Morlet wavelet, the conversion formula has the form:

$$1/f = \frac{4\pi s}{\omega_0 + \sqrt{2+\omega_0^2}}. \tag{59}$$

For $\omega_0=6$, $s \cdot f$ is approximately one.

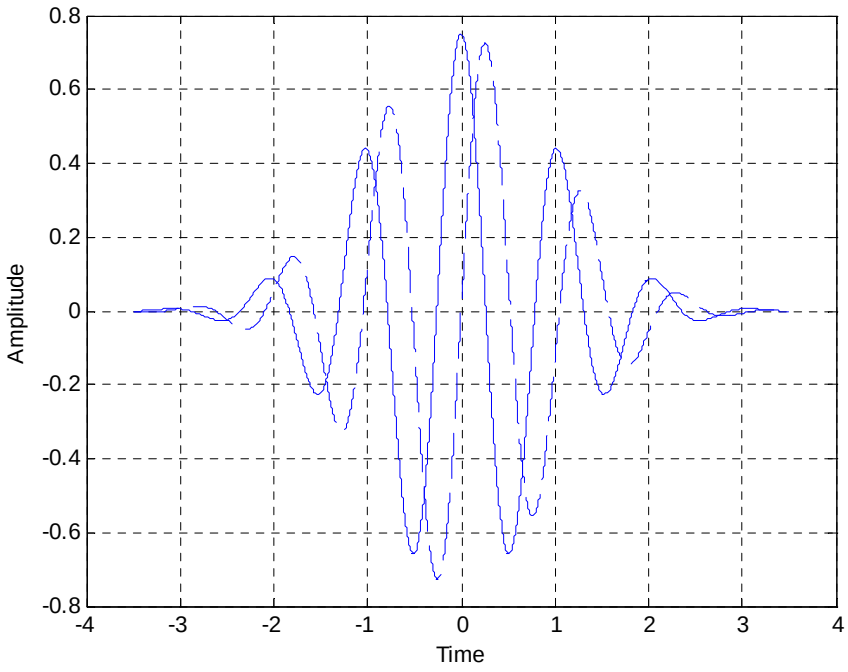

Fig. 4. The Morlet wavelet for $\omega_0=6$. Real part (solid line), imaginary part (dashed line).

The CWT of time series $(x_n, n=1,\ldots,N)$ sampled uniformly with step dt is defined as the convolution of x_n with the scaled and normalized wavelet and is given by:

$$W_n^X(s) = \sqrt{\frac{dt}{s}} \sum_{n'=1}^{N} x_{n'} \psi[(n'-n)\frac{dt}{s}]. \tag{60}$$

Since the above equation is a convolution its computation can be efficiently implemented in the frequency domain by using the FFT algorithm. The details are omitted here but they can be found in the cited literature [195,196,197,454]. The wavelet power is defined as $\left|W_n^X(s)\right|^2$. The complex argument of $W_n^X(s)$ can be interpreted as the local phase.

The CWT has edge artifacts because the Morlet wavelet is not completely localized in time. These are taken into account by introducing the Cone of Influence (COI). The COI is the area in which the wavelet power caused by a discontinuity at the edge drops to e^{-2} of the value at the edge.

The cross wavelet transform (XWT) of two time series x_n and y_n is defined as:

$$W^{XY} = W^X W^{Y*}, \tag{61}$$

where: * denotes complex conjugation. Next, we define the cross wavelet power as $\left|W^{XY}\right|$. Cross wavelet power reveals areas in the time-frequency plane with high common power. The complex argument $\arg(W^{XY})$ can be interpreted as the local relative phase between x_n and y_n time series.

We are often interested in the phase relationship between two time series. Following Torrence and Webster [375] we define the wavelet coherence of x_n and y_n time series as:

$$R_n^2(s) = \frac{\left|S(s^{-1}W_n^{XY}(s)\right|^2}{S(s^{-1}\left|W_n^X(s)\right|^2)\cdot S(s^{-1}\left|W_n^Y(s)\right|^2)}, \tag{62}$$

where: S is a smoothing operator. The wavelet coherence can be interpreted as a localized correlation coefficient in the time-frequency plane. The smoothing operator S has a form:

$$S(W) = S_{scale}(S_{time}(W_n(s))), \tag{63}$$

where: S_{scale} denotes smoothing along the wavelet scale axis and S_{time} smoothing in time. A suitable smoothing operator is given by Torrence and Webster [375]:

$$S_{scale}(W)\big|_s = (W_n(s) * c_1 e^{-\frac{t^2}{2s^2}})\big|_s \tag{64}$$

$$S_{time}(W)\big|_n = (W_n(s) * c_2 \Pi(0.6s))\big|_n, \tag{65}$$

where: c_1 and c_2 are normalization factors and Π is the boxcar function. The value of 0.6 is the optimal for the Morlet wavelet.

The wavelet coherence phase difference is given by the following equation:

$$\phi_n(s) = \tan^{-1}\left(\frac{\mathrm{Im}(S(s^{-1}W_n^{XY}(s)))}{\mathrm{Re}(S(s^{-1}W_n^{XY}(s)))}\right) \tag{66}$$

The statistical significance of wavelet power can be estimated by comparison with the power spectrum of a first order autoregressive AR(1) process. This approach is based on the findings that many geophysical time series show red noise characteristics. The power spectrum of an AR(1) process is given by:

$$P_k = \frac{1-\alpha^2}{\left|1-\alpha e^{-i2\pi k}\right|^2}, \tag{67}$$

where: k is the Fourier frequency index and α autocorrelation at lag equal to 1. Torrence and Compo [374] showed that for a given background spectrum P_k, the corresponding wavelet power at each time n and scale s is distributed as:

$$D\left(\frac{\left|W_n^X(s)\right|^2}{\sigma_X^2} < p\right) = \frac{1}{2} P_k \chi_\upsilon^2(p), \tag{68}$$

where: ν is equal to 1 for real and 2 for complex wavelets, p is the desired significance (p = 0.05 for the 95 % confidence interval).

Similarly, Torrence and Compo [374] have developed a formula for the joint distribution of the cross wavelet power to two time series with background power spectra P_k^X and P_k^Y. It is expressed here as a:

$$D\left(\frac{\left|W_n^X(s)W_n^{Y*}(s)\right|}{\sigma_X \sigma_Y} < p\right) = \frac{Z_\upsilon(p)}{\upsilon}\sqrt{P_k^X P_k^Y}, \tag{69}$$

where: $Z_\nu(p)$ is the confidence level associated with the probability p for the resulting probability density function defined as a square root of the product of two chi-square distributions. For ν = 2, $Z_2(95\%)$ = 3.999.

The wavelet and cross-wavelet transform were computed with the package available at http://www.pol.ac.uk/home/research/waveletcoherence/.

4.3.The results of wavelet transform

Fig. 5 show the CWT of the air temperature. The daily component is clearly seen. However, the seasonal component with a period greater than 128 hours for hours between 200 and 800 in the figure is much stronger. One can also notice the weak high-frequency component with the period of 8 hours. Fig. 6 show the CWT of the topsoil temperature. The similarities with the previous figure are obvious. One can note the reduced dynamics in the topsoil temperature variations. Both daily and seasonal components are of the comparable strength. High frequency variations are now shifted to the band around 12 hours. Fig. 7 shows the CWT of the solar radiation. Obviously, the daily component is strongest one. The seasonal component is the much weaker. One can also see a few little spots of the power along time in the band for 12 hours. In general, the daily course of the topsoil temperature follows closely the solar radiation for a given time. Fig. 8 show the CWT of the air humidity. The power variations with time for daily components are visible. Also long-term features are noticeable. The cross wavelet transform of the solar radiation and air temperature is shown in Fig. 9. The 5% significance level is shown as a thick contour. The arrows indicate the phase relationship between both time series. The time series are in-phase for arrows pointing right, anti-phase pointing left. As it is seen the air temperature is shifted in phase about 45° as compared to the solar radiation. In addition, this shift is noticeably greater for seasonal components. Fig. 10 show the cross wavelet transform of the solar radiation and topsoil temperature. Accordingly, the phase shift is now about 60°.

The above results agree qualitatively with the theory of heat transfer, since the air and soil respond with the delay to driving force, i.e., the solar radiation. Fig. 11 show the cross wavelet transform of the solar radiation and air humidity. Comparing figures 9 and 11 one can conclude that the air temperature and humidity are in anti-phase. Moreover, the air humidity advances the solar radiation. According to the adopted convention, the phase shift is about –45°. Finally, Fig. 12 show the squared wavelet coherence between the solar radiation and air temperature. Again, the 5% significance level is shown as a thick contour. The coherence and constant phase relationship for daily and seasonal components are significant. We conclude that the cross wavelet analysis and wavelet coherence are powerful methods for testing causal relationship between two time series.

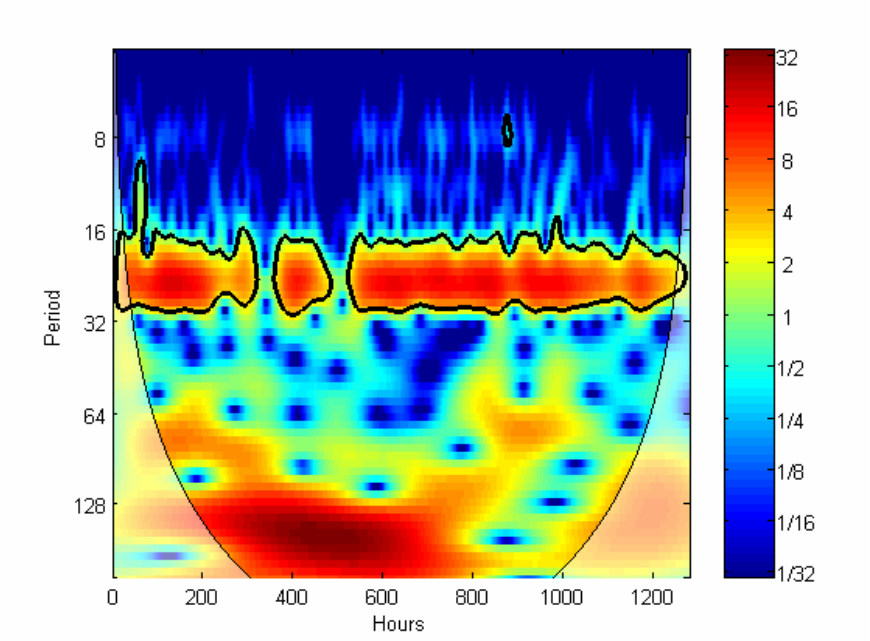

Fig. 5. The wavelet transform of the air temperature.

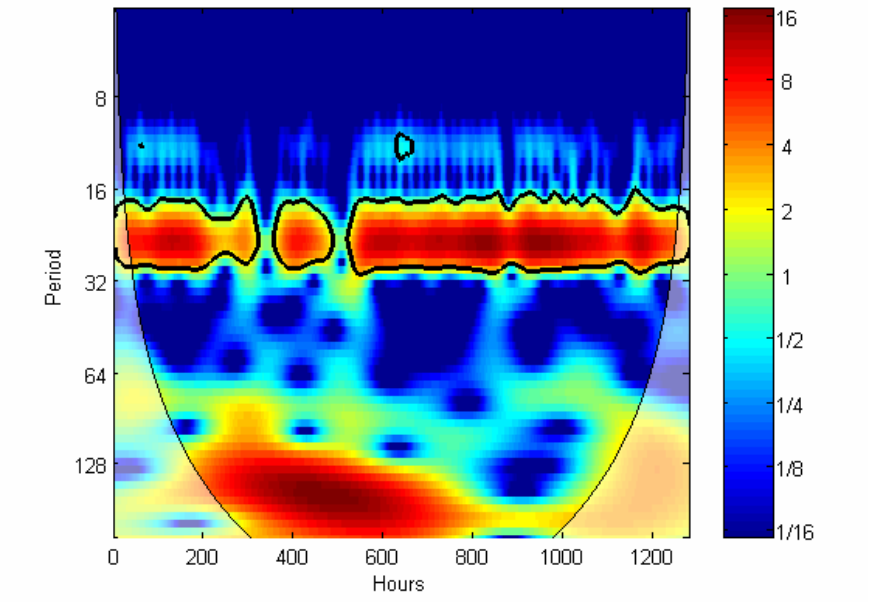

Fig. 6. The wavelet transform of the topsoil temperature.

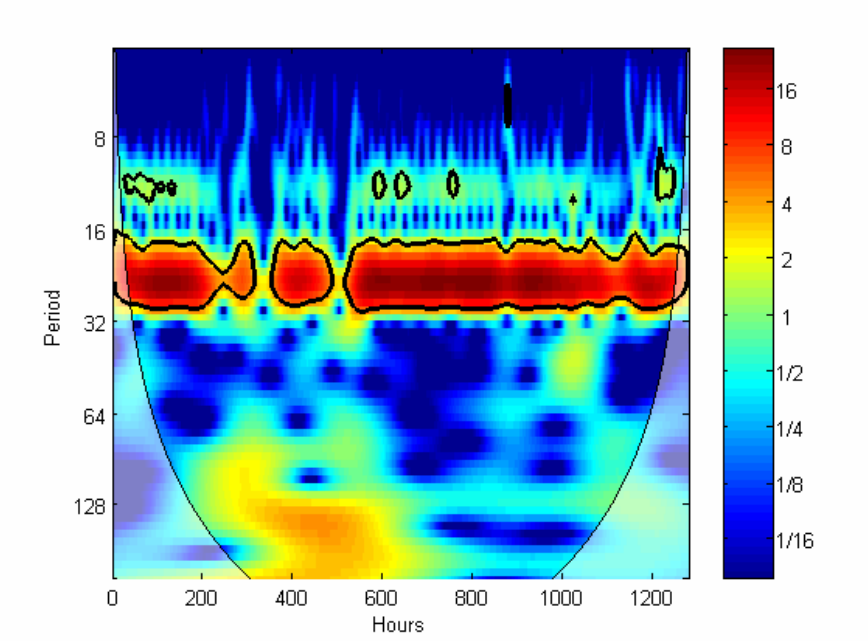

Fig. 7. The wavelet transform of the solar radiation.

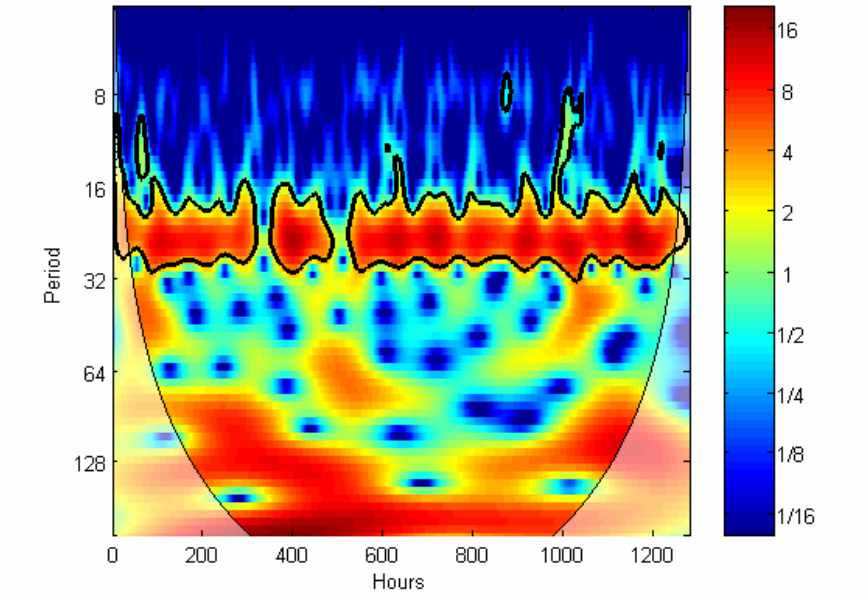

Fig. 8. The wavelet transform of the air humidity.

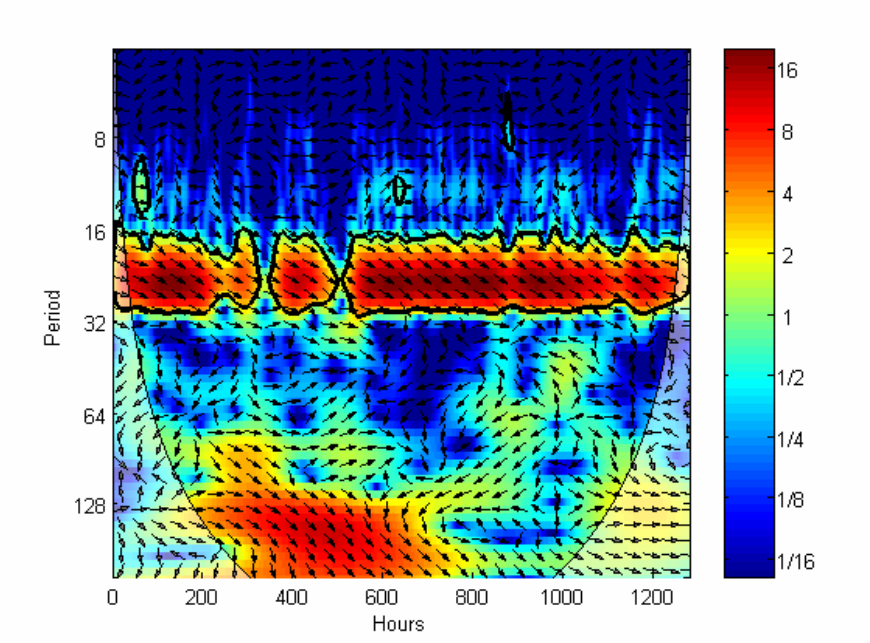

Fig. 9. Cross wavelet transform of the solar radiation and air temperature.

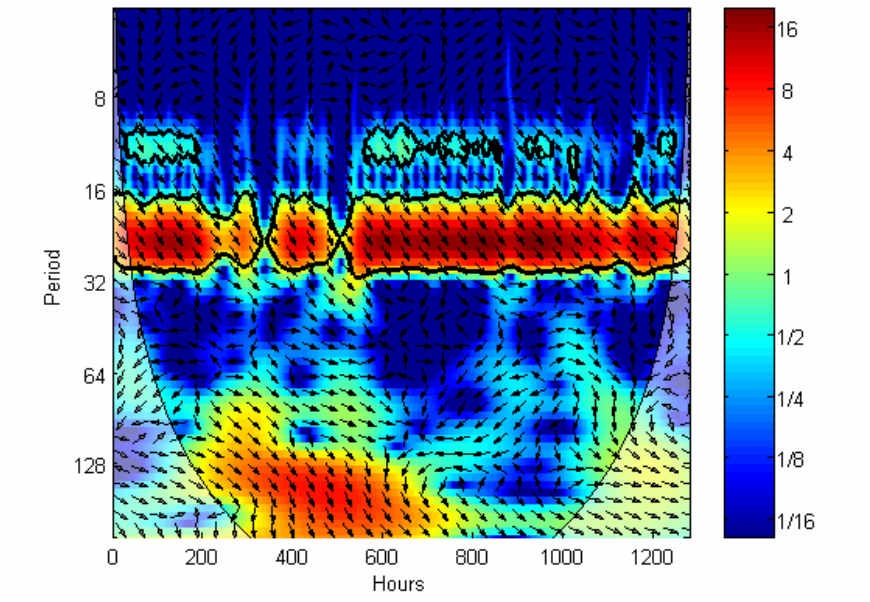

Fig. 10. Cross wavelet transform of the solar radiation and soil temperature.

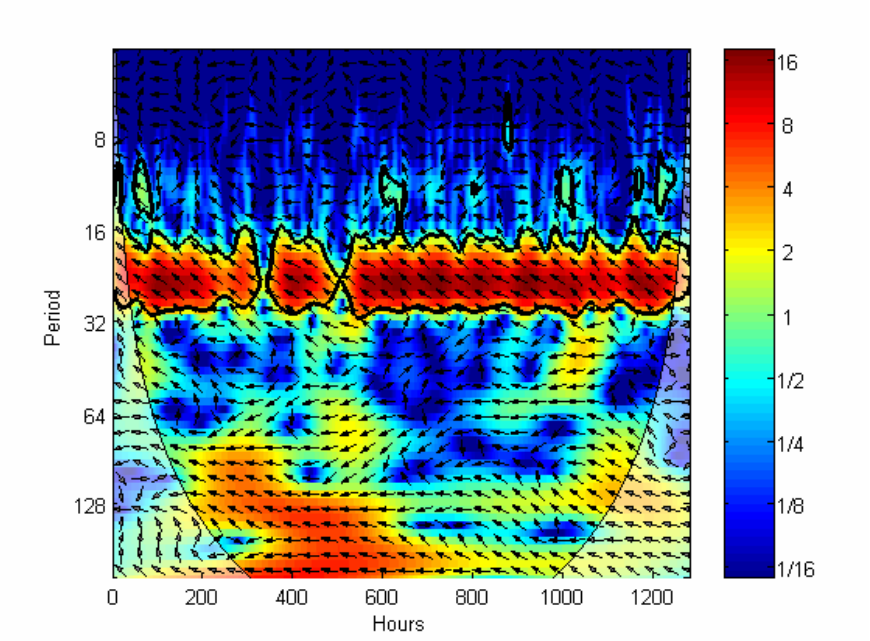

Fig. 11. Cross wavelet transform of the solar radiation and humidity.

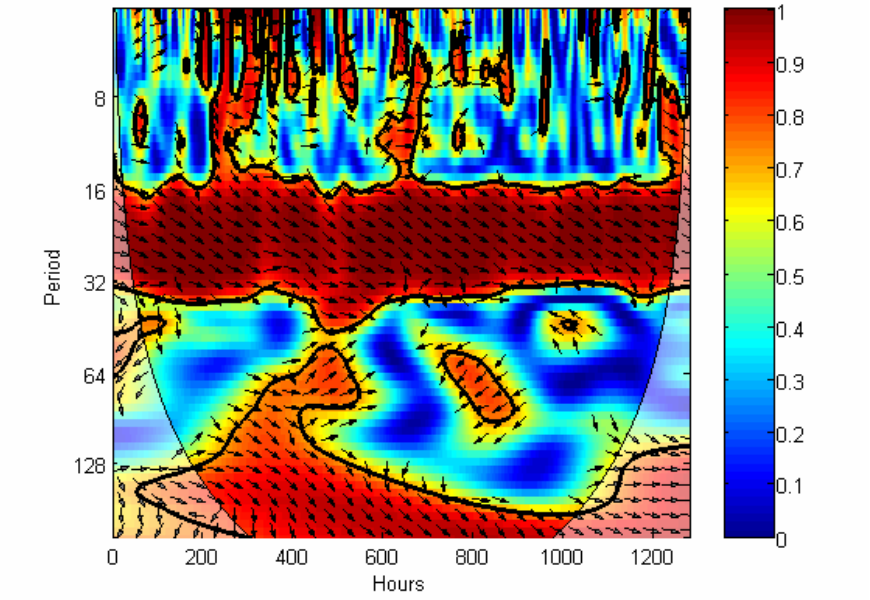

Fig. 12. Squared wavelet coherence between the standardized solar radiation and air temperature.

4.4.Empirical Mode Decomposition

Empirical Mode Decomposition (EMD) has been pioneered by Huang et al. [148,149] for analysis of nonlinear and non-stationary time series. It has gained a lot of popularity in data analysis and is widely considered as a major breakthrough in applied mathematics in the 20th century.

This technique adaptively decomposes the given oscillatory signal into a few AM-FM components which are referred to as *Intrinsic Mode Functions* (IMFs). IMFs are calculated in an iterative procedure called *sifting process*. As a rule, the last IMF represents long-term trend in the data. It is worth to note that this is local and fully data-driven technique. The EMD is in fact a type of adaptive wavelet decomposition whose subbands are built up in accordance with the frequency content of the signal.

The original signal can be reconstructed by summing up all IMFs. However, we are often more interested in partial reconstructions. In other words, we want to analyze various components of the given signal separately. For example, one usually needs to detrend the data or to perform some kind of filtering. One should note that this can be realized completely easily with the IMFs. Estimation of the trend in data or band-pass filtering is equivalent to summing up suitably chosen the mutually orthogonal pairs of IMFs. The above approach is adopted in the present analysis of soil temperature and humidity data. The time-frequency spectrum, a post-processing aspect of EMD, which is estimated with Hilbert transform, will not be considered here.

The EMD assumes that IMFs should:

(1) have the same number of zero crossings and extrema;
(2) be symmetric with respect to the local mean

Given a signal $x(t)$, the EMD algorithm works as follows:

(1) find all the extrema of $x(t)$;
(2) connect all the local maxima by a cubic spline as an upper envelope $e_{max}(t)$; repeat the procedure for the local minima to obtain the lower envelope $e_{min}(t)$;
(3) compute the average $m(t) = (e_{min}(t) + e_{max}(t))/2$;
(4) extract the detail $d(t) = x(t) - m(t)$;
(5) iterate on the residual $m(t)$.

In practice, the above main loop is refined by a sifting process, an inner loop that iterates step (1) to (4) upon the detail signal $d(t)$, until this latter can be considered as zero-mean according to some stopping criterion. Once this is achieved, the detail is considered as the effective IMF, the corresponding residual is computed and only then algorithm goes to step (5).

In summary, the original signal $x(t)$ is first decomposed through the main loop as

$$x(t) = d_1(t) + m_1(t), \tag{70}$$

and the first residual $m_1(t)$ is itself decomposed as

$$m_1(t) = d_2(t) + m_2(t), \tag{71}$$

so that

$$\begin{aligned} x(t) &= d_1(t) + m_1(t) \\ &= d_1(t) + d_2(t) + m_2(t) \\ &= \ldots \\ &= \sum_{k=1}^{K} d_k(t) + m_K(t) \end{aligned} \tag{72}$$

Although the EMD principle is very simple and appealing and its implementation easy, the exact mathematical theory of this method is not available yet. Due to the lack of analytical formulas its performance analysis is difficult. In spite of that, the EMD is widely used in different branches of science as a one of the best methods for the analysis of non-stationary time series.

The reconstruction of signal components is done in a process of visual inspection and selection of the appropriate IMFs. Although the selection criterion is a bit arbitrary, one can readily identify particular IMSs which correspond to a given sub-band. Finally, the signal components are restored by summing up the carefully selected IMFs. Let us emphasize that the above very simple procedure is equivalent to the adaptive sub-band filtering.

We illustrate how the EMD works using the same data we have analyzed with the CWT.

4.5.The results of EMD

Fig. 13 show the EMD of the air temperature. As can be seen, the original time series is decomposed into eight IMFs. The reconstructed components, high-frequency variations (C1), periodic (daily) variations (sum of C2 to C4) and long-term (seasonal) variations (sum of C5 to C8) are shown in Fig. 14. The seasonal component is superimposed on the original time series, while the remaining

components are shown below in the figure. This same convention is used in subsequent figures. Note that the mean value of these two components is relative and equal to zero. Fig. 15 show the EMD of the topsoil temperature. In this case the high-frequency variations are not present. Of course, this is caused by greater thermal inertia of the soil as compared to the air. Fig. 16 show the two reconstructed components. The daily component comprises of C1 and C2 IMFs while the seasonal component the remaining IMFs (sum of C3 to C6). Fig. 18 shows the EMD of the air humidity. In this case, one can observe readily an increase of the air humidity caused by the precipitation. Fig. 19 show the three reconstructed components of the air humidity. The high-frequency component comprises of C1 IMF, the daily component (sum of C2 to C4), the seasonal (sum of C5 to C8). Note that the daily component is additionally shifted to the level – 50 % for presentation clarity. Finally, the EMD of the solar radiation is shown in Fig. 20 and the reconstructed components in Fig. 21. The visible valleys in the course of solar radiation are caused by the weather breakings. This intermittent behavior is instantly reflected in other measured quantities. The EMD of the solar radiation contains of nine IMFs. The high-frequency component comprises of C1 IMF, the daily component (sum of C2 to C4), the seasonal component (sum of C5 to C9). The daily component is additionally shifted to the level -1.5 kW/m^2 for presentation clarity.

The heat transfer regime at the air-soil interface can be studied with details by using the Empirical Mode Decomposition as demonstrated above. Two main factors play a major role here - solar radiation and intermittency in the weather.

The dynamics of the air and topsoil temperature variations can be represented on the so-called phase-space plots. Fig. 17 shows such a plot for the daily and seasonal reconstructed components. As can be seen the dynamical picture of both variatiations is rather complex.

It is worth to note that such representation is very useful in qualitative assessment of the heat transfer regime at the air-soil interface.

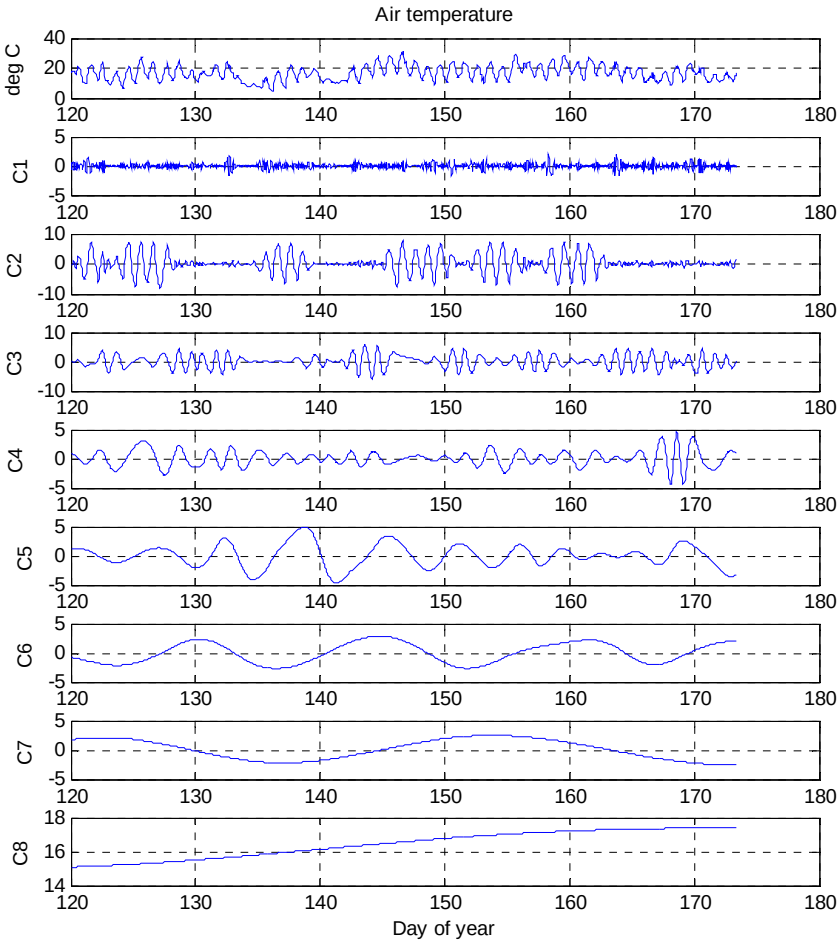

Fig. 13. The Empirical Mode Decomposition of the air temperature.

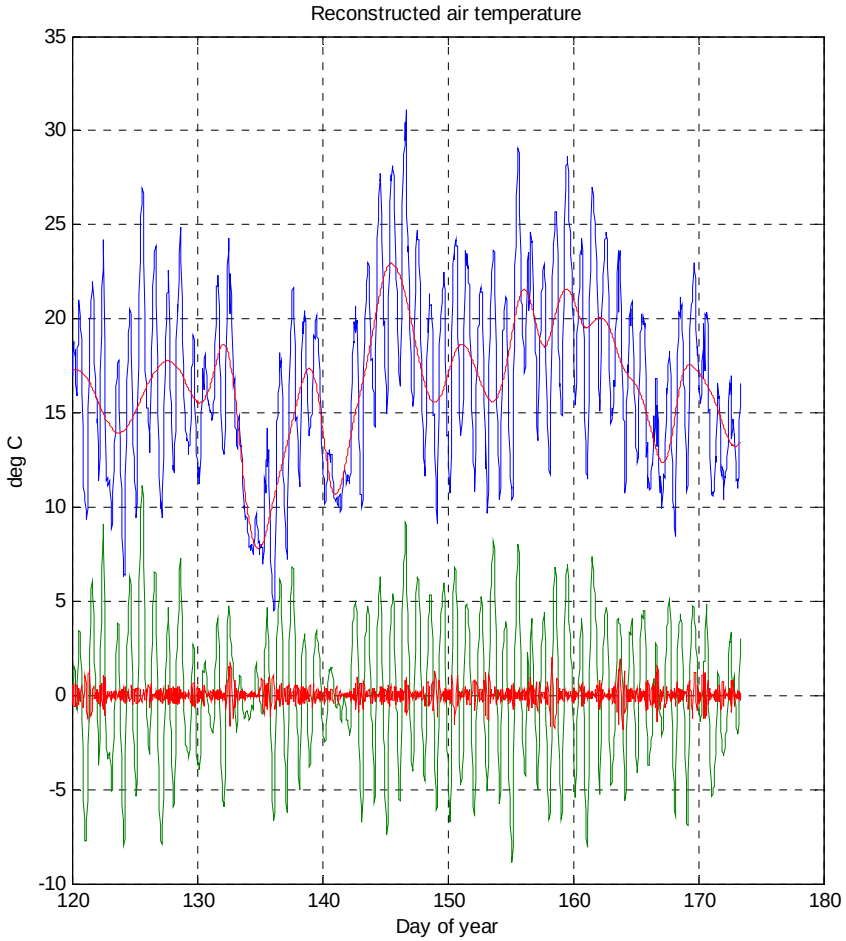

Fig. 14. The reconstructed three components of the air temperature.

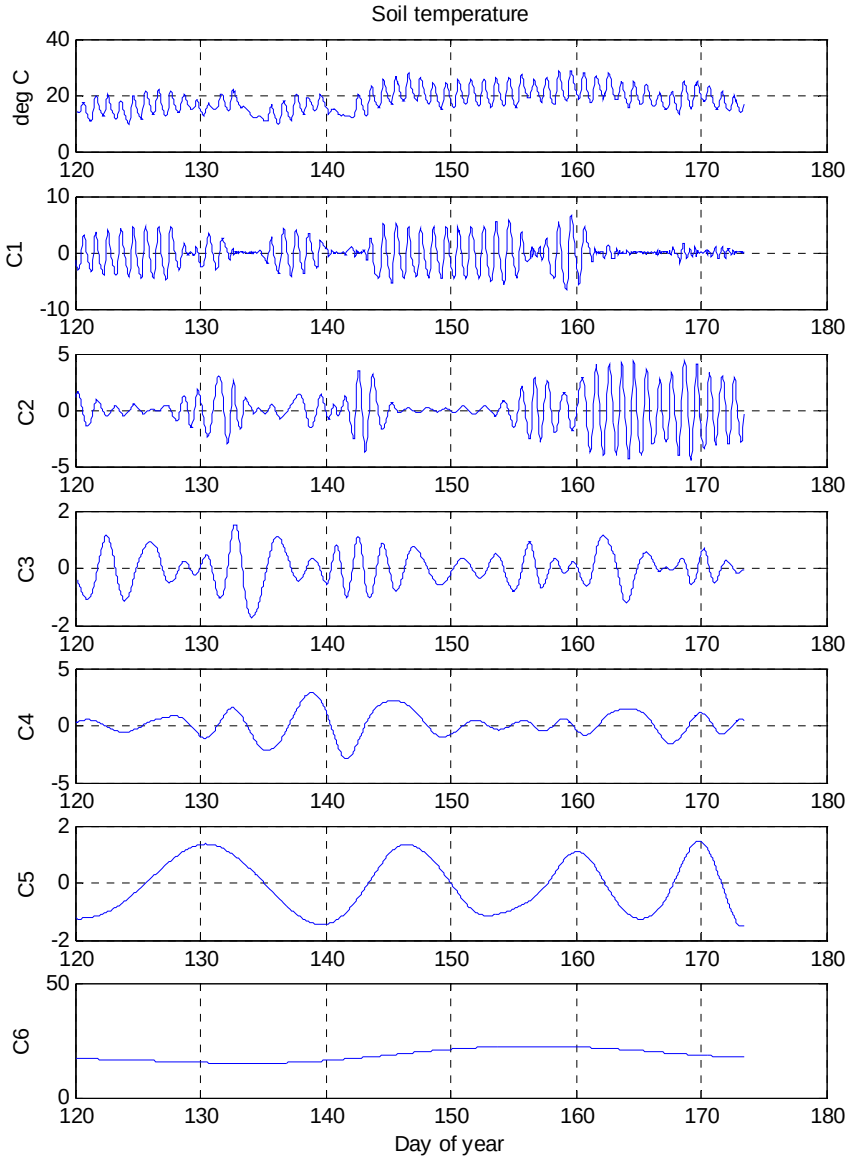

Fig. 15. The Empirical Mode Decomposition of the topsoil temperature.

Fig. 16. The reconstructed two components of the topsoil temperature.

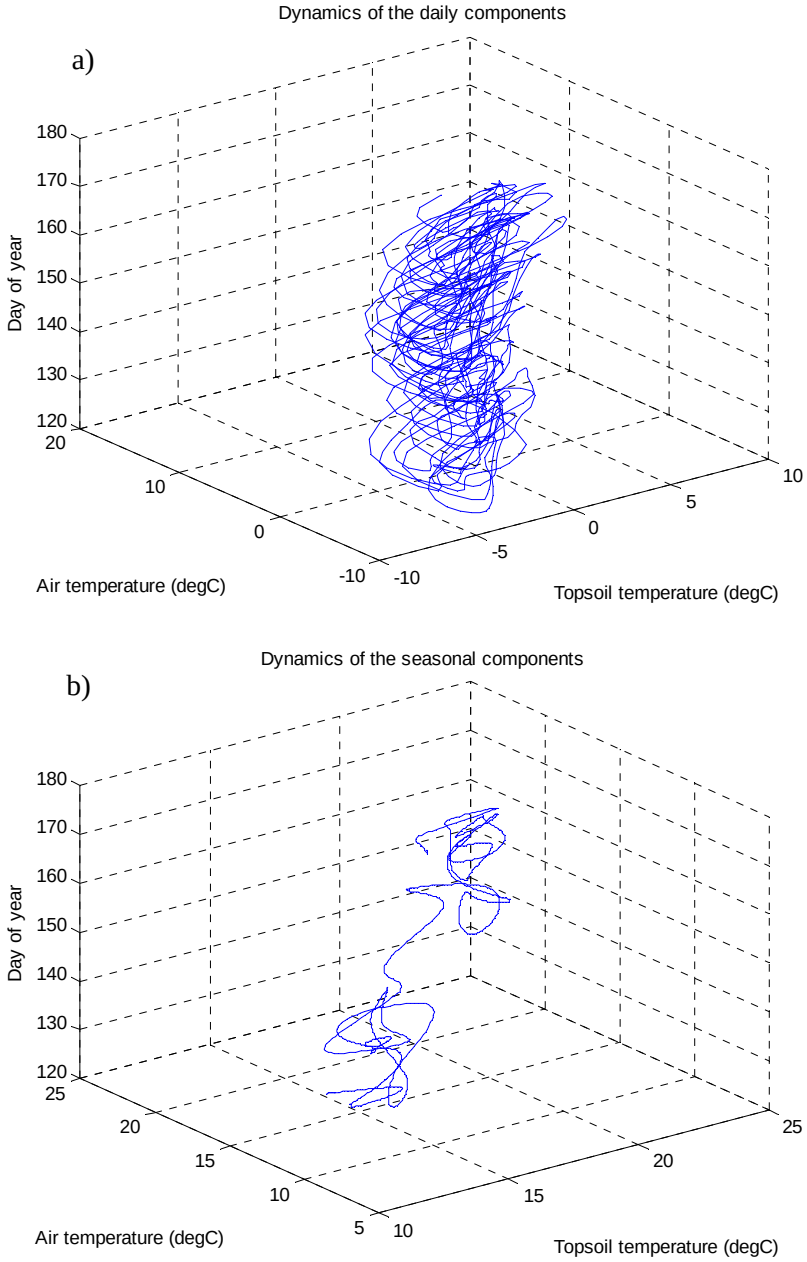

Fig. 17. Phase space plot of the air and topsoil temperature, (a) reconstructed daily components, (b) reconstructed seasonal components.

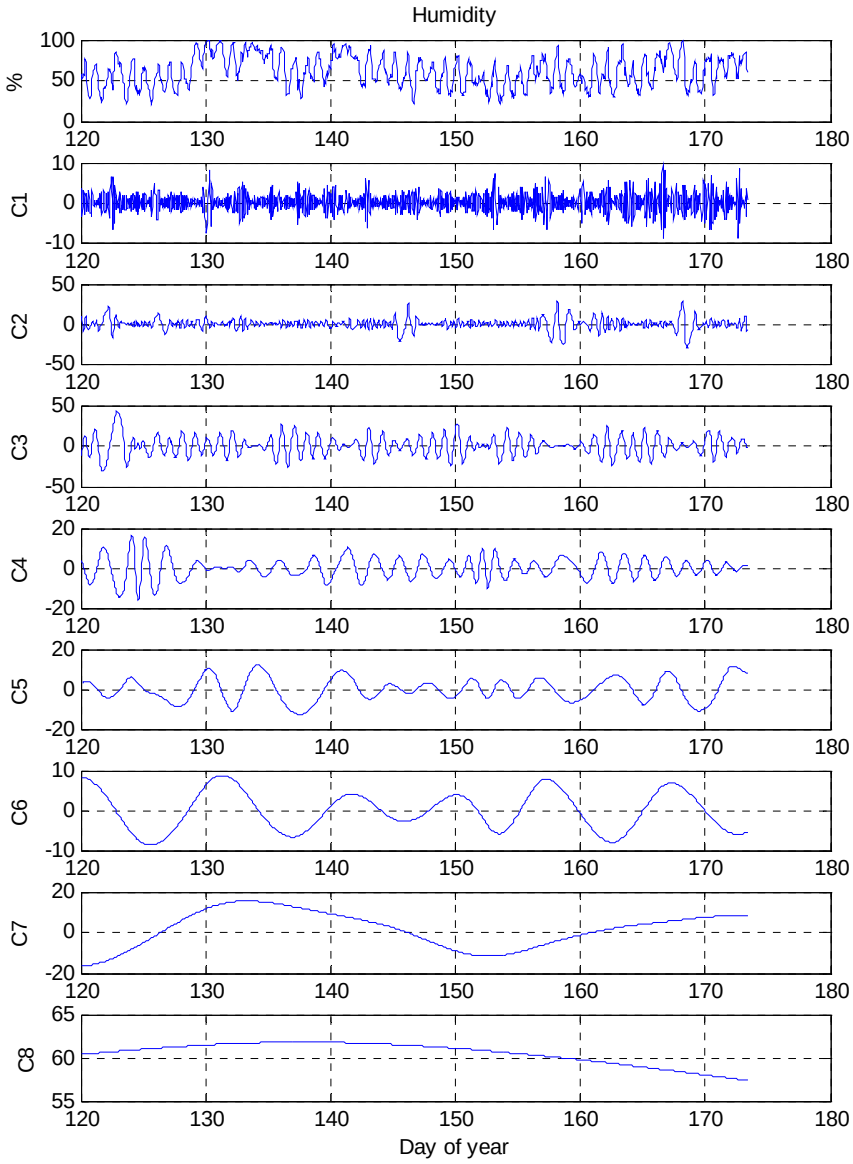

Fig. 18. The Empirical Mode Decomposition of the air humidity.

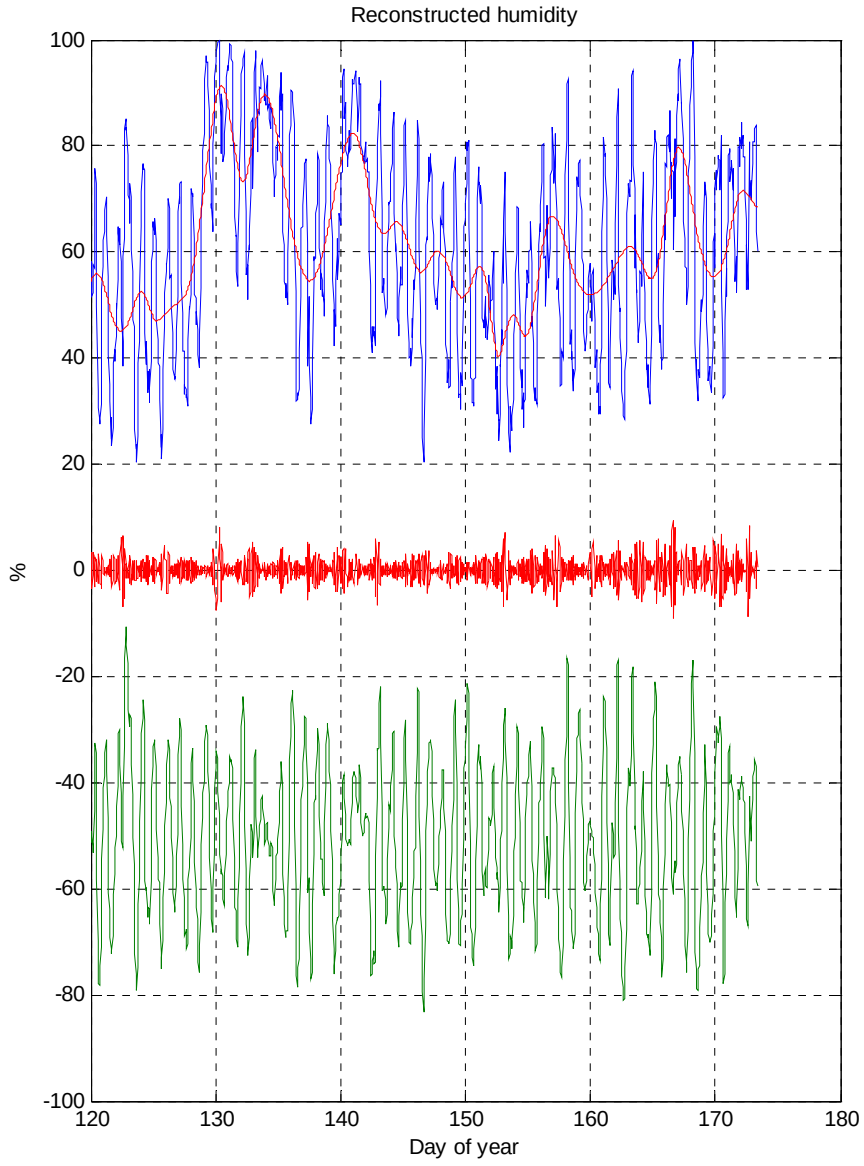

Fig. 19. The reconstructed three components of the air humidity.

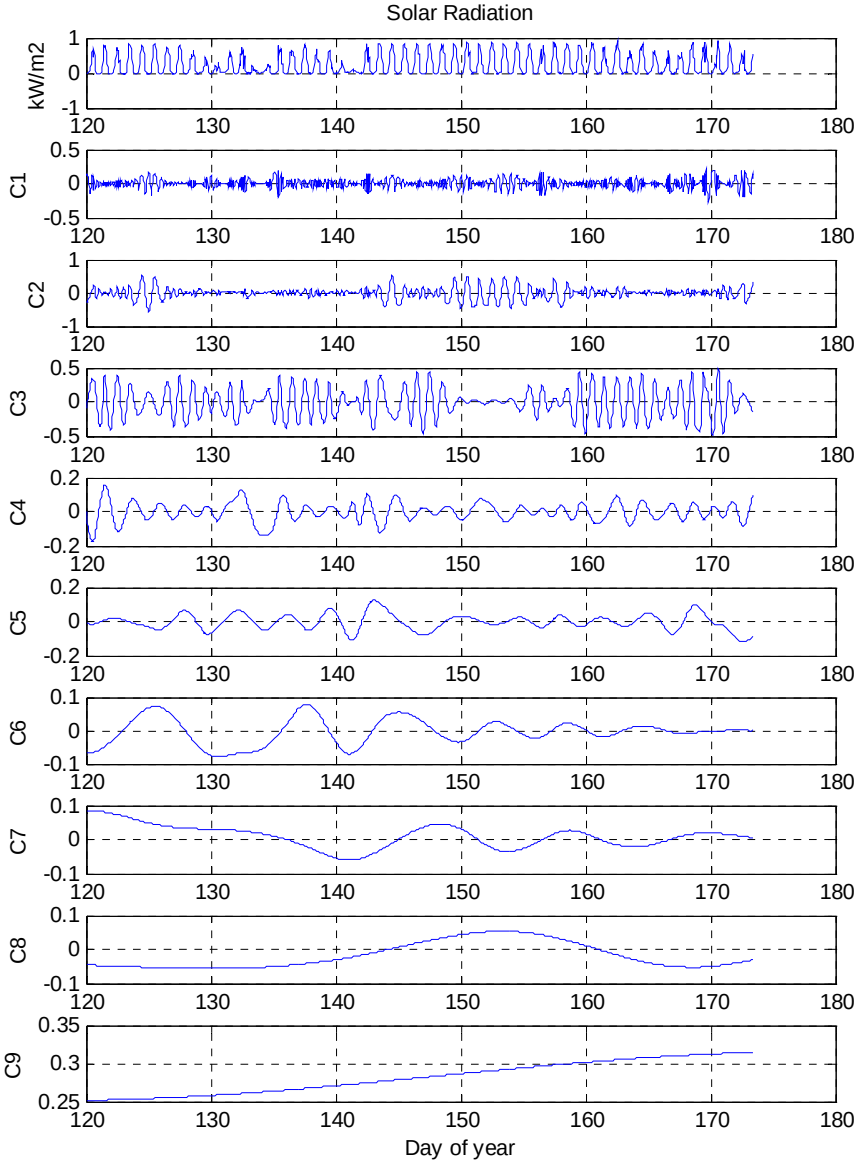

Fig. 20. The Empirical Mode Decomposition of the solar radiation.

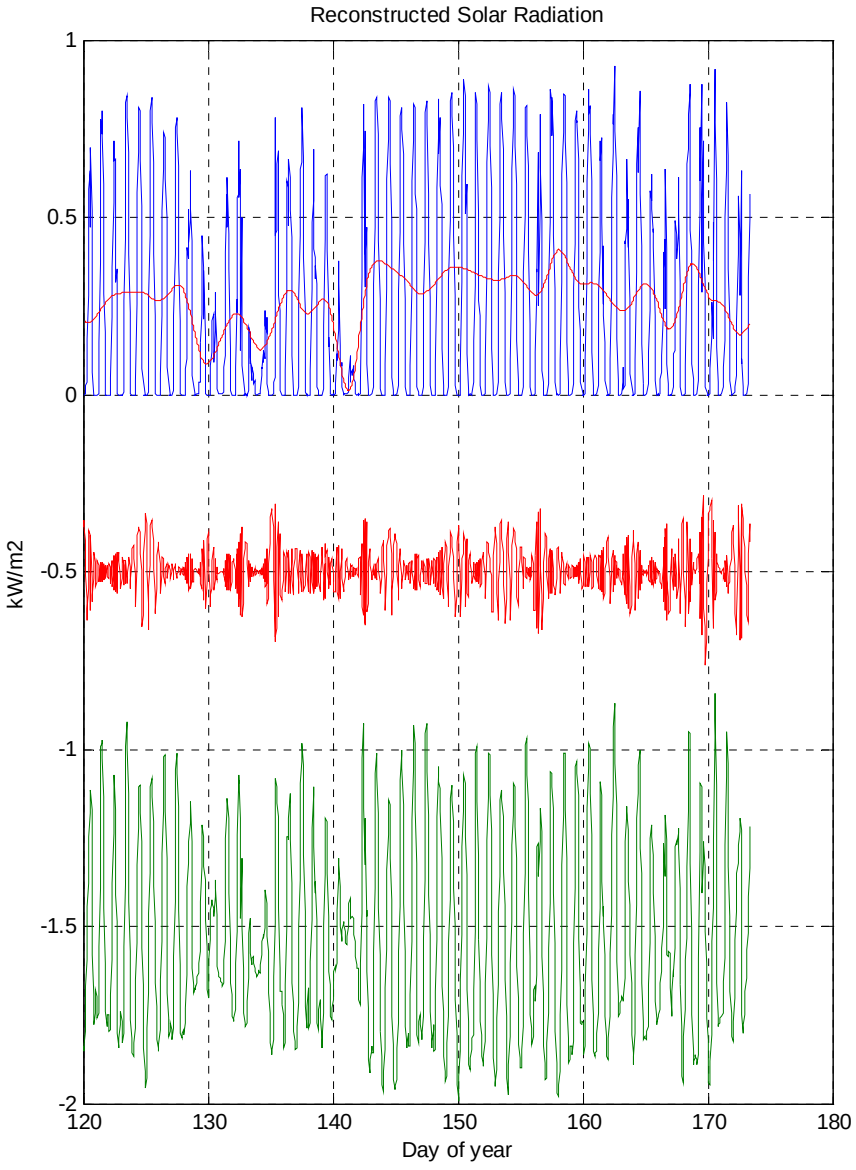

Fig. 21. The reconstructed three components of the solar radiation.

4.6.The Multitaper Method

Usually, the power spectrum of a time series is estimated as the squared absolute value of its Fourier Transform. This simple approximation is called the periodogram. To reduce leakage in the spectral estimation, a time series is often windowed before applying the Fourier Transform. Although windowing reduces the bias, it does not reduce the variance of the spectral estimate. The multitaper method [290,371] is designed to reduce spectral leakage. First the dates are windowed with different, orthogonal tapers, and next spectra for all the tapers are averaged. The resulting multitaper spectral estimator is superior to the periodogram in terms of reduced bias and variance. There are some similarities with the Welch method of modified periodogram.

The multitaper spectrum estimator is given by:

$$S(f) = \frac{1}{L}\sum_{k=0}^{L-1} \alpha_k S_k(f) \tag{73}$$

with

$$S_k(f) = \left| \sum_{n=0}^{N-1} w_k(n) x(n) e^{-j2\pi fn} \right|^2 \tag{74}$$

where: α_k is the corresponding weighting factor, N is the data length and $w_k(n)$ is the k-th data taper used for the spectral estimate $S_k(f)$, which is also called k-th eigenspectrum. The tapers are orthonormal, i.e., $\sum_n w_k(n) w_j(n) = 0$ for $j \neq k$ and equal to 1 for $j = k$. The discrete prolate spheroidal sequences (dpss) or Slepian sequences are usually chosen as tapers because of their good leakage properties. The number of tapers L is always chosen to be less than $2NW$, where W is expressed in units of normalized frequency, i.e., $0 < W < ½$. The Slepian sequences maximize the spectral concentration of the window main lobe within $[-W,W]$.

The multitaper cross spectral transform for time series x_n and y_n is given as

$$S^{XY}(f) = \frac{1}{L}\sum_{k=0}^{L-1} F_k^X(f) F_k^{Y*}(f), \tag{75}$$

where:

$$F_k^X(f) = \sum_{n=0}^{N-1} w_k(n) x(n) e^{-j2\pi fn}, \tag{76}$$

and similarly for y_n. The multitaper coherence is defined here as:

$$C^{XY}(f) = \frac{\left|S^{XY}\right|}{\sqrt{S^X}\sqrt{S^Y}}, \tag{77}$$

and phase difference is given by:

$$\phi = \arctan\left(\frac{\mathrm{Im}(C^{XY})}{\mathrm{Re}(C^{XY})}\right), \tag{78}$$

We have used the improved matlab scripts for the computation of both the multitaper spectrum and coherence. These scripts were delivered by Peter Huybers and are available in the Matlab Central archive or in his home page http://web.mit.edu/~phuybers/www/Mfiles/index.html.

It is worthwhile to note that these scripts use a fast approximation to compute the 95% confidence limits for a chi-squared distribution and computes the equivalent degrees of freedom as given by Percival and Walden, 1993, p256 and p370 [290]. Also the adaptive weights α_k is determined iteratively (see above, pp.368-370).

4.7.The results of the Multitaper Method

We have shown that the adaptive sub-band filtering of a given time series can be implemented readily with the EMD. How efficient is this technique? We answer this question by comparing the MTM power spectra of both the original time series and the reconstructed components. Fig. 22 shows the power spectrum of the air temperature. The background spectrum really resembles the red noise, since the power increases at low frequencies. There are apparent three distinct peaks in the spectrum. The strongest peak corresponds to the diurnal cycle; the next ones have periods of 12 and 8 hours. The high-frequency noise is also apparent. Fig. 23 shows the reconstructed daily components of the air and topsoil temperature. These components are quite similar. However, one can also notice minor differences in their course.

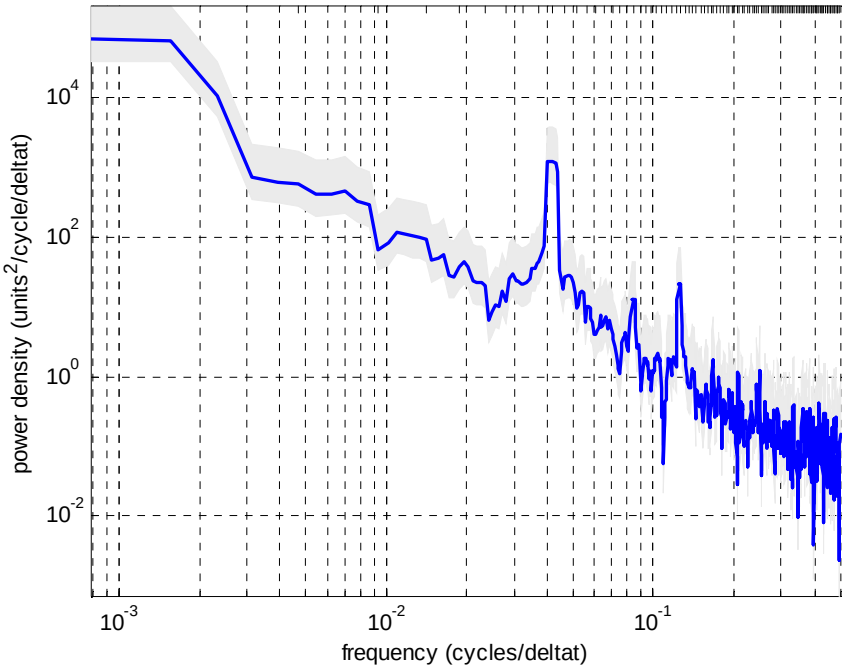

Fig. 22. The multitaper power spectrum density of the air temperature.

Fig. 24 shows the MTM spectrum of the daily component of the air temperature. It is evident that low- and high-frequency power is diminished. Fig. 25 shows the high-frequency component of the air-temperature. The MTM power spectrum of this noisy component is shown in Fig. 26. Obviously, this confirms again that the EMD is highly efficient when one tries to filter out or isolate signal components.

Fig.27 shows the coherence and phase difference for the daily components of the air and topsoil temperature. We draw our attention to the following frequencies, 0.04, 0.08 and 0.12 (cycles/delta t). Almost perfect coherence is seen for the main variation, still high for variation at frequencies 0.08 and 0.12. Notice also the progressive phase difference at these frequencies.

Fig. 28 shows the seasonal components of the air and topsoil temperature. These are also quite similar. It is also apparent that the soil accumulates the thermal energy especially for days 145 to 175. Fig. 29 shows the coherence and the phase difference for the seasonal components. The coherence is also high and phase difference is increasing with the frequency. The above results agree well

with the wavelet analysis. However, we should emphasize here that the combined EMD-MTM analysis enables much deeper insight into the thermal regime at the air-soil interface.

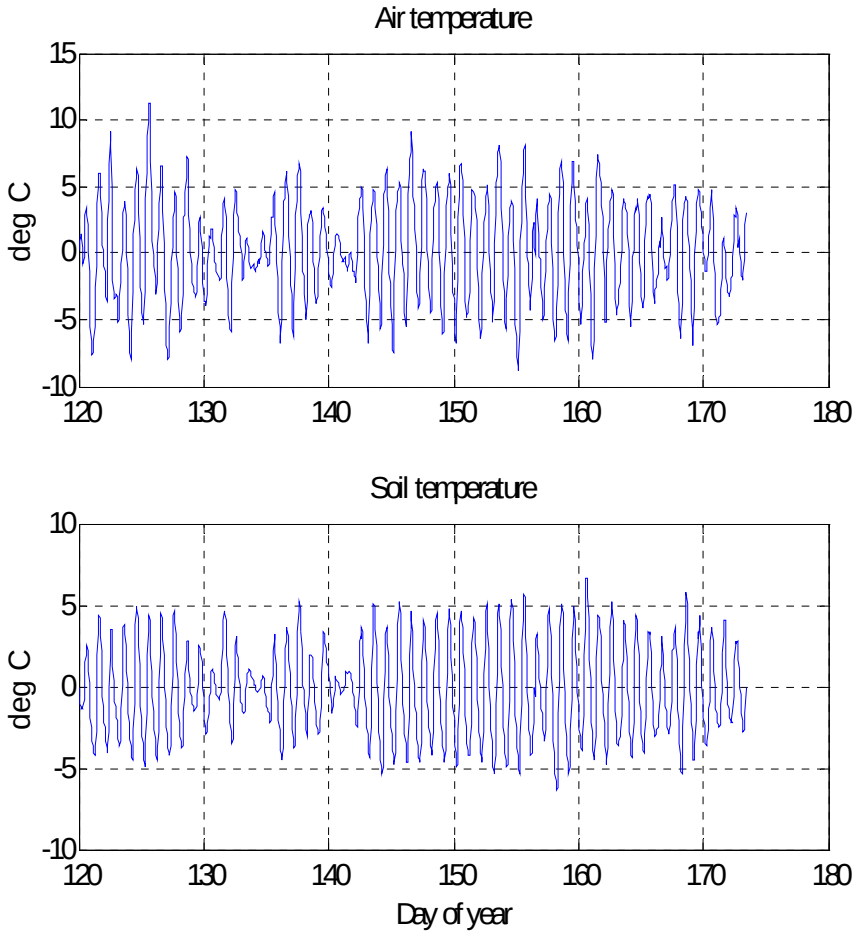

Fig. 23. The reconstructed daily components of the air and topsoil temperature.

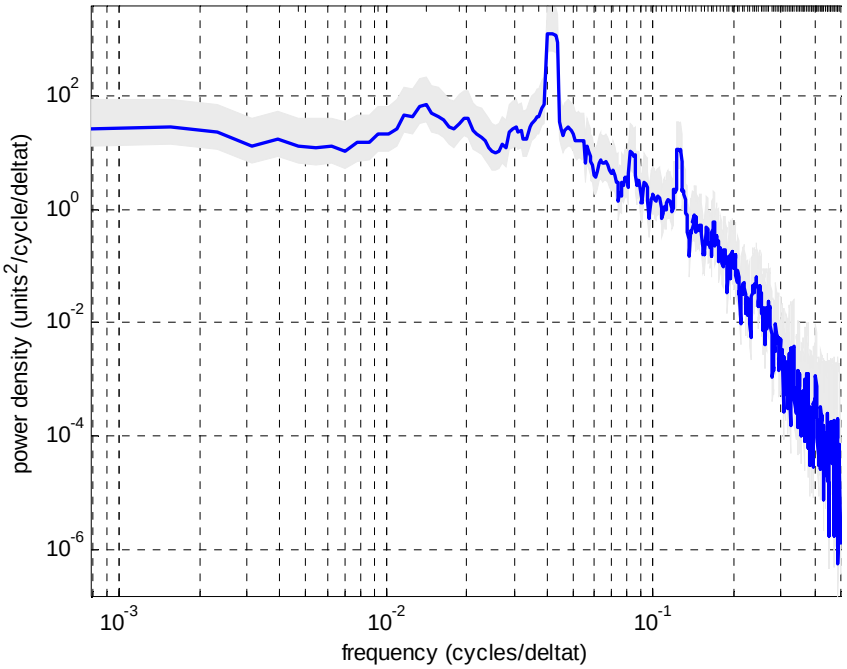

Fig. 24. The multitaper power spectrrum density of the daily component of air temperature.

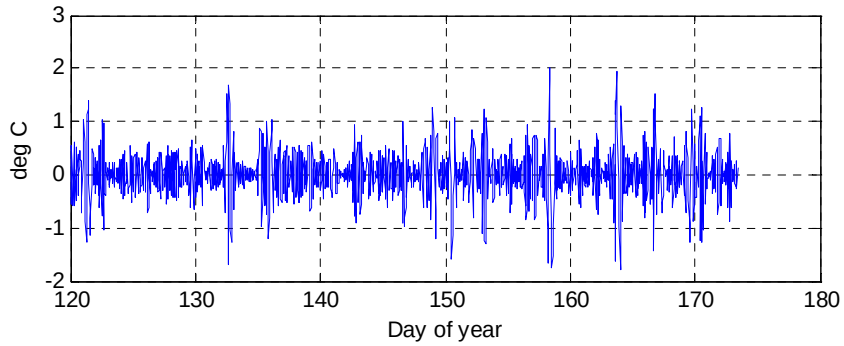

Fig. 25. The high-frequency (noisy) component of the air temperature.

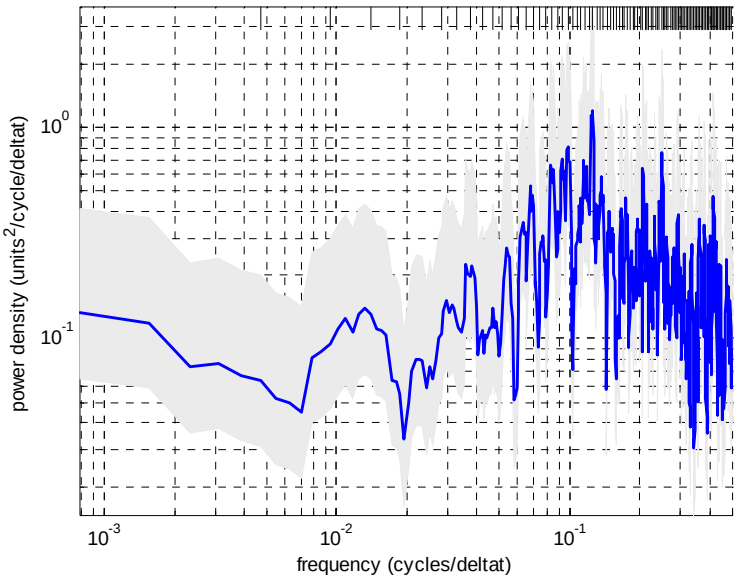

Fig. 26. The multitaper power spectrum density of the noisy component of air temperature.

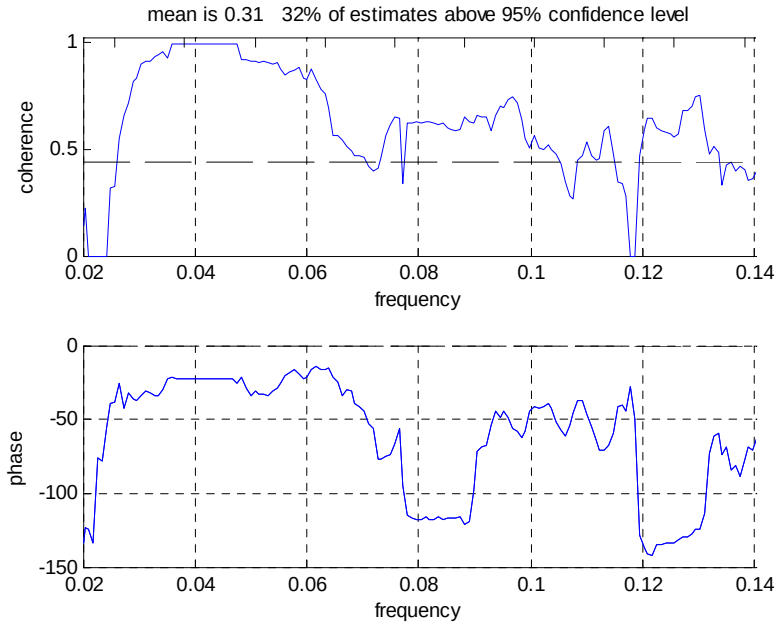

Fig. 27. The multitaper coherence and phase difference for daily components of air and topsoil temperature.

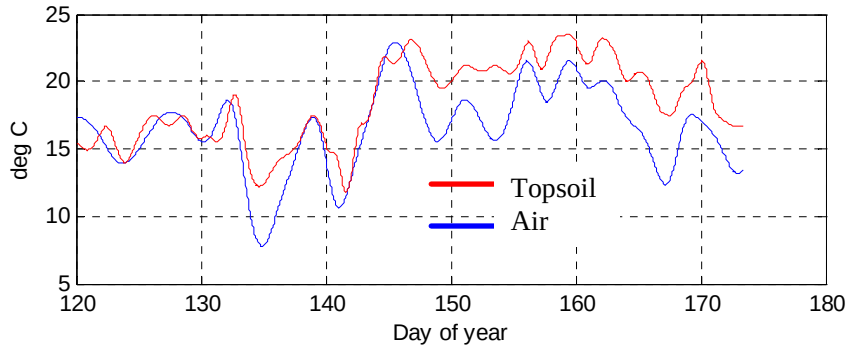

Fig. 28. The reconstructed seasonal components of the air and topsoil temperature.

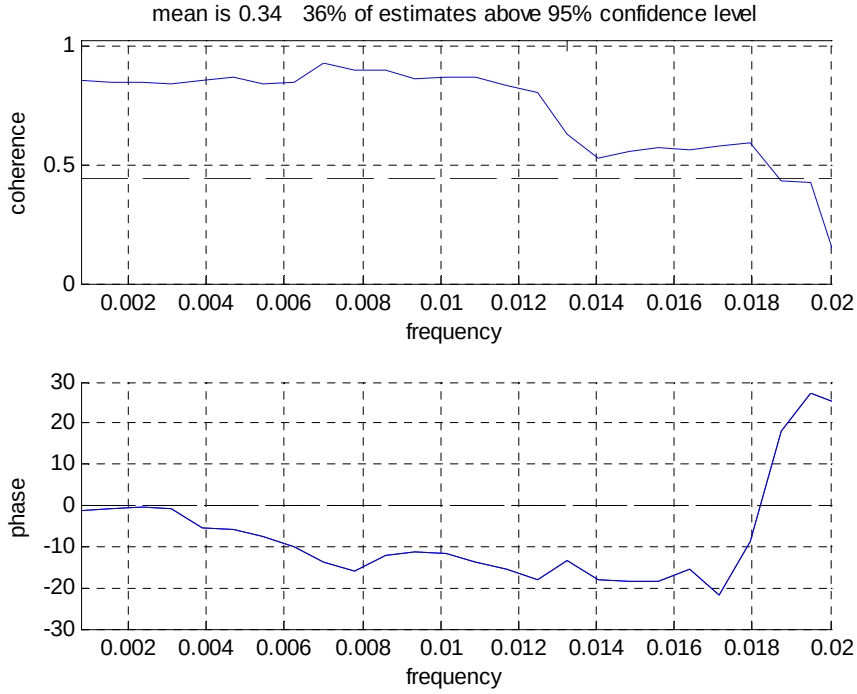

Fig. 29. The multitaper coherence and phase difference for the seasonal components of air and topsoil temperature.

5. STATISTICAL AND GEOSTATISTICAL ANALYSES OF TIME SERIES OF THE PHYSICAL VALUES AND PROPERTIES OF SOIL

5.1. Field experiment

The data analyzed in this monograph originated from two sources. The first was the measurement data acquired within the research project „Structure of radiation balance and the thermal-moisture relations of soil", Grant KBN, No. PB 1679/5/91 headed by Prof. R.T. Walczak [416]. The second – data collected within the research project KBN No. 6 P06H 029 20 (2001-2003) „Investigation of spatial variability of physicochemical soil properties as a base for precision agriculture„ State Committee for Scientific Research, during the period of 2001-2003, headed by the first of the authors of this monograph.

In the case of the first object of investigation, measurements were taken in an experimental plot of the Agrometeorological Station, University of Agriculture, Lublin, in the field of the Agricultural Experimental Station, University of Agriculture, located next to the Institute of Agrophysics in Lublin (Felin, 51°13'29" N 22°38'42" E). The soil at Felin is classified as a grey brown podzolic soil. R. Turski (verbal information) classified the soil at Felin as a grey brown podzolic soil developed from a loess-like formation, incomplete, on a chalk formation. In the object studied, the following soil profile was determined: from 0 to about 20 cm – humus horizon with brown-grey colouring, distinctly separated from the next layer with reddish colouring, below 30 cm somewhat lighter in colour with yellow spots and with high sand content. From the depth of about 45 dm there appear fragments of weathered lime rock which becomes a significant material component of the soil below 90 cm [169]. The Table 2 presents the granulometric composition and some physical-chemical properties of the soil at the Agricultural Experimental Station, University of Agriculture (further referred to as the RZD AR Station) at Felin near Lublin [207].

The measurements were taken on the object with plant canopy and without plants (as reference). The measurements were taken within the period of April-July, 1993. The arrangement of the experimental plots, 50 x 40 m in size, was such that they were strung along a road passing through the middle of the station area. The fallow plot and the meteorological station plot had constant positions during the measurement seasons, while particular cultures were located on plots with an annual cycle of rotation (a specific culture would be moved in successive years by one plot in anticlockwise direction). TDR probes, spaced at 0.2 m from one another, were installed opposite the midpoints of the plots, in a row at the

distance of 3 m from the path. Each of the probes had one moisture sensor. The moisture sensors covered 5 cm soil layers and were installed in the plots in the soil layers of 0-0.05, 0.05-0.1, 0.1-0.15, 0.2-0.25, 0.3-0.35, 0.4-0.45, 0.5-0.55, 0.8-0.85 m. Measurements of soil moisture were taken once a day, in the afternoon hours. The time required to take measurements at all the measurement points in he experiment was approximately half an hour.

Soil density was determined according to the gravimetric method, on the basis of soil cores sampled with cylinders 100 cm^3 in volume and 5 cm high from the levels of TDR probe installation, down to the depth of 85 cm. The density measurements were taken in close proximity to the moisture sensors (about 0.5 m from the sensors) at the end of the moisture measurement sessions. Three soil cores were sampled from each horizon.

The main mineral components of the soil, i.e. quartz and other minerals, were determined from the granulometric distribution assuming that the 1-0.02 mm fraction contains mainly quartz, and other minerals are contained in the fraction below 0.02 mm [78,390].

Table 2. Granulometric composition and some physical-chemical properties of the soil at the RZD AR Station, Felin near Lublin [207].

Layer (cm)	% content of granulometric fraction < 1 mm						pH (KCl)	OM (%)	PD (Mgm^{-3})
	1-0.1	0.1 -0.05	0.05 -0.02	0.02 -0.006	0.006 -0.002	< 0.002			
0-15	20	6	42	23	3	6	5.8	1.48	2.61
30-40	16	10	42	13	6	13	5.4	-	2.63
80-90	66	10	9	4	3	8	5.6	-	2.58

OM – organic matter, PD – particle density of solid fraction.

5.2. Results of statistical analysis

The distribution of atmospheric precipitation during the period of the study is presented in Fig. 30a. The sum of precipitation for that period was 167.5 mm in total; the maximum recorded precipitation occurred on the 174th day of the year and amounted to 27.9 mm. The effect of precipitation is most visibly reflected in the plot without plants, in the surface horizon of the soil (Fig. 31c), while the presence of plant canopy has a distinctly damping effect on the temporal runs of soil moisture. The extent to which plants could change the time runs of soil moisture depended on their stage of development (i.e. the intensity of water

uptake by their roots), on the water interception on a given plant, and on the surface runoff which in turn was determined by the degree of compaction of the surface horizon of the soil (Fig. 30b).

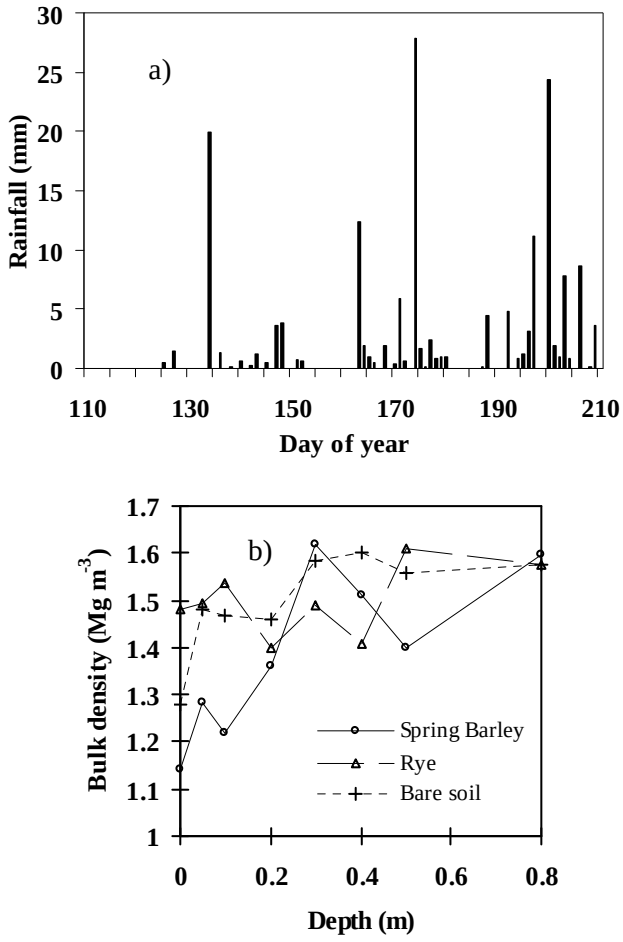

Fig. 30. Precipitation (a) as a function of time and soil bulk density (b) of spring barley, rye and bare soil.

The mean values of soil density measured in the plots are shown, with relation to depth, in Fig. 30b. The lowest density was observed in the field with barley, in the arable layer, and the highest in the field with rye. Below the arable layer, the differentiation of soil density in the objects studied was only slight. The soil density distributions observed in the particular plots were related primarily to the time that elapsed from the last tillage applied, to the meteorological conditions,

and to the occurrence of the same genetic horizons at different depths in particular cultivation plots.

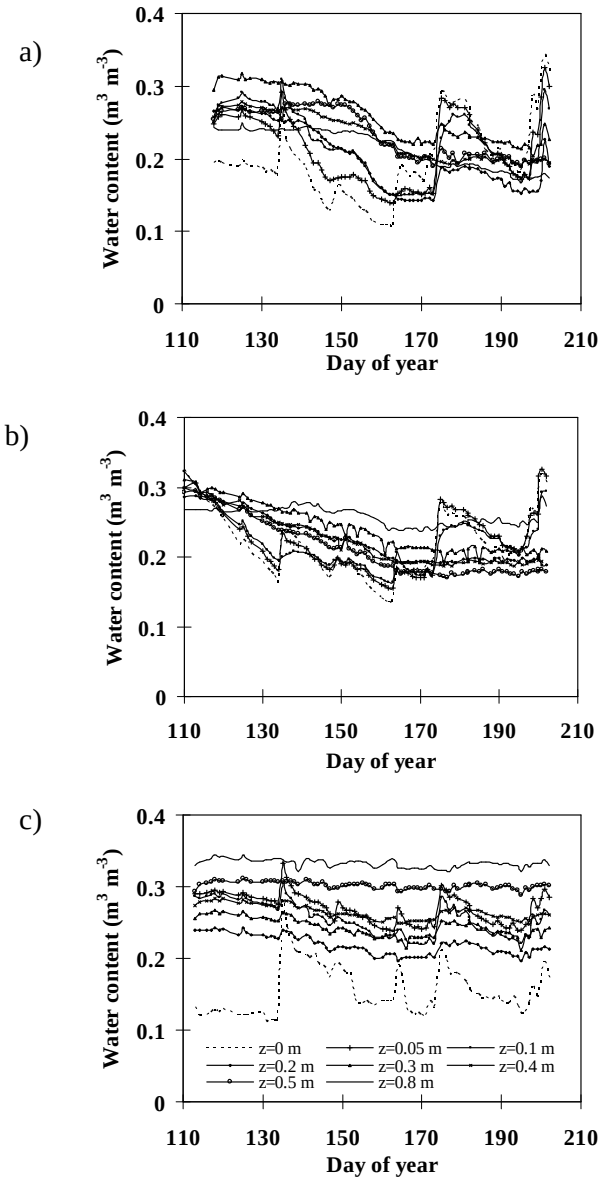

Fig. 31. Soil water content as a function of time for different depths (a - spring barley, b - rye, c - bare soil) during growing season.

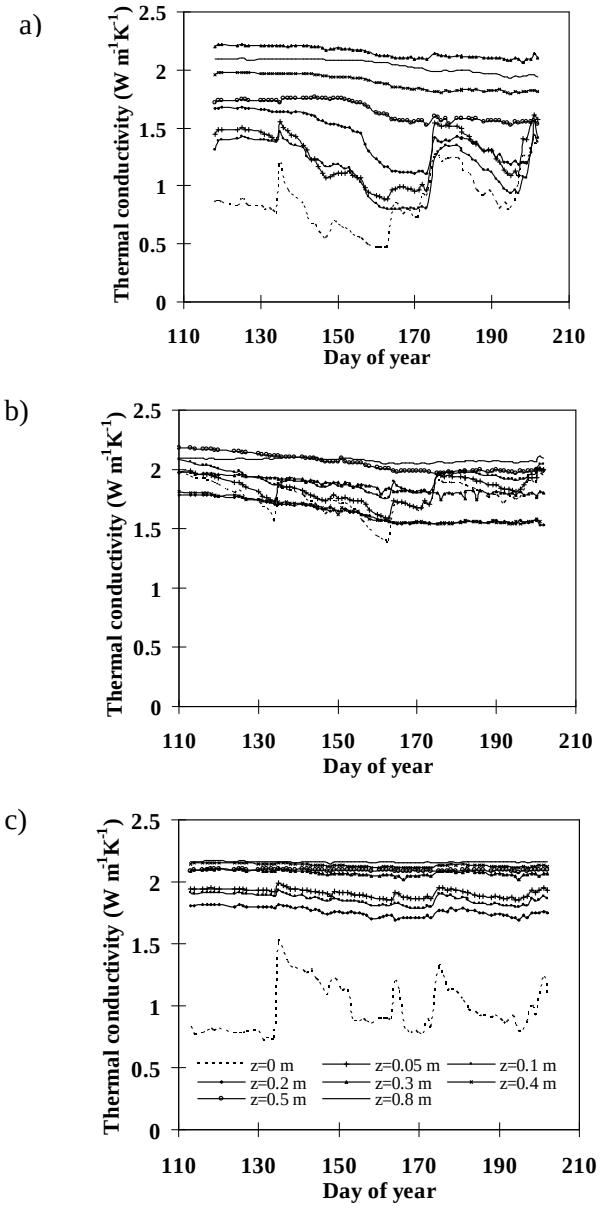

Rys. 32. Soil thermal conductivity as a function of time for different depths (a - spring barley, b - rye, c - bare soil) during growing season.

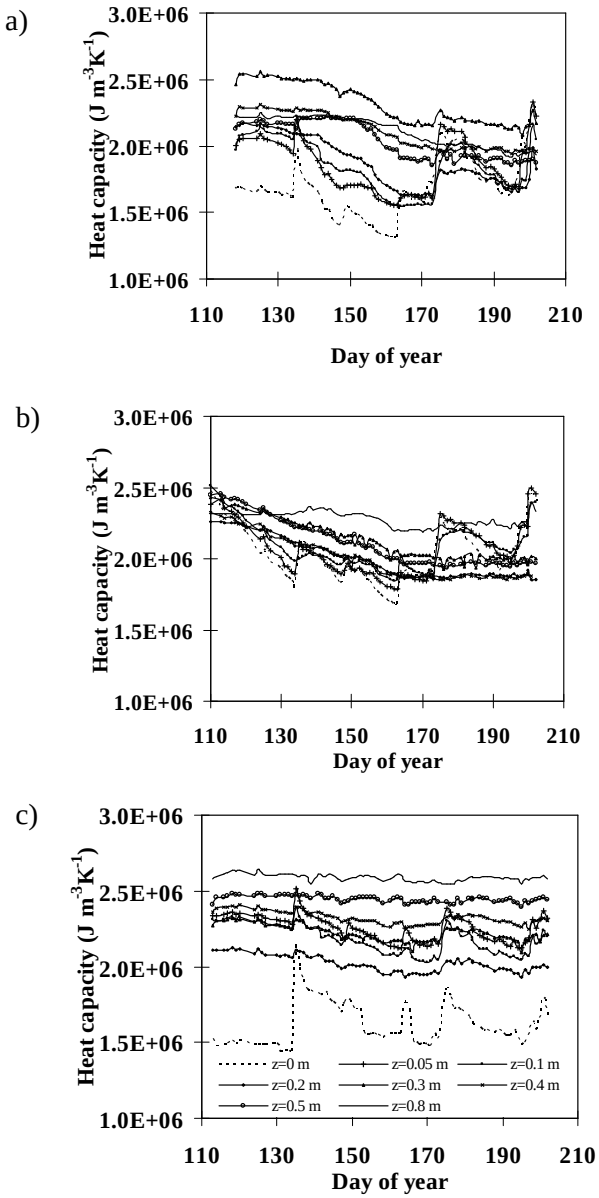

Rys. 33. Soil heat capacity as a function of time for different depths (a - spring barley, b - rye, c - bare soil) during growing season.

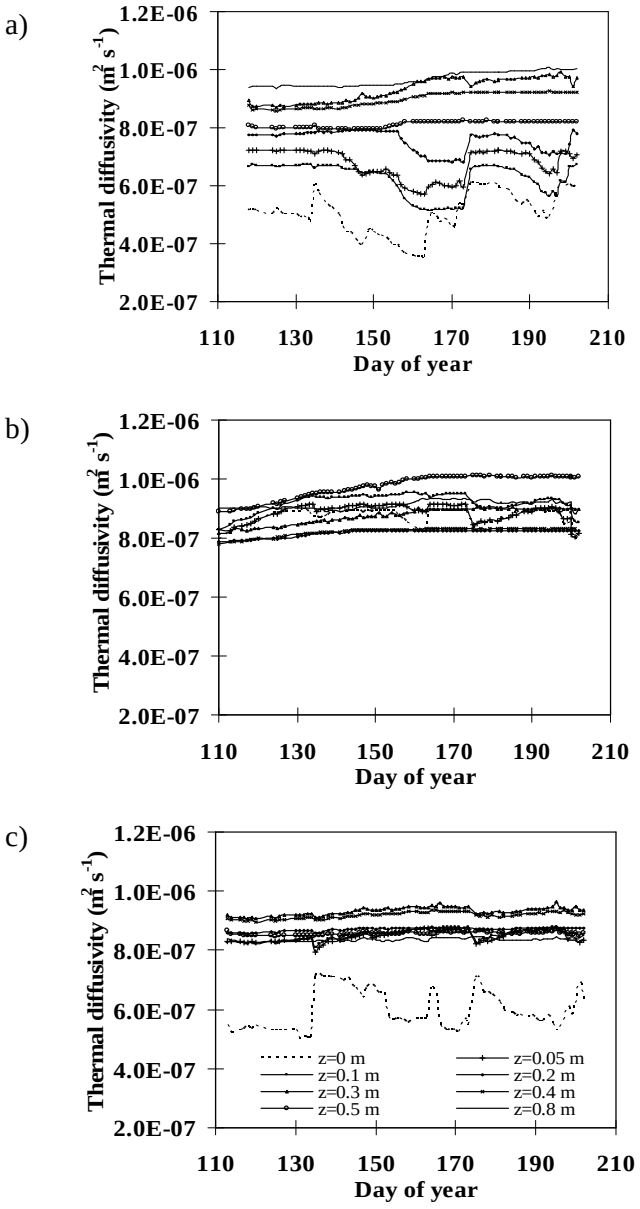

Rys. 34. Soil thermal diffusivity as a function of time for different depths (a - spring barley, b - rye, c - bare soil) during growing season.

Table 3. Summary statistics for water content, thermal conductivity, heat capacity and thermal diffusivity of spring barley.

Depth (m)	0	0.5	0.1	0.2	0.3	0.4	0.5	0.8	Whole profile
					Water content (m^3 m^{-3})				
Mean	0.195	0.21	0.219	0.199	0.258	0.229	0.232	0.214	0.219
Minimum	0.108	0.14	0.149	0.142	0.204	0.19	0.189	0.167	0.108
Maximum	0.343	0.325	0.31	0.272	0.318	0.278	0.278	0.249	0.343
Std.Dev.	0.054	0.049	0.047	0.043	0.036	0.031	0.033	0.027	0.045
Coef.Var(%)	27.8	23.1	21.4	21.7	13.9	13.7	14.4	12.5	20.5
Skewness	0.612	0.276	-0.009	0.305	0.283	0.211	0.150	-0.294	0.021
Kurtosis	2.969	1.823	1.798	1.685	1.435	1.310	1.208	1.441	2.362
					Thermal conductivity (W m^{-1} K^{-1})				
Mean	0.771	1.185	1.086	1.340	2.111	1.840	1.603	1.995	1.491
Minimum	0.361	0.644	0.691	0.960	2.034	1.743	1.416	1.888	0.361
Maximum	1.355	1.583	1.404	1.626	2.191	1.942	1.721	2.070	2.191
Std.Dev.	0.268	0.250	0.242	0.225	0.052	0.081	0.089	0.066	0.479
Coef.Var(%)	34.8	21.1	22.3	16.8	2.5	4.4	5.6	3.3	32.1
Skewness	0.253	-0.273	-0.403	-0.216	0.030	0.038	0.119	-0.374	-0.401
Kurtosis	2.364	1.875	1.839	1.782	1.467	1.247	1.327	1.579	2.145
					Heat capacity × 10^6 (J m^{-3} K^{-1})				
Mean	1.683	1.852	1.841	1.865	2.309	2.107	2.033	2.107	1.975
Minimum	1.318	1.559	1.550	1.629	2.083	1.943	1.852	1.912	1.318
Maximum	2.300	2.333	2.223	2.172	2.560	2.311	2.224	2.255	2.560
Std.Dev.	0.227	0.203	0.196	0.181	0.150	0.131	0.140	0.112	0.253
Coef.Var(%)	13.5	11.0	10.6	9.7	6.5	6.2	6.9	5.3	12.8
Skewness	0.612	0.276	-0.009	0.305	0.283	0.211	0.150	-0.295	-0.181
Kurtosis	2.968	1.824	1.798	1.685	1.436	1.311	1.208	1.442	2.546
					Thermal diffusivity × 10^{-7} (m^2 s^{-1})				
Mean	4.454	6.331	5.824	7.135	9.166	8.742	7.892	9.475	7.377
Minimum	2.738	4.129	4.455	5.892	8.561	8.404	7.649	7.177	2.738
Maximum	6.002	7.147	6.623	7.790	9.763	8.997	8.118	9.873	9.873
Std.Dev.	1.011	0.738	0.759	0.593	0.372	0.173	0.126	0.203	1.752
Coef.Var(%)	22.7	11.7	13.0	8.3	4.1	2.0	1.6	2.1	23.8
Skewness	-0.402	-1.043	-0.814	-0.960	-0.315	-0.274	0.035	0.274	-0.604
Kurtosis	2.118	3.472	2.215	2.855	1.435	1.643	1.635	1.447	2.578

Table 4. Summary statistics for water content, thermal conductivity, heat capacity and thermal diffusivity of rye.

Depth (m)	0	0.5	0.1	0.2	0.3	0.4	0.5	0.8	Whole profile
					Water content (m^3 m^{-3})				
Mean	0.215	0.221	0.218	0.221	0.237	0.221	0.209	0.258	0.225
Minimum	0.135	0.156	0.163	0.188	0.190	0.187	0.171	0.236	0.135
Maximum	0.325	0.326	0.322	0.287	0.310	0.300	0.295	0.287	0.326
Std.Dev.	0.044	0.044	0.036	0.032	0.033	0.035	0.038	0.012	0.038
Coef.Var(%)	20.6	19.8	16.6	14.3	13.9	15.8	18.0	4.8	16.9
Skewness	0.470	0.527	0.771	0.789	0.600	0.820	0.865	-0.026	0.292
Kurtosis	2.592	2.260	3.072	2.248	2.072	2.368	2.480	1.885	2.195
					Thermal conductivity (W m^{-1} K^{-1})				
Mean	1.705	1.773	1.863	1.591	1.809	1.598	1.996	2.038	1.797
Minimum	1.368	1.479	1.676	1.423	1.694	1.432	1.914	2.004	1.368
Maximum	1.939	1.973	2.037	1.761	1.955	1.717	2.142	2.087	2.142
Std.Dev.	0.141	0.122	0.085	0.087	0.076	0.093	0.081	0.016	0.181
Coef.Var(%)	8.3	6.9	4.6	5.5	4.2	5.8	4.1	0.8	10.1
Skewness	-0.631	-0.470	-0.049	0.647	0.167	0.519	0.454	-0.321	-0.147
Kurtosis	2.983	2.681	2.445	2.039	1.783	2.085	1.674	4.228	2.041
					Heat capacity × 10^6 (J m^{-3} K^{-1})				
Mean	2.018	2.059	2.077	1.990	2.121	1.992	2.096	2.275	2.078
Minimum	1.684	1.788	1.849	1.851	1.925	1.850	1.938	2.185	1.684
Maximum	2.479	2.499	2.513	2.264	2.427	2.323	2.456	2.398	2.513
Std.Dev.	0.185	0.183	0.151	0.132	0.138	0.146	0.157	0.521	0.171
Coef.Var(%)	9.2	8.9	7.3	6.7	6.5	7.3	7.5	2.3	8.2
Skewness	0.470	0.529	0.771	0.789	0.601	0.821	0.866	-0.027	0.276
Kurtosis	2.594	2.265	3.070	2.247	2.074	2.369	2.481	1.884	2.054
					Thermal diffusivity × 10^{-7} (m^2 s^{-1})				
Mean	8.457	8.627	8.986	8.001	8.542	8.029	9.541	8.958	8.643
Minimum	7.823	7.898	8.107	7.691	8.055	7.652	8.721	8.702	7.652
Maximum	8.838	9.019	9.381	8.160	8.840	8.210	9.879	9.176	9.879
Std.Dev.	0.248	0.269	0.262	0.129	0.215	0.159	0.319	0.147	0.533
Coef.Var(%)	2.9	3.1	2.9	1.6	2.5	2.0	3.3	1.6	6.2
Skewness	-0.615	-0.686	-1.173	-0.839	-0.750	-0.816	-1.176	0.080	0.359
Kurtosis	2.516	2.677	4.236	2.324	2.507	2.411	3.206	1.434	2.477

Table 5. Summary statistics for water content, thermal conductivity, heat capacity and thermal diffusivity of bare soil.

Depth (m)	0	0.5	0.1	0.2	0.3	0.4	0.5	0.8	Whole profile
					Water content (m^3 m^{-3})				
Mean	0.155	0.270	0.254	0.218	0.243	0.264	0.302	0.333	0.255
Minimum	0.111	0.239	0.219	0.197	0.212	0.247	0.289	0.322	0.111
Maximum	0.278	0.332	0.305	0.243	0.267	0.284	0.311	0.345	0.345
Std.Dev.	0.034	0.021	0.023	0.013	0.013	0.010	0.005	0.005	0.053
Coef.Var(%)	22.1	7.7	9.0	6.0	5.2	3.7	1.6	1.6	20.9
Skewness	1.056	0.243	0.189	0.309	0.071	0.332	-0.196	-0.081	-0.631
Kurtosis	3.870	2.415	1.833	1.973	2.299	2.026	2.384	2.481	3.207
					Thermal conductivity (W m^{-1} K^{-1})				
Mean	0.821	1.867	1.817	1.706	2.032	2.095	2.062	2.132	1.816
Minimum	0.239	1.814	1.730	1.642	1.981	2.077	2.056	2.115	0.550
Maximum	0.406	1.954	1.900	1.776	2.059	2.127	2.066	2.162	2.162
Std.Dev.	0.254	0.037	0.045	0.050	0.024	0.017	0.002	0.007	0.413
Coef.Var(%)	30.9	2.0	2.5	2.9	1.2	0.8	0.1	0.3	22.7
Skewness	-1.056	-0.206	-0.084	0.170	-0.599	0.836	-0.168	1.315	-1.943
Kurtosis	3.870	1.840	1.957	1.440	2.025	2.214	2.131	12.955	5.834
					Heat capacity × 10^6 (J m^{-3} K^{-1})				
Mean	1.621	2.254	2.177	2.019	2.221	2.322	2.445	2.589	2.206
Minimum	1.436	2.125	2.030	1.931	2.091	2.251	2.391	2.544	1.436
Maximum	2.134	2.513	2.390	2.124	2.321	2.405	2.483	2.641	2.641
Std.Dev.	0.143	0.872	0.955	0.549	0.524	0.410	0.204	0.220	0.284
Coef.Var(%)	8.8	3.9	4.4	2.7	2.4	1.8	0.8	0.9	12.9
Skewness	1.057	0.243	0.194	0.306	0.066	0.334	-0.200	-0.088	-0.919
Kurtosis	3.869	2.411	1.832	1.973	2.307	2.029	2.385	2.600	3.510
					Thermal diffusivity × 10^{-7} (m^2 s^{-1})				
Mean	4.977	8.292	8.351	8.446	9.148	9.022	8.432	8.235	8.113
Minimum	3.832	7.774	7.951	8.316	8.870	8.844	8.319	8.094	3.832
Maximum	6.993	8.537	8.653	8.603	9.472	9.228	8.597	8.401	9.472
Std.Dev.	1.091	0.164	0.174	0.071	0.124	0.093	0.061	0.061	1.291
Coef.Var(%)	21.9	2.0	2.1	0.8	1.4	1.0	0.7	0.7	15.9
Skewness	0.433	-0.507	-0.136	0.025	-0.405	0.202	0.235	0.189	-2.285
Kurtosis	1.597	2.647	2.138	2.351	2.908	2.106	2.423	2.900	7.361

The time runs of soil moisture, thermal conductivity, capacity and diffusivity in the plots with barley and rye and in the bare plot are presented in Fig. 31, 32, 33, 34. The dynamics of particular variables was related to the stage of plant development in the plots under study. Rye, which was already well grown and had time to consume most of the water available in the soil, caused a continual decrease in the soil moisture. In turn, the condition of the plants did not permit the soil to be re-supplied with water from precipitation, as only the surface horizon of the soil increased its moisture content slightly after a rainfall. Barley, which during the period of the experiment went through all of its development stages, shows in the soil moisture distribution both the amount of water used for plant growth and the amount of water that reached the soil surface. The bare field was characterized by the most uniform distribution of moisture in the soil profile. The surface horizon of the fallow plot was characterized by the strongest dynamics and effect of precipitation on soil moisture.

The thermal properties of the soil (Fig. 32, 33, 34) reflected primarily the moisture status of the soil (Fig. 31), and to a lesser extent – the soil compaction condition (Fig. 30b). The time runs of the heat capacity of the soil conformed with the soil moisture runs. Slightly less similar to the moisture runs were the time runs of the thermal conductivity. In the case of the thermal diffusivity they were distinctly different from the moisture runs. In some of the diffusivity runs a certain reflection of the moisture runs could be noticed, but in most of them the diffusivity increased with a reduction in the soil moisture content (Fig 34). This type of time runs indicates that with a certain soil density the thermal diffusivity of the soil was already beyond its maximum, and a decrease in the soil moisture resulted in a diffusivity shift towards its maximum.

The mean values of soil moisture within the whole profile were similar in the plots with plants, and somewhat different in the bare plot. The plots with plants had relatively uniform moisture distributions within the profile; the bare plot was characterized by a considerable drop in soil moisture values in the surface horizon, below which the values were more homogeneous.

The mean values of soil density in the rye plot and in the fallow were almost the same; in the barley plot the mean soil density was lower than in the fallow. The mean values of the thermal properties in the soil profile did reflect the water content in the soil, but in the case of thermal conductivity and diffusivity the barley plot had values somewhat lower than the rye plot, even though the soil moisture of the barley plot was higher, but in this case the conductivity and diffusivity were also significantly affected by the soil density which was higher in

the rye plot. The heat capacity of the soil conformed to the soil moisture distribution in the plots.

Standard deviation was used as a measure of the scatter of soil moisture values. The greatest scatter was observed in the plots with plant canopy, the smallest in the bare plot. Coefficients of variability calculated for the whole profile in particular plots were the highest for the moisture in the rye plot and for the thermal properties in the barley plot. The lowest variability was observed in the case of moisture in the bare plot and the thermal properties in the rye plot. Analyzing the soil profiles, the greatest variability was observed for the moisture and thermal properties in the barley plot, and the smallest variability within the profile for moisture, heat capacity, and thermal conductivity and diffusivity of soil for horizons below 0.1 m was observed in the bare plot. In the case of thermal conductivity and diffusivity of soil in the 0-0.1 m the lowest values were observed in the rye plot.

Statistics characterizing the soil moisture distributions – histograms (asymmetry and kurtosis) indicate mainly a slight right-hand asymmetry and a somewhat smaller than normal distribution concentration of soil moisture values around its mean value (normal distribution - asymmetry equal 0, kurtosis equal 3). Distribution of the heat capacity of the soil were similar to those of soil moisture. Thermal conductivity and diffusivity of the soil showed a largely left-hand asymmetry in the distribution of values and somewhat smaller than normal distribution concentration of values of those thermal properties of the soil around their mean values.

5.3. Results of correlation analysis

Calculations of linear correlation of the soil features under consideration were performed at the significance level of $p<0,05$, and the results of the calculations are presented in Table 6, 7, 8 (statistically significant correlations are highlighted with bold type). Three objects were considered – two with plant cover and one bare. Correlations were calculated for the soil moisture, thermal conductivity, heat capacity, and thermal diffusivity. The results of the correlation analysis indicate that the presence of plants affected both the values of the correlations and their significance at a given depth. In a significant majority of cases, high and significant coefficients of correlation were obtained for the particular thermal and moisture properties of the soil between the particular horizons. The lowest number of significant correlations was observed in the rye plot, the highest in the barley plot. In the barley plot, between the soil surface and horizons below

z=0.2 m, and in the fallow plot only in the surface horizon of down to z=0.1 m, significant negative correlations were observed – in the barley plot for all the features under consideration, and in the fallow plot for the thermal diffusivity. In the other cases the correlations were positive. Lack of correlation between the surface of the soil z=0 m and the horizon of z=0.2 m, and between the horizon of z=0.05 m and below z=0.4 m was observed in the barley plot, though for the thermal diffusivity in that plot lack of correlation was observed only in two cases. The rye plot was characterized by a lack of correlation between the levels of z=0, z=0.05m and below z=0.2 m, the situation being varied for the particular thermal properties and moisture of the soil. Thermal conductivity in this object had the highest number of no correlation. The bare plot showed no significant correlation for all the variables under consideration only between the surface of the soil, z=0 m, and the level below z=0.2 m.

5.4. Analysis of soil moisture semivariograms

The temporal-spatial variability of soil moisture and thermal properties of soil was also studied with the help of semivariograms. The nugget values, sills and ranges of temporal autocorrelation were determined, semivariogram models were fitted to the empirical values, and model fitting parameters were determined (Table 9, 10, 11). The quality of fitting of the theoretical semivariogram models to the empirical data was defined by means of the determination coefficient R^2 and residual squares sum RSS of the model values and the empirical values of the semivariogram. High values of the determination coefficient and low RSS values (in most cases $R^2 > 0.9$, $RSS < 10^{-6}$) indicate a very high quality of theoretical models fitting to the empirical values of the semivariograms.

Temporal autocorrelation was noted for all the features studied in the soil profile. The form of the temporal autocorrelation in the arable horizon was spherical in all the plots, and below the arable horizon changed to the Gaussian in the plots with plants and to exponential in the bare plot. The highest values of the temporal autocorrelation range were observed for the rye plot below the arable horizon (210 days), and the lowest in the surface horizon of the rye plot (9.5 days for diffusivity), the barley plot and the bare plot (17.4 and 18.1 days, respectively). The results indicate that the shortest “memory” in terms of the event (cause) resulting in changes in the distribution of soil moisture or thermal property is most often displayed by the surface horizon of the soil, with its non-stabilized structure (loose soil). The deeper horizons, where the processes of mass exchange occur more slowly and where soil density does not change much within

the period under study, the causes of changes in the soil moisture are „visible" for a longer period of time, approximately half a year. The rye plot, in which the soil density in the surface horizon was the highest, was characterized by an over a month-and-a-half radius of autocorrelation in the arable horizon.

5.5. Analysis of the fractal dimension of soil moisture

Fractal dimensions calculated on the basis of smovariograms, and parameters of line fitting to the empirical data of semivariance in the logarithmic system of coordinates, are presented in Fig. 35 and in Tables 9, 10, 11. In a clear majority of cases the standard fitting error was below 0.1, while the determination coefficient R^2 was above 0.9, the *n* number being the population of data for which the standard fitting error and the determination coefficient were calculated. These values indicate that the obtained results of line slope indexes provide a good indicator of semivariance change direction in the objects under study, and thus permit satisfactory determination of the fractal dimensions.

The course of the fractal dimension of the thermal properties of soil was similar to that for the soil moisture. Slight differences in the form of the courses for the thermal properties may have resulted from the distribution of soil density in the soil profile. High values of the fractal dimensions of soil moisture and thermal properties in the surface horizon of the soil indicate a high level of randomness in their distribution. Such a situation in the distribution of soil moisture and thermal properties is observed in the fallow throughout the soil profile. A clear decrease in the fractal dimension values with increasing depth, however, was observed in the plots with plant cover. The decrease can be interpreted in terms of determination of the soil moisture distribution in time by an external factor. In this the external factor was the plant. It is also possible to interpret the decrease in another way, saying that the plants caused a decrease in the randomness of the soil moisture distribution in those plots.

Table 6. Correlation coefficients between the variables measured at the eighth depths (a - spring barley). The correlation coefficients are significant (bold type) at $p < 0.05$, N=75.

Water content	z=0 m	z=0.05 m	z=0.1 m	z=0.2 m	z=0.3 m	z=0.4 m	z=0.5 m	z=0.8 m
z=0 m	1.00	**0.79**	**0.47**	-0.01	**-0.27**	**-0.42**	**-0.44**	**-0.57**
z=0.05 m	**0.79**	1.00	**0.89**	**0.55**	**0.30**	0.14	0.10	-0.06
z=0.1 m	**0.47**	**0.89**	1.00	**0.84**	**0.66**	**0.53**	**0.50**	**0.33**
z=0.2 m	-0.01	**0.55**	**0.84**	1.00	**0.95**	**0.88**	**0.85**	**0.73**
z=0.3 m	**-0.27**	**0.30**	**0.66**	**0.95**	1.00	**0.97**	**0.95**	**0.89**
z=0.4 m	**-0.42**	0.14	**0.53**	**0.88**	**0.97**	1.00	**0.96**	**0.94**
z=0.5 m	**-0.44**	0.10	**0.50**	**0.85**	**0.95**	**0.96**	1.00	**0.92**
z=0.8 m	**-0.57**	-0.06	**0.33**	**0.73**	**0.89**	**0.94**	**0.92**	1.00

Thermal conductivity	z=0 m	z=0.05 m	z=0.1 m	z=0.2 m	z=0.3 m	z=0.4 m	z=0.5 m	z=0.8 m
z=0 m	1.00	**0.76**	**0.46**	-0.01	**-0.29**	**-0.48**	**-0.45**	**-0.58**
z=0.05 m	**0.76**	1.00	**0.90**	**0.60**	**0.33**	0.12	0.14	-0.07
z=0.1 m	**0.46**	**0.90**	1.00	**0.84**	**0.65**	**0.46**	**0.51**	**0.27**
z=0.2 m	-0.01	**0.60**	**0.84**	1.00	**0.94**	**0.84**	**0.84**	**0.68**
z=0.3 m	**-0.29**	**0.33**	**0.65**	**0.94**	1.00	**0.96**	**0.96**	**0.88**
z=0.4 m	**-0.48**	0.12	**0.46**	**0.84**	**0.96**	1.00	**0.97**	**0.94**
z=0.5 m	**-0.45**	0.14	**0.51**	**0.84**	**0.96**	**0.97**	1.00	**0.91**
z=0.8 m	**-0.58**	-0.07	**0.27**	**0.68**	**0.88**	**0.94**	**0.91**	1.00

Heat capacity	z=0 m	z=0.05 m	z=0.1 m	z=0.2 m	z=0.3 m	z=0.4 m	z=0.5 m	z=0.8 m
z=0 m	1.00	**0.79**	**0.47**	-0.01	**-0.27**	**-0.42**	**-0.44**	**-0.57**
z=0.05 m	**0.79**	1.00	**0.89**	**0.55**	**0.30**	0.14	0.10	-0.06
z=0.1 m	**0.47**	**0.89**	1.00	**0.84**	**0.66**	**0.53**	**0.50**	**0.33**
z=0.2 m	-0.01	**0.55**	**0.84**	1.00	**0.95**	**0.88**	**0.85**	**0.73**
z=0.3 m	**-0.27**	**0.30**	**0.66**	**0.95**	1.00	**0.97**	**0.95**	**0.89**
z=0.4 m	**-0.42**	0.14	**0.53**	**0.88**	**0.97**	1.00	**0.96**	**0.94**
z=0.5 m	**-0.44**	0.10	**0.50**	**0.85**	**0.95**	**0.96**	1.00	**0.92**
z=0.8 m	**-0.57**	-0.06	**0.33**	**0.73**	**0.89**	**0.94**	**0.92**	1.00

Continuation - Table 6

Thermal diffusivity	z=0 m	z=0.05 m	z=0.1 m	z=0.2 m	z=0.3 m	z=0.4 m	z=0.5 m	z=0.8 m
z=0 m	1.00	**0.68**	**0.41**	0.06	**0.24**	**-0.37**	**-0.41**	**-0.55**
z=0.05 m	**0.68**	1.00	**0.89**	**0.63**	**-0.38**	**0.25**	**0.24**	0.00
z=0.1 m	**0.41**	**0.89**	1.00	**0.90**	**-0.59**	**0.46**	**0.52**	**0.27**
z=0.2 m	0.06	**0.63**	**0.90**	1.00	**-0.72**	**0.62**	**0.72**	**0.52**
z=0.3 m	**0.24**	**-0.38**	**-0.59**	**-0.72**	1.00	**-0.98**	**-0.95**	**-0.89**
z=0.4 m	**-0.37**	**0.25**	**0.46**	**0.62**	**-0.98**	1.00	**0.96**	**0.94**
z=0.5 m	**-0.41**	**0.24**	**0.52**	**0.72**	**-0.95**	**0.96**	1.00	**0.92**
z=0.8 m	**-0.55**	0.00	**0.27**	**0.52**	**-0.89**	**0.94**	**0.92**	1.00

Table 7. Correlation coefficients between the variables measured at the eighth depths (Rye). The correlation coefficients are significant (bold type) at $p < 0.05$, N=81.

Water content	z=0 m	z=0.05 m	z=0.1 m	z=0.2 m	z=0.3 m	z=0.4 m	z=0.5 m	z=0.8 m
z=0 m	1.00	**0.97**	**0.90**	0.20	0.14	**0.22**	**0.22**	**0.25**
z=0.05 m	**0.97**	1.00	**0.94**	0.20	0.12	0.22	0.22	**0.25**
z=0.1 m	**0.90**	**0.94**	1.00	0.40	**0.32**	**0.41**	**0.41**	**0.32**
z=0.2 m	0.20	0.20	**0.40**	1.00	**0.98**	**1.00**	**0.99**	**0.70**
z=0.3 m	0.14	0.12	**0.32**	**0.98**	1.00	**0.99**	**0.98**	**0.70**
z=0.4 m	**0.22**	0.22	**0.41**	**1.00**	**0.99**	1.00	**0.99**	**0.71**
z=0.5 m	**0.22**	0.22	**0.41**	**0.99**	**0.98**	**0.99**	1.00	**0.70**
z=0.8 m	**0.25**	**0.25**	**0.32**	**0.70**	**0.70**	**0.71**	**0.70**	1.00

Thermal conductivity	z=0 m	z=0.05 m	z=0.1 m	z=0.2 m	z=0.3 m	z=0.4 m	z=0.5 m	z=0.8 m
z=0 m	1.00	**0.95**	**0.88**	0.15	0.05	0.16	0.13	**0.26**
z=0.05 m	**0.95**	1.00	**0.96**	0.18	0.05	0.18	0.15	**0.30**
z=0.1 m	**0.88**	**0.96**	1.00	**0.31**	0.18	**0.30**	**0.28**	**0.34**
z=0.2 m	0.15	0.18	**0.31**	1.00	**0.96**	**0.99**	**0.99**	**0.74**
z=0.3 m	0.05	0.05	0.18	**0.96**	1.00	**0.97**	**0.97**	**0.71**
z=0.4 m	0.16	0.18	**0.30**	**0.99**	**0.97**	1.00	**0.99**	**0.76**
z=0.5 m	0.13	0.15	**0.28**	**0.99**	**0.97**	**0.99**	1.00	**0.75**
z=0.8 m	**0.26**	**0.30**	**0.34**	**0.74**	**0.71**	**0.76**	**0.75**	1.00

Continuation - Table 7

Heat capacity	z=0 m	z=0.05 m	z=0.1 m	z=0.2 m	z=0.3 m	z=0.4 m	z=0.5 m	z=0.8 m
z=0 m	1.00	**0.97**	**0.90**	0.20	0.14	**0.22**	**0.22**	**0.25**
z=0.05 m	**0.97**	1.00	**0.94**	0.20	0.12	0.22	0.22	**0.26**
z=0.1 m	**0.90**	**0.94**	1.00	**0.40**	**0.32**	**0.41**	**0.41**	**0.32**
z=0.2 m	0.20	0.20	**0.40**	1.00	**0.98**	**1.00**	**0.99**	**0.70**
z=0.3 m	0.14	0.12	**0.32**	**0.98**	1.00	**0.99**	**0.98**	**0.70**
z=0.4 m	**0.22**	0.22	**0.41**	**1.00**	**0.99**	1.00	**0.99**	**0.71**
z=0.5 m	**0.22**	0.22	**0.41**	**0.99**	**0.98**	**0.99**	1.00	**0.70**
z=0.8 m	**0.25**	**0.26**	**0.32**	**0.70**	**0.70**	**0.71**	**0.70**	1.00

Thermal diffusivity	z=0 m	z=0.05 m	z=0.1 m	z=0.2 m	z=0.3 m	z=0.4 m	z=0.5 m	z=0.8 m
z=0 m	1.00	**0.85**	**0.68**	**0.26**	0.11	**0.30**	0.15	0.08
z=0.05 m	**0.85**	1.00	**0.90**	**0.35**	0.13	**0.37**	0.20	0.14
z=0.1 m	**0.68**	**0.90**	1.00	**0.61**	**0.40**	**0.63**	**0.47**	**0.29**
z=0.2 m	**0.26**	**0.35**	**0.61**	1.00	**0.92**	**0.99**	**0.95**	**0.49**
z=0.3 m	0.11	0.13	**0.40**	**0.92**	1.00	**0.93**	**0.99**	**0.69**
z=0.4 m	**0.30**	**0.37**	**0.63**	**0.99**	**0.93**	1.00	**0.95**	**0.50**
z=0.5 m	0.15	0.20	**0.47**	**0.95**	**0.99**	**0.95**	1.00	**0.67**
z=0.8 m	0.08	0.14	**0.29**	**0.49**	**0.69**	**0.50**	**0.67**	1.00

Table 8. Correlation coefficients between the variables measured at the eighth depths (Bare soil). The correlation coefficients are significant (bold type) at $p < 0.05$, N=79.

Water content	z=0 m	z=0.05 m	z=0.1 m	z=0.2 m	z=0.3 m	z=0.4 m	z=0.5 m	z=0.8 m
z=0 m	1.00	**0.49**	**0.31**	0.15	0.17	0.14	0.02	-0.13
z=0.05 m	**0.49**	1.00	**0.95**	**0.85**	**0.83**	**0.83**	**0.50**	**0.38**
z=0.1 m	**0.31**	**0.95**	1.00	**0.94**	**0.92**	**0.92**	**0.59**	**0.52**
z=0.2 m	0.15	**0.85**	**0.94**	1.00	**0.96**	**0.99**	**0.74**	**0.66**
z=0.3 m	0.17	**0.83**	**0.92**	**0.96**	1.00	**0.96**	**0.70**	**0.61**
z=0.4 m	0.14	**0.83**	**0.92**	**0.99**	**0.96**	1.00	**0.74**	**0.66**
z=0.5 m	0.02	**0.50**	**0.59**	**0.74**	**0.70**	**0.74**	1.00	**0.88**
z=0.8 m	-0.13	**0.38**	**0.52**	**0.66**	**0.61**	**0.66**	**0.88**	1.00

Continuation - Table 8

Thermal conductivity	z=0 m	z=0.05 m	z=0.1 m	z=0.2 m	z=0.3 m	z=0.4 m	z=0.5 m	z=0.8 m
z=0 m	1.00	**0.46**	**0.31**	0.17	0.17	0.13	-0.01	-0.15
z=0.05 m	**0.46**	1.00	**0.95**	**0.85**	**0.82**	**0.82**	**0.49**	**0.38**
z=0.1 m	**0.31**	**0.95**	1.00	**0.94**	**0.90**	**0.91**	**0.58**	**0.51**
z=0.2 m	0.17	**0.85**	**0.94**	1.00	**0.96**	**0.98**	**0.73**	**0.64**
z=0.3 m	0.17	**0.82**	**0.90**	**0.96**	1.00	**0.95**	**0.69**	**0.61**
z=0.4 m	0.13	**0.82**	**0.91**	**0.98**	**0.95**	1.00	**0.74**	**0.65**
z=0.5 m	-0.01	**0.49**	**0.58**	**0.73**	**0.69**	**0.74**	1.00	**0.87**
z=0.8 m	-0.15	**0.38**	**0.51**	**0.64**	**0.61**	**0.65**	**0.87**	1.00

Heat capacity	z=0 m	z=0.05 m	z=0.1 m	z=0.2 m	z=0.3 m	z=0.4 m	z=0.5 m	z=0.8 m
z=0 m	1.00	**0.49**	**0.31**	0.15	0.17	0.14	0.02	-0.13
z=0.05 m	**0.49**	1.00	**0.95**	**0.85**	**0.83**	**0.83**	**0.50**	**0.38**
z=0.1 m	**0.31**	**0.95**	1.00	**0.94**	**0.92**	**0.92**	**0.59**	**0.52**
z=0.2 m	0.15	**0.85**	**0.94**	1.00	**0.96**	**0.99**	**0.74**	**0.66**
z=0.3 m	0.17	**0.83**	**0.92**	**0.96**	1.00	**0.96**	**0.70**	**0.61**
z=0.4 m	0.14	**0.83**	**0.92**	**0.99**	**0.96**	1.00	**0.75**	**0.66**
z=0.5 m	0.02	**0.50**	**0.59**	**0.74**	**0.70**	**0.75**	1.00	**0.88**
z=0.8 m	-0.13	**0.38**	**0.52**	**0.66**	**0.61**	**0.66**	**0.88**	1.00

Thermal diffusivity	z=0 m	z=0.05 m	z=0.1 m	z=0.2 m	z=0.3 m	z=0.4 m	z=0.5 m	z=0.8 m
z=0 m	1.00	**-0.40**	**-0.23**	0.06	-0.08	-0.07	0.05	0.18
z=0.05 m	**-0.40**	1.00	**0.95**	**0.78**	**0.83**	**0.83**	**0.50**	**0.38**
z=0.1 m	**-0.23**	**0.95**	1.00	**0.89**	**0.92**	**0.92**	**0.59**	**0.52**
z=0.2 m	0.06	**0.78**	**0.89**	1.00	**0.92**	**0.94**	**0.69**	**0.66**
z=0.3 m	-0.08	**0.83**	**0.92**	**0.92**	1.00	**0.96**	**0.69**	**0.61**
z=0.4 m	-0.07	**0.83**	**0.92**	**0.94**	**0.96**	1.00	**0.74**	**0.66**
z=0.5 m	0.05	**0.50**	**0.59**	**0.69**	**0.69**	**0.74**	1.00	**0.88**
z=0.8 m	0.18	**0.38**	**0.52**	**0.66**	**0.61**	**0.66**	**0.88**	1.00

Table 9. Fractal summary statistics and semivariogram parameters for water content, thermal conductivity, heat capacity and thermal diffusivity of spring barley.

Depth (m)	0	0.05	0.1	0.2	0.3	0.4	0.5	0.8
				Water content				
SE	0.079	0.103	0.062	0.016	0.019	0.014	0.021	0.016
R^2	0.94	0.913	0.964	0.991	0.987	0.991	0.985	0.989
n	29	24	24	79	66	66	66	66
Model	Sph	Sph	Sph	Lin	Gauss	Gauss	Gauss	Gauss
Nugget Co	3.34E-4	1.00E-6	1.00E-6	1.00E-6	4.00E-5	1.00E-5	2.00E-5	1.00E-6
Sill Co +C	3.31E-3	2.67E-3	2.42E-3	5.36E-3	4.66E-3	3.34E-3	2.60E-3	2.54E-3
Range	23.4	17.5	21.7	79	90	85	65	90
R^2	0.944	0.995	0.996	0.977	0.998	0.996	0.976	0.995
RSS	1.46E-6	8.19E-8	1.07E-7	4.65E-6	3.66E-7	2.86E-7	1.50E-6	2.43E-7
				Thermal conductivity				
SE	0.063	0.077	0.071	0.039	0.021	0.015	0.02	0.017
R^2	0.961	0.945	0.95	0.962	0.984	0.99	0.987	0.988
n	29	24	24	66	66	66	66	66
Model	Exp	Sph	Sph	Exp	Gauss	Gauss	Gauss	Gauss
Nugget Co	8.00E-4	1.00E-4	1.00E-4	0.0001	9.00E-5	1.00E-5	1.40E-4	1.00E-5
Sill Co +C	8.87E-2	6.25E-2	5.80E-2	8.24E-2	7.87E-3	1.39E-2	1.92E-2	1.23E-2
Range	48.3	22.5	22.1	112	95	80	65	93
R^2	0.979	0.996	0.993	0.982	0.997	0.994	0.979	0.996
RSS	2.44E-4	4.31E-5	1.25E-4	5.33E-4	1.19E-6	8.47E-6	5.92E-5	3.39E-6
				Heat capacity				
SE	0.08	0.105	0.062	0.016	0.019	0.014	0.02	0.018
R^2	0.939	0.911	0.964	0.99	0.986	0.991	0.985	0.986
n	29	24	24	79	66	66	66	66
Model	Exp	Sph	Sph	Lin	Gauss	Gauss	Gauss	Gauss
Nugget Co $\times 10^{12}$	1.00E-4	0.0001	1.00E-4	0.00E+0	7.00E-4	1.00E-4	3.00E-4	1.00E-4
Sill Co +C $\times 10^{12}$	6.74E-2	4.64E-2	4.24E-2	9.34E-2	8.12E-2	0.059	4.59E-2	4.49E-2
Range	36	17.4	21.7	79	90	85.4	62	89
R^2	0.97	0.995	0.996	0.975	0.998	0.996	0.979	0.995
RSS	2.41E-4	2.61E-5	3.58E-5	1.52E-3	9.56E-5	8.47E-5	3.35E-4	6.51E-5
				Thermal diffusivity				
SE	0.042	0.037	0.073	0.05	0.018	0.014	0.029	0.017
R^2	0.975	0.985	0.943	0.978	0.987	0.991	0.975	0.986
n	39	24	24	19	66	66	66	66
Model	Sph	Sph	Sph	Sph	Gauss	Gauss	Gauss	Gauss
Nugget Co $\times 10^{-14}$	0.032	0.001	0.001	0.000	0.004	0.0001	1.10E-3	1.00E-4
Sill Co +C $\times 10^{-14}$	0.888	0.497	0.485	1.67E-1	0.566	0.1962	2.81E-2	1.95E-1
Range	34.5	38.3	22.5	16.5	90	85	53	82
R^2	0.989	0.991	0.985	0.763	0.998	0.998	0.962	0.994
RSS	3.00E-2	4.59E-3	1.75E-2	3.29E-2	2.93E-3	6.86E-4	2.33E-4	1.64E-3

R^2 – determination coefficient, RSS – residual squares sum of model values and empirical data, N – data population, Sph – spherical, Exp – exponential, Lin – linear

Table 10. Fractal summary statistics and semivariogram parameters for water content, thermal conductivity, heat capacity and thermal diffusivity of rye.

Depth (m)	0	0.05	0.1	0.2	0.3	0.4	0.5	0.8
				Water content				
SE	0.093	0.101	0.078	0.044	0.046	0.019	0.011	0.039
R^2	0.854	0.841	0.889	0.917	0.917	0.98	0.993	0.967
n	60	55	57	80	80	80	80	59
Model	Sph	Sph	Sph	Gauss	Gauss	Gauss	Gauss	Sph
Nugget Co	4.08E-4	3.32E-4	1.50E-5	3.00E-5	1.00E-5	2.00E-5	2.00E-5	8.00E-7
Sill Co +C	2.87E-3	3.15E-3	2.22E-3	6.83E-3	6.95E-3	8.82E-3	1.13E-2	2.49E-3
Range	47.3	52.7	53.5	155	145	160	170	47.1
R^2	0.848	0.954	0.981	0.996	0.997	0.994	0.993	0.98
RSS	6.68E-6	2.12E-6	5.44E-7	4.94E-7	5.53E-7	1.04E-6	1.56E-6	7.16E-9
				Thermal conductivity				
SE	0.065	0.065	0.058	0.049	0.069	0.023	0.016	0.041
R^2	0.932	0.924	0.934	0.902	0.872	0.974	0.987	0.964
n	50	55	57	80	80	80	80	59
Model	Sph	Sph	Sph	Gauss	Gauss	Gauss	Gauss	Sph
Nugget Co	4.30E-3	9.00E-4	1.00E-5	1.00E-4	1.00E-5	1.00E-4	1.00E-5	1.00E-6
Sill Co +C	2.77E-2	1.79E-2	9.72E-3	3.33E-2	1.87E-2	3.95E-2	2.38E-2	4.62E-4
Range	44	40.5	44	116	116	118	123	45.7
R^2	0.882	0.955	0.964	0.997	0.994	0.996	0.996	0.979
RSS	3.87E-4	7.57E-5	2.07E-5	1.74E-5	1.03E-5	2.81E-5	8.85E-6	2.63E-8
				Heat capacity				
SE	0.077	0.101	0.079	0.043	0.044	0.024	0.009	0.038
R^2	0.902	0.842	0.89	0.92	0.922	0.97	0.995	0.97
n	55	55	55	80	80	80	80	59
Model	Sph	Sph	Sph	Gauss	Gauss	Gauss	Gauss	Sph
Nugget Co $\times 10^{12}$	7.60E-3	5.80E-3	3.00E-4	5.00E-4	1.00E-4	4.00E-4	1.00E-4	4.00E-5
Sill Co +C $\times 10^{12}$	5.49E-2	5.54E-2	3.87E-2	1.19E-1	1.27E-1	1.54E-1	1.72E-1	4.48E-3
Range	54.5	53	53.7	155	150	160	154	49
R^2	0.929	0.954	0.981	0.996	0.997	0.994	0.991	0.981
RSS	9.30E-4	6.46E-4	1.65E-4	1.48E-4	1.33E-4	3.06E-4	6.31E-4	2.13E-6
				Thermal diffusivity				
SE	0.0437	0.162	0.096	0.023	0.025	0.14	0.009	0.04
R^2	0.487	0.693	0.847	0.986	0.97	0.99	0.995	0.967
n	20	55	55	80	80	80	79	59
Model	Sph	Sph	Sph	Gauss	Gauss	Gauss	Gauss	Sph
Nugget Co $\times 10^{-14}$	0.0001	0.0285	0.0067	1.10E-3	0.001	0.0011	1.00E-3	0.00
Sill Co +C $\times 10^{-14}$	0.0682	0.15	0.1574	1.46E-1	0.486	0.2022	1.33	2.91E-2
Range	9.3	81.4	67.9	210	161	205	182	46.7
R^2	0.284	0.858	0.98	0.959	0.996	0.954	0.991	0.98
RSS	2.02E-2	9.05E-3	2.12E-3	8.31E-4	2.41E-3	1.99E-3	2.32E-2	9.79E-5

Table 11. Fractal summary statistics and semivariogram parameters for water content, thermal conductivity, heat capacity and thermal diffusivity of bare soil.

Depth (m)	0	0.05	0.1	0.2	0.3	0.4	0.5	0.8
				Water content				
SE	0.219	0.091	0.042	0.023	0.4	0.28	0.09	0.0116
R^2	0.716	0.851	0.96	0.987	0.962	0.979	0.848	0.781
n	29	70	70	70	70	70	70	70
Model	Sph	Sph	Sph	Sph	Exp	Exp	Lin	Sph
Nugget Co	3.74E-4	1.86E-4	1.33E-4	1.73E-5	1.29E-5	6.00E-7	8.58E-7	1.07E-5
Sill Co +C	1.48E-3	6.06E-4	9.36E-4	3.22E-4	2.77E-4	2.07E-4	4.48E-5	4.08E-5
Range	18.7	60.2	82.3	80.3	96.3	128.1	70	60.1
R^2	0.675	0.765	0.933	0.968	0.921	0.972	0.865	0.738
RSS	1.34E-6	3.54E-7	2.85E-7	1.85E-8	2.57E-8	4.58E-9	1.18E-9	2.06E-9
				Thermal conductivity				
SE	0.187	0.097	0.051	0.037	0.05	0.029	0.094	0.114
R^2	0.769	0.832	0.941	0.967	0.945	0.978	0.838	0.786
n	29	70	70	70	70	70	70	70
Model	Sph	Sph	Sph	Sph	Exp	Exp	Lin	Sph
Nugget Co	1.06E-2	4.57E-4	4.47E-4	2.18E-4	2.50E-5	4.00E-6	9.76E-6	8.81E-6
Sill Co +C	4.93E-2	1.44E-3	2.73E-3	2.17E-3	5.78E-4	3.55E-4	5.01E-5	3.42E-5
Range	18.6	57.8	73.1	66.4	73.5	130.5	70	60.9
R^2	0.75	0.759	0.914	0.949	0.898	0.972	0.854	0.747
RSS	1.17E-3	2.02E-6	3.26E-6	1.38E-6	1.53E-7	1.30E-8	1.58E-9	1.41E-9
				Heat capacity				
SE	0.218	0.092	0.043	0.024	0.039	0.03	0.093	0.144
R^2	0.717	0.847	0.957	0.985	0.965	0.977	0.844	0.702
n	29	70	70	70	70	70	70	70
Model	Sph	Sph	Sph	Sph	Exp	Exp	Lin	Sph
Nugget Co $\times 10^{12}$	6.60E-3	3.20E-3	2.27E-3	3.20E-4	2.70E-4	4.00E-5	1.70E-4	2.23E-4
Sill Co +C $\times 10^{12}$	2.58E-2	1.05E-2	1.67E-2	5.54E-3	5.05E-3	3.61E-3	7.94E-4	7.22E-4
Range	18.8	58.9	84.9	76.2	106.5	126	70	59.9
R^2	0.677	0.759	0.93	0.967	0.926	0.971	0.852	0.655
RSS	4.07E-4	1.10E-4	9.20E-5	5.86E-6	7.39E-6	1.44E-6	3.83E-7	8.50E-7
				Thermal diffusivity				
SE	0.171	0.087	0.038	0.026	0.038	0.028	0.09	0.116
R^2	0.798	0.861	0.967	0.98	0.966	0.98	0.848	0.781
n	29	70	70	70	70	70	70	70
Model	Sph	Sph	Sph	Lin	Exp	Exp	Lin	Sph
Nugget Co $\times 10^{-14}$	0.098	0.0141	0.0082	1.00E-5	0.0014	0.0001	8.58E-4	1.07E-3
Sill Co +C $\times 10^{-14}$	0.551	0.047	0.0661	7.82E-3	0.0346	0.0244	4.48E-3	4.08E-3
Range	18.1	60.9	89	70	109.8	127.8	70	60.1
R^2	0.811	0.774	0.941	0.987	0.927	0.972	0.865	0.738
RSS	1.12E-1	2.07E-3	1.17E-3	5.65E-6	3.42E-4	6.19E-5	1.18E-5	2.06E-5

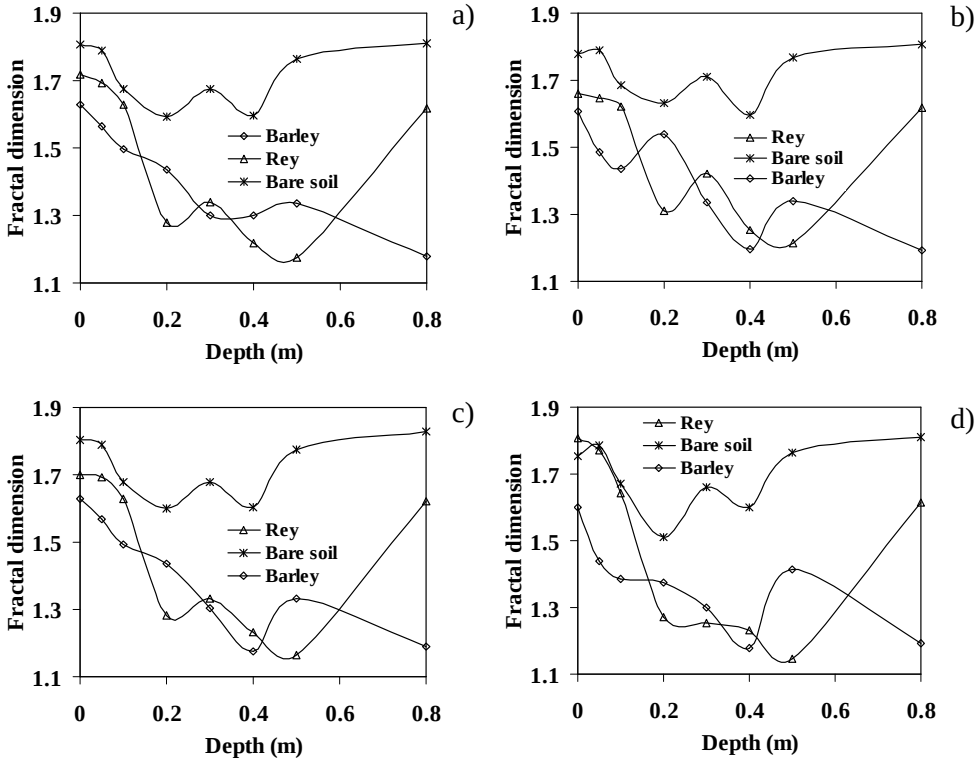

Rys. 35. Fractal dimension as a function of depth a) water content, b) thermal conductivity, c) heat capacity and d) thermal diffusivity for rye, bare soil, and spring barley.

5.6. Results of reciprocal correlation analysis

For the determination of reciprocal correlation, precipitation data and data from soil moisture measurements with the TDR meter were used. The lack of precipitation of a given day was represented in the data set as 0 mm precipitation. Calculations of reciprocal correlation of precipitation and soil moisture at various depths were made for three objects – spring barley, rye, and bare soil, at the level of significance of $p<0.05$. The results of the calculations are presented in Table 12. No significant reciprocal correlation was found between the precipitation and soil moisture in the soil profile for any of the objects studied. The lack of reciprocal correlation could have been the result of the population of data that were used for the study, or of the effect of other factors, e.g. plants, that had a more significant effect on the soil moisture in a given object than that of precipitation. The earlier analysis of correlation (Table 6, 7, 8) partially supports

this observation. Although the correlation analysis indicates a lack of correlation between the variables under consideration, observation of the soil moisture runs in particular objects and of precipitation distribution shows clearly that rainfall has an effect on the soil moisture. The amount of precipitation water that increased the soil moisture depended on the strength of the rainfall, on the hydrological properties of the soil (primarily the soil density), the status of the plant cover, and surface runoff. It can be assumed that the runoff was not overly large and similar in all of the objects studied. Basing on the precipitation distribution and on the soil moisture runs, an attempt was made at finding a temporal and spatial relationship between those variables, employing for the purpose the geostatistical methods which permit time and space to be included in the analysis.

Table 12. Correlation between rainfall and water content for different depths - z.

Rainfall	z=0 m	z=0.05 m	z=0.1 m	z=0.2 m	z=0.3 m	z=0.4 m	z=0.5 m	z=0.8 m
				Barley				
Rainfall 1.00	0.22	0.14	0.01	-0.10	-0.13	-0.18	-0.15	-0.19
				Rye				
Rainfall 1.00	0.04	0.05	-0.04	-0.18	-0.18	-0.18	-0.18	-0.16
				Bare soil				
Rainfall 1.00	0.06	0.04	0.01	-0.09	-0.09	-0.10	-0.13	-0.15

5.7. Results of cross-semivariance analysis

Analysis of semivariance and cross-semivariance of precipitation and soil moisture was performed for the three objects under study. The results of analyses concerned with precipitation and soil moisture at the level of z=0 m for each of the objects under study are shown in figures (Fig. 36, 37, 38); for the other levels the results are presented in tables 13, 14, 15. The tables, apart from the model and cross-semivariogram parameters, provide also statistics of theoretical cross-semivariogram model fitting to empirical data, i.e. determination coefficients R^2 and residual squares sums RSS of the values from the model and the empirical data of the cross-semivariogram. In a majority of cases high values were observed in the case of the determination coefficient, and low values of the RSS. These data indicate good agreement in the fitting of the theoretical models to the empirical data of the corss-semivariograms. In a notable majority of cases, the

fitted cross-semivariogram models were Gaussian models, both in the plots with plants and in the bare plot.

The earlier analyses of autocorrelation using semivariograms showed the existence of a temporal relationship in the soil moisture distribution (Table 9, 10, 11, Fig. 36a). The temporal autocorrelation radii varied with the depth, but were also related to the status of the plant cover on a given object. Precipitation, subjected to semivariance analysis, displayed a total lack of temporal dependence (Fig. 36b). This result indicates the random character of precipitation in time. The calculated cross-semivariance between precipitation and the soil moisture (Fig. 36c, Table 13) indicates the existence of a temporal relationship. The nugget and sill values were positive in the surface horizon of the soil and varied negatively in the deeper layers. In the plot with plants, the change occurred already at z = 0.2 m, and in the bare plot not until z = 0.4 m (Table 13, 14, 15). This difference in the transition from positive to negative values at different depths in the soil profile should be attributed to the influence of plants on the reduction of the amount of rainfall water reaching the soil surface, and to the use of water for plant growth through the root system which is located primarily in the arable horizon of the soil. Positive values of cross-semivariance indicate that the increase in soil moisture is due to rainfall. Negative values show that changes in soil moisture were related to another factor, probably water upflow from lower soil horizons.

a)

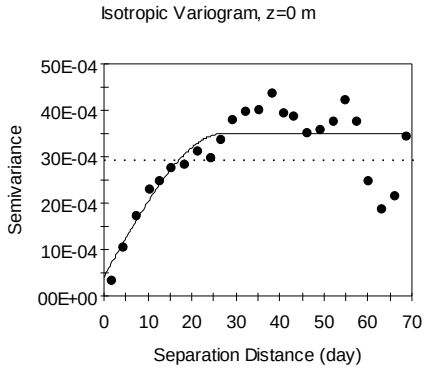

b)

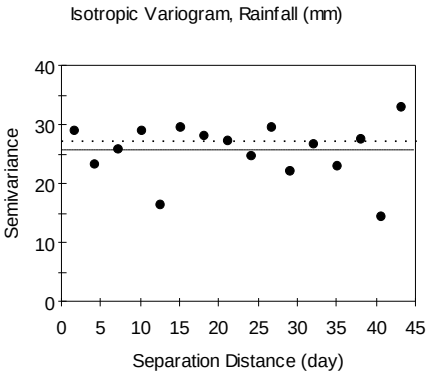

c)

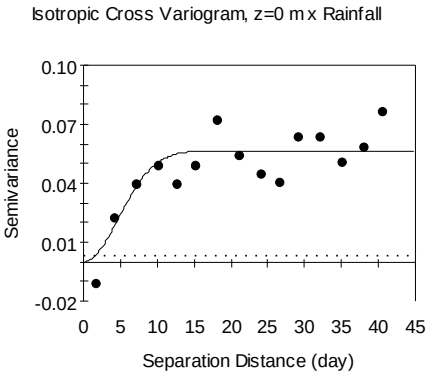

Fig. 36. Semivariograms (a, b), cross-semivariogram (c), and estimated mathematical models of water content and rainfall for spring barley

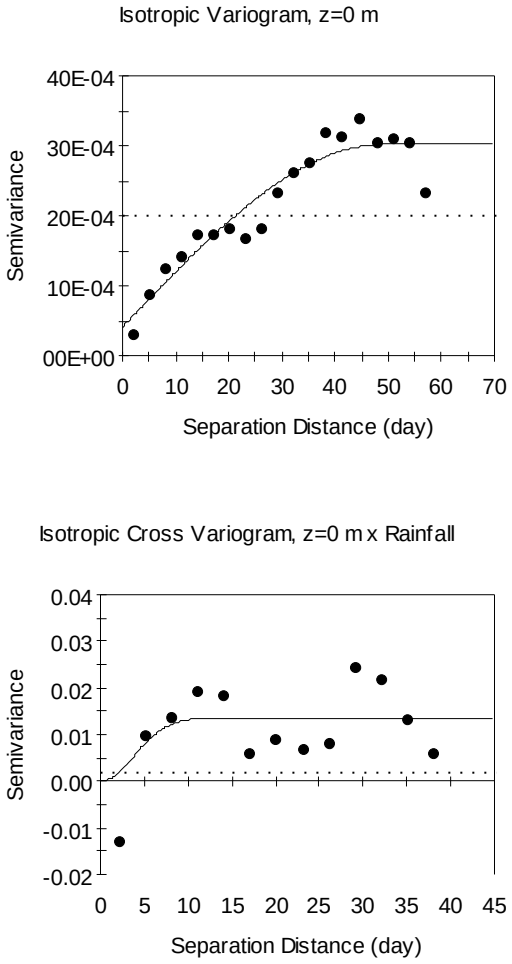

Fig. 37. Semivariogram (a) and cross-semivariogram (b), and estimated mathematical models of water content and rainfall for rye

The ranges of the temporal relationship of cross-semivariance of precipitation and soil moisture were the largest below the arable horizon. Barley showed a correlation radius of from 2 to 6 days in the soil horizon from z=0 m to z=0.1 m and an over 80-day correlation below the level of z=0.1 m. Rye was characterized by an over 5-day correlation on the soil surface, over 30-day at the next level studied, and an 80-100-day radius of correlation at deeper soil horizons. The bare

plot had an approximately 3-day radius of reciprocal correlation in the soil layer from z=0 m to z=0.2 m; below that level it increased to about 20 days, and at the deeper level even exceeded 100 days.

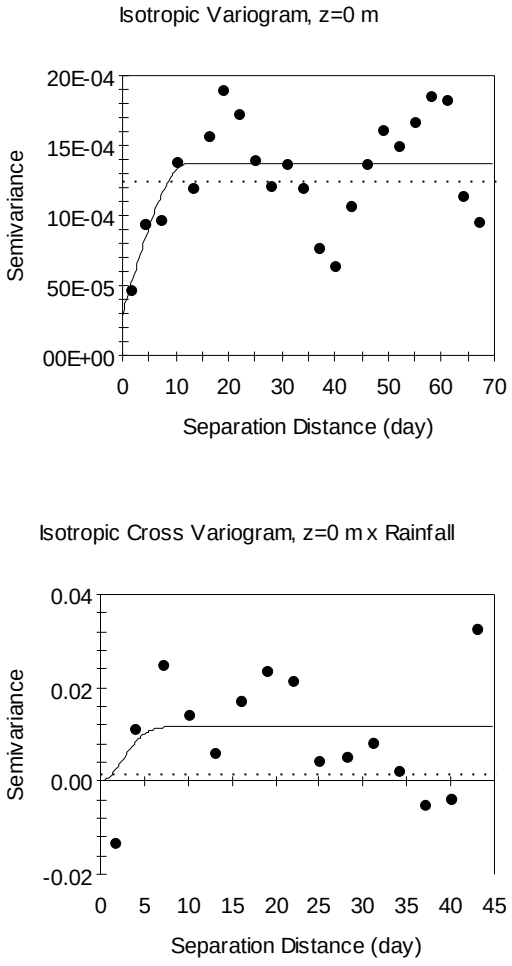

Fig. 38. Semivariogram (a) and cross-semivariogram (b), and estimated mathematical models of water content and rainfall for bare soil

Table 13. Cross-semivariogram parameters for water content and validation statistics of kriging and cokriging method for spring barley.

Barley	Rainfall	z=0 cm	z=0.05 m	z=0.1 m	z=0.2 m	z=0.3 m	z=0.4 m	z=0.5 m	z=0.8 m
Model	Lin	Gauss	Gauss	Gauss	Gauss	Gauss	Gauss	Lin	Gauss
Nugget Co	25.72	0.0001	0.0001	0.00001	-0.0001	-0.0001	-0.0005	-0.0001	-0.0023
Sill Co +C	25.72	0.0566	0.0376	0.00992	-0.137	-0.1674	-0.2108	-0.069	-0.199
Range	43	6.76	3.81	2.2	91	91	89.92	83.9	88.4
R^2	0.005	0.741	0.477	0.024	0.597	0.847	0.868	0.81	0.923
RSS	357	1.68E-3	1.45E-3	2.49E-3	1.17E-3	7.75E-4	3.54E-4	5.38E-4	1.79E-4
Kriging									
Regression coefficient		1.057	0.996	0.994	0.989	1.023	1.01	1.014	1
Intercept		-0.01	0	0	0	-0.01	0	0	0
SE		0.04	0.036	0.028	0.026	0.028	0.016	0.023	0.017
R^2		0.904	0.912	0.947	0.953	0.949	0.982	0.965	0.98
SE Prediction		0.017	0.014	0.011	0.01	0.008	0.004	0.006	0.004
Cokriging									
Regression coefficient		0.99	0.989	0.995	0.966	0.983	0.993	0.996	0.999
Intercept		0	0	0	0	0	0	0	0
SE		0.036	0.036	0.028	0.026	0.025	0.016	0.023	0.016
R^2		0.91	0.911	0.946	0.951	0.955	0.982	0.963	0.982
SE Prediction		0.016	0.015	0.011	0.01	0.008	0.004	0.006	0.004

Table 14. Cross-semivariogram parameters for water content and validation statistics of kriging and cokriging method for rye.

Rye	Rainfall	z=0 cm	z=0.05 m	z=0.1 m	z=0.2 m	z=0.3 m	z=0.4 m	z=0.5 m	z=0.8 m
Model	Lin	Gauss	Gauss	Gauss	Gauss	Gauss	Gauss	Gauss	Gauss
Nugget Co	25.72	0.00001	0.00588	0.0001	-0.0026	0.0001	-0.0019	-0.0044	-0.0025
Sill Co +C	25.72	0.01362	0.02706	0.0343	-0.1813	-0.2	-0.2127	-0.2088	-0.0456
Range	43	5.39	30.2	83.3	101	97	101	99.1	84.3
R^2	0.005	0.506	0.364	0.373	0.748	0.863	0.839	0.81	0.507
RSS	357	6.81E-4	7.54E-4	1.22E-3	5.04E-4	3.67E-4	3.99E-4	4.93E-4	1.60E-4
Kriging									
Regression coefficient		1.109	1.062	1.02	1.006	1.012	1.008	1.008	1.033
Intercept		-0.02	-0.01	0	0	0	0	0	-0.01
SE		0.044	0.023	0.027	0.015	0.023	0.014	0.015	0.059
R^2		0.889	0.923	0.948	0.982	0.96	0.985	0.983	0.795
SE Prediction		0.015	0.011	0.008	0.004	0.007	0.004	0.005	0.006
Cokriging									
Regression coefficient		1.02	992	1.019	0.995	0.977	0.998	0.991	0.935
Intercept		0	0	0	0	0.01	0	0	0.02
SE		0.032	0.029	0.027	0.015	0.028	0.015	0.0014	0.046
R^2		0.929	0.937	0.948	0.983	0.939	0.982	0.984	0.839
SE Prediction		0.012	0.009	0.008	0.004	0.008	0.005	0.005	0.005

Table 15. Cross-semivariogram parameters for water content and validation statistics of kriging and cokriging method for bare soil.

Bare soil	Rainfall	z=0 cm	z=0.05m	z=0.1 m	z=0.2 m	z=0.3 m	z=0.4 m	z=0.5 m	z=0.8 m
Model	Lin	Gauss	Gauss	Gauss	Gauss	Gauss	Gauss	Gauss	Exp
Nugget Co	25.72	0.0001	0.00001	0.00001	0	0	-0.00001	-0.00001	-0.00197
Sill Co +C	25.72	0.01172	0.01282	0.01182	0.0008	0.00061	-0.00347	-0.01407	-0.01231
Range	43	3.59	3.4	2.98	2.42	19.94	101	101	70.1
R^2	0.005	0.229	0.542	0.588	0.115	0.031	0.432	0.615	0.396
RSS	357	1.88E-3	2.92E-4	1.64E-4	2.29E-5	4.14E-5	1.44E-4	3.33E-5	4.62E-5
Kriging									
Regression coefficient		1.052	1.139	1.066	1.021	1.031	1.017	0.978	0.968
Intercept		-0.01	-0.04	-0.02	0	-0.01	0	0.01	0.01
SE		0.083	0.084	0.052	0.046	0.053	0.05	0.112	0.139
R^2		0.678	0.705	0.844	0.863	0.83	0.841	0.498	0.389
SE Prediction		0.02	0.011	0.009	0.005	0.005	0.004	0.004	0.005
Cokriging									
Regression coefficient		0.946	0.956	0.978	0.946	0.946	0.972	0.867	0.768
Intercept		0.01	0.01	0.01	0.01	0.01	0.01	0.04	0.08
SE		0.069	0.054	0.043	0.048	0.05	0.046	0.086	0.098
R^2		0.706	0.801	0.871	0.837	0.821	0.853	0.568	0.43
SE Prediction		0.019	0.009	0.008	0.005	0.005	0.004	0.004	0.005

5.8. Estimation of soil moisture distributions with the methods of kriging and cokriging

In the calculations conducted according to the methods of kriging and cokriging, soil moisture was chosen as the basic variable, and precipitation was the auxiliary (secondary) variable. The determined semivariogram models of soil moisture and precipitation and the cross-semivariogram of soil moisture and precipitation were used in the estimation of soil moisture. Measured values of soil moisture (dots), calculated values (solid line) and standard deviations (broken line) for the surface horizon of soil z=0 m, for the three objects under study, are presented in Fig. 39, 40, 41. The conformity of calculated and measured values was examined by means of linear regression equation, standard error SE, and determination coefficients R^2. Results of the comparisons are presented in Fig. 42, 43, 44 and in Table 13, 14, 15. The statistics presented show good agreement between the measured values of soil moisture and the values calculated with the help of the two methods of calculation.

The kriging method permited fairly accurate estimation of soil moisture on the basis of determined semivariogram and soil moisture values measured in prior (Fig. 42a, 43a, 44a and Tables 13, 14, 15). However, the estimated standard deviation of kriging clearly indicated a considerable area of uncertainty that was the greatest at the beginning and at the end of measurements.

The application of the cokriging method results in a slight improvement of soil moisture estimations – in some cases the estimations were at the same level as with the kriging method but with a significant reduction of the area of uncertainty as expressed by standard deviation (Fig. 42b, 43b, 44b and Tables 13, 14, 15). Standard deviation was also small at the beginning and end of estimation.

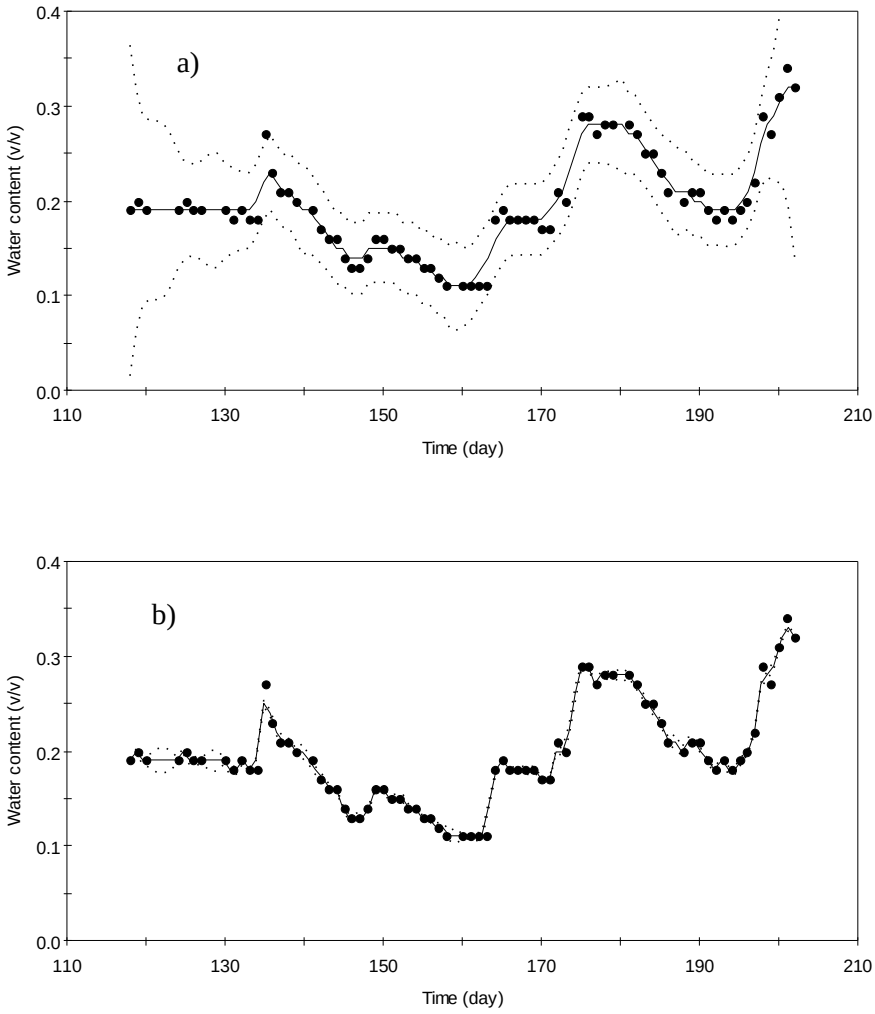

Fig. 39. Measured (dots) and estimated (solid line) - with the kriging (a) and cokriging (b) methods - values of soil moisture in the surface horizon of soil z = 0 m in the spring barley plot. Broken line is used to mark standard deviations of kriging and cokriging.

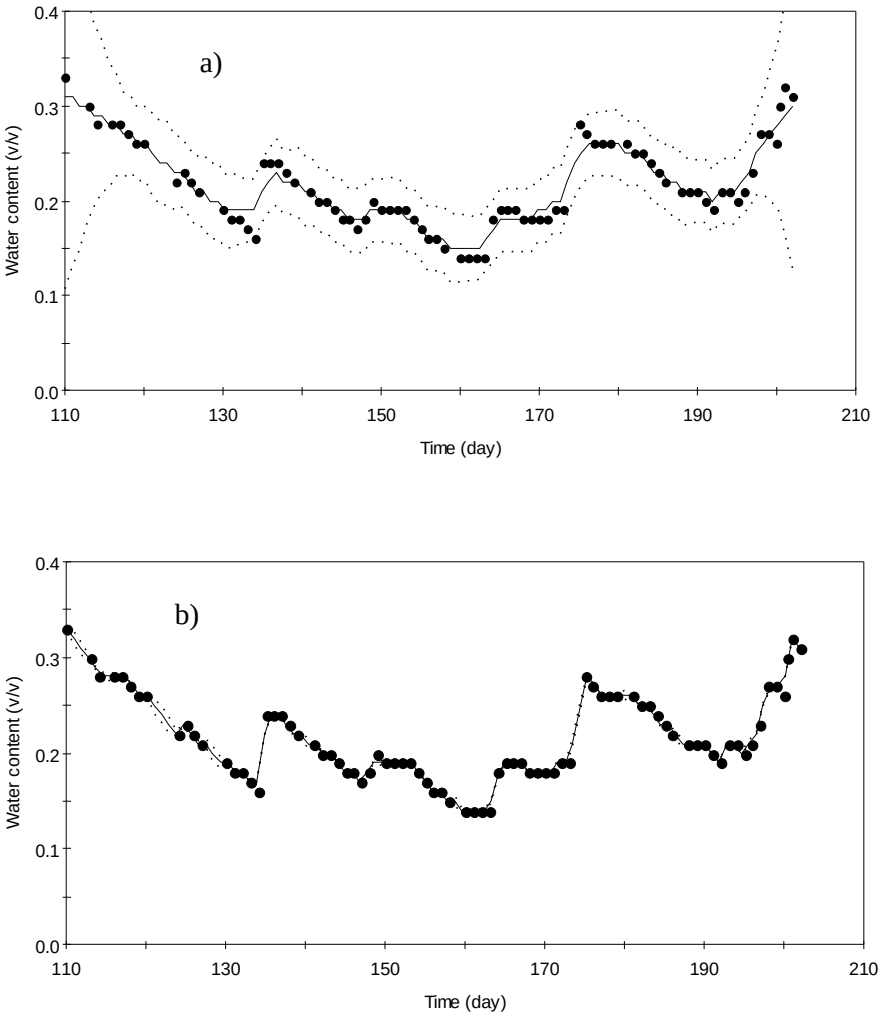

Fig. 40. Measured (dots) and estimated (solid line) - with the kriging (a) and cokriging (b) methods - values of soil moisture in the surface horizon of soil z = 0 m in the rye plot. Broken line is used to mark standard deviations of kriging and cokriging

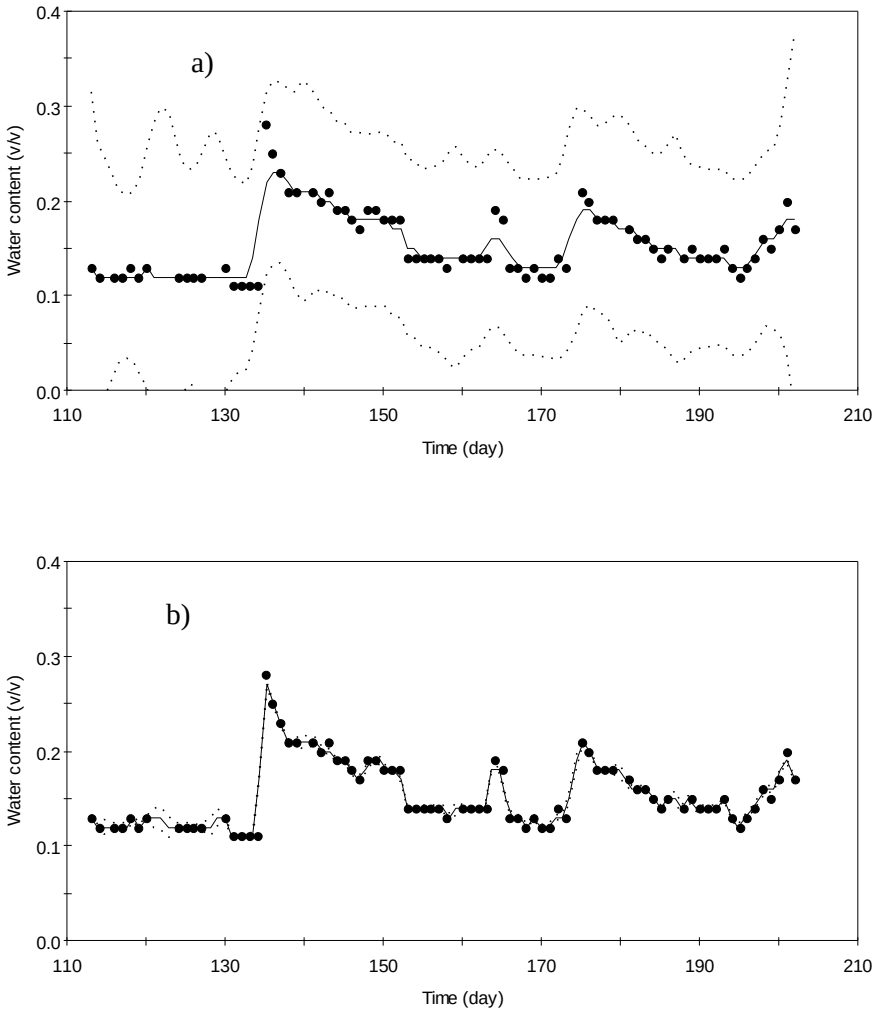

Fig. 41. Measured (dots) and estimated (solid line) - with the kriging (a) and cokriging (b) methods - values of soil moisture in the surface horizon of soil z = 0 m in the bare plot. Broken line is used to mark standard deviations of kriging and cokriging

5.9. Assessment of conformance of kriging and cokriging estimations

The assessment of conformance of soil moisture values estimated with the kriging and cokriging methods was performed with the help of the cross-validation method. From the time series, data were removed one at a time and, on the basis of neighbouring data, soil moisture value was estimated for the point of removal. The completion of the procedure for all the data possible yielded a set of calculated data equivalent to the measurement data. The measured and estimated data are presented in a system of coordinates (Fig. 42, 43, 44) and the statistical parameters illustrating the goodness of conformance are presented in Tables 13, 14, 15.

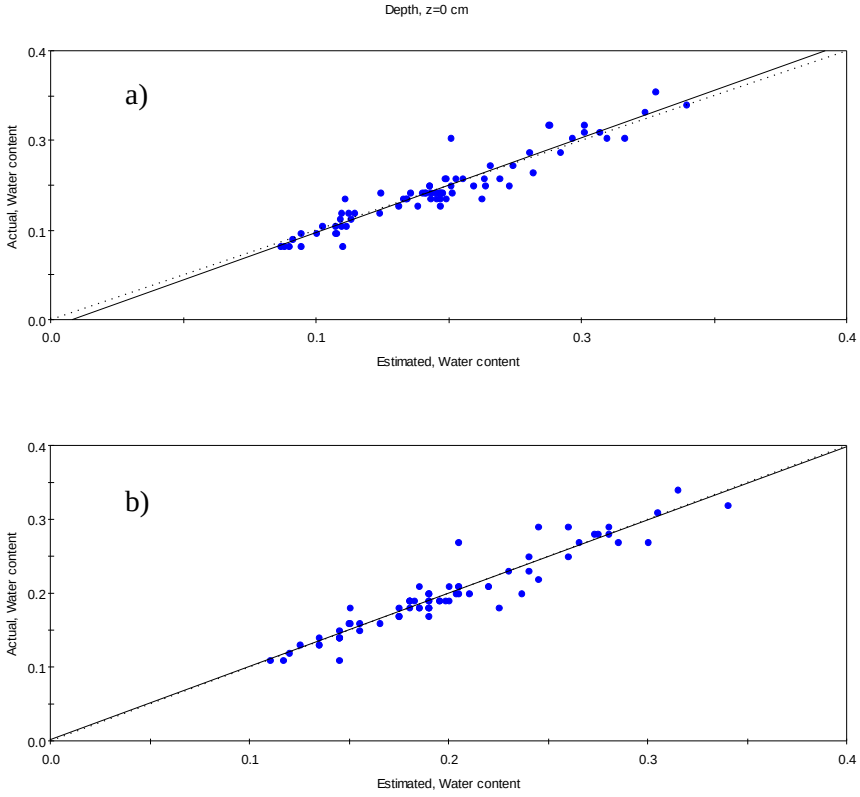

Fig. 42. Comparison of soil moisture values - measured and calculated with the kriging (a) and cokriging (b) methods for the plot with spring barley (Water content – $m^3\ m^{-3}$).

Solid lines represent the linear regression equations which were fitted to the measurement-calculation data. The broken line represented 1:1 relationship. High concentration of dots around the 1:1 axis and the overlapping of the solid line with the broken line indicate improvement of estimation with the cokriging method as compared to the kriging method. The kriging method also gives good conformance of measured and calculated data, but with somewhat divergent conformance of the linear regression equation to the 1:1 line. The standard error SE and the SE Prediction term, defined as $SD \cdot \sqrt{1-R^2}$, where *SD* = standard deviation of the actual data (Table 13, 14, 15) were low and thus indicated good conformance of the measured and calculated values. The figures show also that the greatest range of soil moisture values in the surface horizon during the vegetation season was observed in the barley plot, somewhat smaller in the rye plot, and the smallest in the bare field.

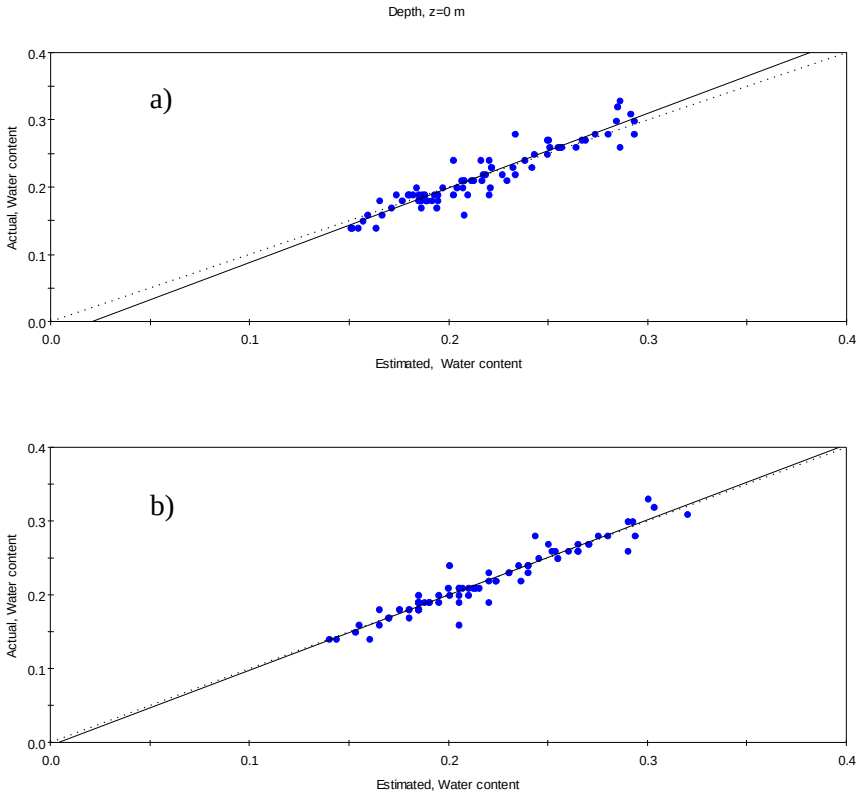

Fig. 43. Comparison of soil moisture values - measured and calculated with the kriging (a) and cokroging (b) methods for the plot with rye (Water content – $m^3\ m^{-3}$).

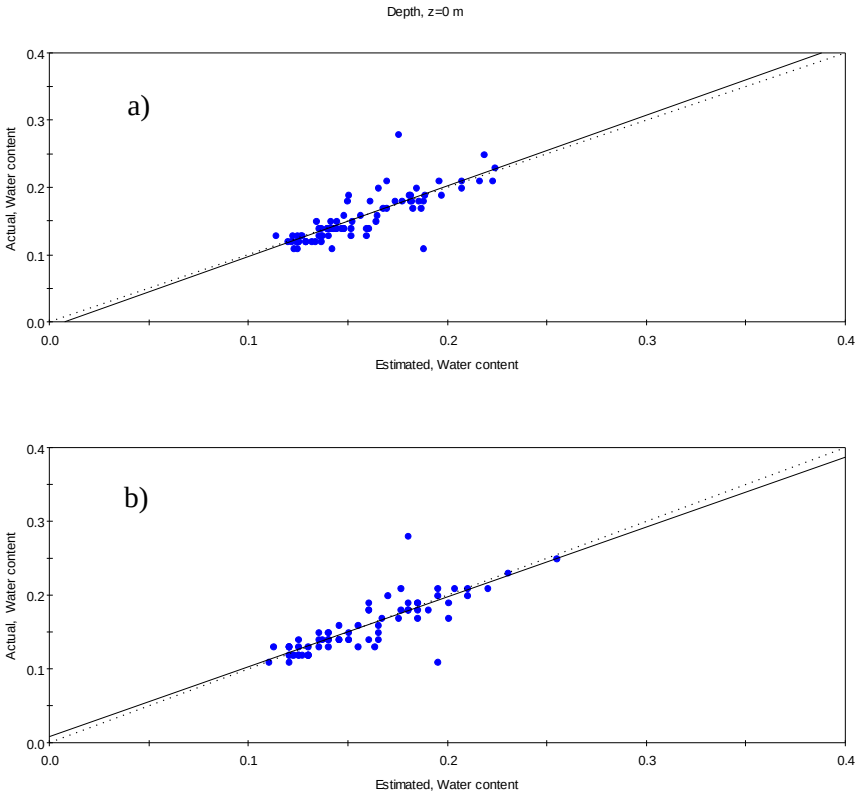

Fig. 44. Comparison of soil moisture values - measured and calculated with the kriging (a) and cokroging (b) methods for the bare field (Water content – $m^3\ m^{-3}$).

5.10. Conclusion

This part of the work was concerned with the assessment of the temporal and spatial variability of soil moisture and thermal properties in the soil profile in a field with plant cover and without, using the methods of geostatistical analysis and fractal theory.

The basic statistical parameters were calculated and it was shown that the lowest and the highest values of soil moisture within the spring-summer season occurred in the bare field; the lowest in the surface horizon, and the highest in

deeper soil layers. The greatest variability of soil moisture within the soil profile was observed in the plots with plant cover, and the smallest in the bare field.

The geostatistical parameters determined showed the temporal dependence of moisture distribution in the soil profile, with the autocorrelation radius increasing with increasing depth in the profile. The highest values of the radius were observed in the plots with plant cover below the arable horizon, and the lowest in the arable horizon on the barley and fallow plots.

The fractal dimensions showed a clear decrease in values with increasing depth in the plots with plant cover, while in the bare plots they were relatively constant within the soil profile under study. Therefore, they indicated that the temporal distribution of soil moisture within the soil profile in the bare field was more random in character than in the plots with plants.

The results obtained and the analyses indicate that the moisture in the soil profile, its variability and determination, are significantly affected by the type and condition of plant canopy. The differentiation in moisture content between the plots studied resulted from different precipitation interception and different intensity of water uptake by the roots.

In calculations made with the help of the kriging and cokriging methods, soil moisture was chosen as the basic variable and precipitation as the auxiliary (secondary) variable. Semivariogram models were determined for soil moisture and precipitation, and the cross-semivariogram of moisture and precipitation was used for the estimation of soil moisture. The conformance of calculated and measured data was validated with the help of linear regression equations, standard errors SE, and the determination coefficients R^2. The statistics presented indicate good conformance between the soil moisture values measured and calculated with the help of the two calculation methods.

The method of kriging permitted a fairly good estimation of soil moisture on the basis of the semivariogram and the soil moisture values measured beforehand. However, the estimated standard deviation of kriging clearly showed a considerable area of uncertainty. The area of uncertainty was the greatest at the beginning and at the end of the measurements.

The application of the method of cokriging provided a slight improvement in the estimation of soil moisture. Sometimes the estimation results were similar to those obtained with the kriging method, but there was a significant reduction of the area of uncertainty as expressed by the standard deviation. Standard deviation was also low at the beginning and at the end of the estimation.

6.1. Field experiment

In the case of the second object, the basic data considered in the tsudy originated from measurements of granulometric composition, pH, organic matter content and exchangeable cation capacity (CEC) in the surface horizon (0 – 10 cm) of soil in arable fields in the commune of Trzebieszów [399]. The soil was sampled into cloth bags (approx. 1.5 kg of soil per sample). The soil samples were analyzed according to methods commonly used in soil science. Soil moisture was measured using the TDR meter (Soil moisture meter (TDR) elaboreted and pronanced by Institute of Agrophysics PAS Lublin, Poland) [216]. Concurrently, at the same sampling points, the soil was sampled into cylinders 100 cm^3 in volume and 5 cm high, for soil moisture and density determinations according to the gravimetric method. That latter measurement method was used for the validation of data obtained with the reflectometric method (TDR) [394]. For soil moisture determinations, soil samples were taken from selected arable fields, from the arable horizon exclusively, in spring and in summer immediately after harvest. The measurement points within the fields were distributed on a regular grid (Fig. 45). The regular grid was marked out in the fields with the help of measuring tape, and selected reper points were determined with the help of Trimble's GPS GeoExplorer 3 with the accuracy of approx. 1 m.

For each object the basic statistical parameters were determined, i.e. the mean value, standard deviation, coefficient of variability (CV), maximum and minimum values, as well as values characterizing the distribution of the given features, i.e. skewness and kurtosis. Spatial characterization of the data under consideration was performed with the geostatistical methods. The statistics, semivariograms, estimation of the soil features studied and their mapping were obtained with the help of such software packages as the GeoEas, Statistica 6, Variowin 2.21, GS+5 Demo GS+ 7 Demo, Surfer 8 Demo [91, 109, 114, 280, 281].

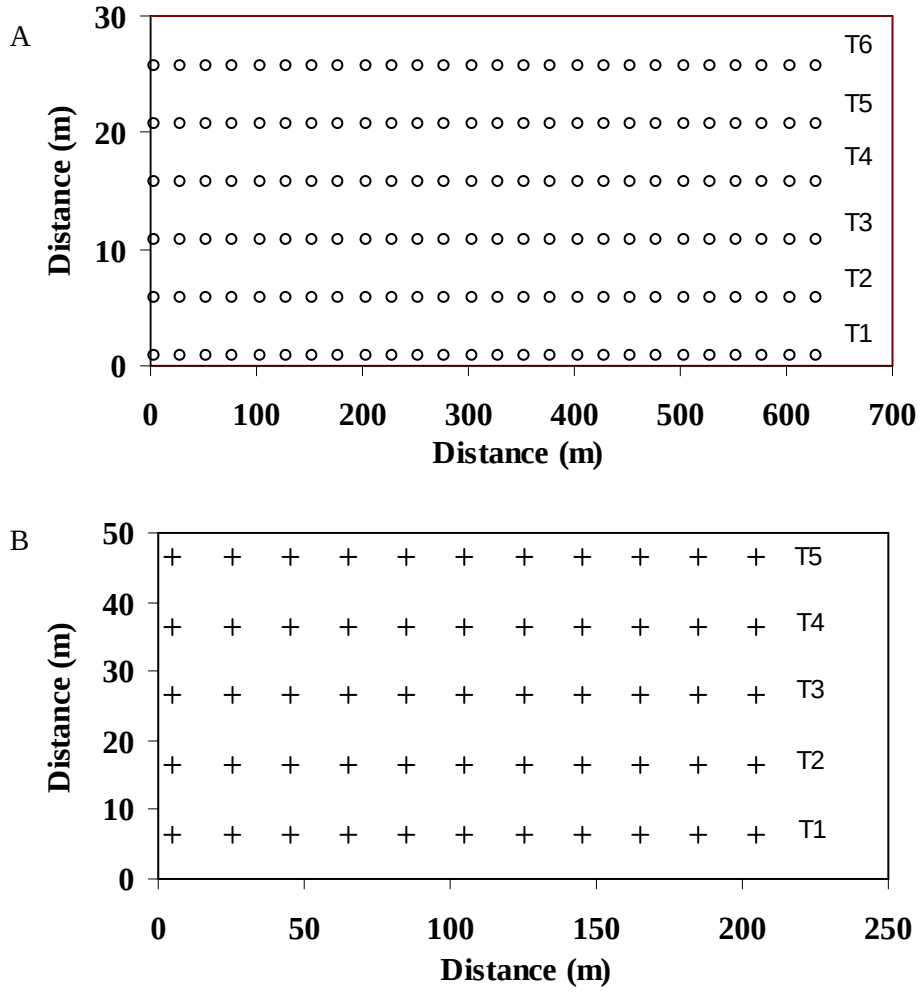

Fig. 45. Location of measurement points on fields A and B, (denoted: T1-T6 transects from 1 to 6, on field A point 0,0 corresponds to 22.53960361° λE and 51.98515° φN, on field B – 22.56809278° λE and 51.98714389° φN) [399].

6.2. Results of statistical analysis

The statistical parameters of the soil features studied for the surface horizon (0-10 cm) of arable fields A and B were calculated and compiled in Tables 16 and 17. The mean value is an especially significant measure of the central trend of distribution of a given variable. Its reliability is increasing with the population of the sample. It is known that with increasing variance of data the reliability of the

mean value decreases. Standard deviations determined for the variables under consideration (Tables 16, 17) were, in most cases, significantly lower than the mean values, which indicates that the mean values obtained were representative for the objects studied.

Table 16. Summary statistics of granulometric fraction, acidity (pH), organic mater content (OM) and cation exchange capacity (CEC) in 0-10 cm layer for cultivated field A [399].

Parameter	Cultivated field A						
	% content of fractions			pH [KCl]	pH [H_2O]	OM	CEC
	1-0.1 [mm]	0.1-0.02 [mm]	<0.02 [mm]	–	–	%	cmol·kg^{-1}
				Layer 0-10 cm			
Number of points	150	150	150	150	150	150	150
Mean	48.8	37.2	14.0	3.905	4.458	0.835	11.8
Variance	50.1	36.9	18.4	0.084	0.099	0.118	12.9
Standard deviation	7.08	6.08	4.29	0.29	0.314	0.344	3.59
Coefficient of variation	14.5	16.3	30.6	7.4	7.0	41.2	30.5
Skewness	0.811	–0.419	–0.125	5.307	2.47	0.276	0.628
Kurtosis	4.298	4.446	2.646	44.47	15.97	3.709	3.672
Minimum	34	16	3	3.56	3.93	0.014	3.69
25th %tile	44	34	11	3.78	4.27	0.650	9.22
Median	48	38	15	3.86	4.39	0.832	11.40
75th %tile	52	40	17	3.96	4.60	1.003	13.49
Maximum	75	54	25	6.49	6.59	1.800	23.80

Table 17. Summary statistics of granulometric fraction, acidity (pH), organic mater content (OM) and cation exchange capacity (CEC) in 0-10 cm layer for cultivated field B [399].

Parameter	Cultivated field B						
	% content of fractions			pH [KCl]	pH [H_2O]	OM	CEC
	1-0.1 [mm]	0.1-0.02 [mm]	<0.02 [mm]	–	–	%	cmol·kg^{-1}
				Layer 0-10 cm			
Number of points	50	50	50	50	50	50	50
Mean	54.7	34.5	10.8	4.18	4.81	0.804	10.3
Variance	57.1	45.5	23.0	0.143	0.173	0.076	14.6
Standard deviation	7.56	6.74	4.79	0.378	0.416	0.276	3.82
Coefficient of variation	13.8	19.5	44.4	9.0	8.6	34.4	37.0
Skewness	0.005	0.273	1.377	1.688	0.918	–0.123	1.164
Kurtosis	2.618	2.213	5.1	6.616	3.521	4.323	4.429
Minimum	39	22	4	3.75	4.21	0.1	4.53
25th %tile	49	30	7.5	3.93	4.51	0.668	7.57
Median	55.5	33	9.5	4.09	4.74	0.832	9.63
75th %tile	59.5	40	13	4.26	4.99	0.973	11.6
Maximum	72	49	26	5.69	6.06	1.675	23.2

The content of granulometric fractions in the objects studied was rather varied in the scale of a field. In terms of mean values, the lowest sand content characterized the soil in the arable field A (48.8%), and the highest – in field B (average of 54.7%). The content of the silt fraction varied within the range from 34.5% (field B) to 37,2% (arable field A), and that of clay - from 10.8% (field B) to 14% (field A). Minimum values of sand, silt and clay content in field A were 34, 16 and 3%, and in field B were somewhat higher, i.e. by 5, 6 and 1, than in field A. Maximum values observed in both the fields were 75-72% for sand, 54-49% for silt, and 25-26% for clay.

Organic matter content in the soil of the arable fields was low at about 0.8%. The lowest and highest values of organic matter content observed at a single measurement point in the surface horizon were 0.1 and 1.8%.

Soil reaction in the fields was acid. The mean pH value in the 0-10 cm horizon, measured in KCl, was 3.91 and in H_2O approximately 4.8. Minimum pH values of soil samples were 3.6 (KCl) and 3.9 (H_2O), and the maximum values - 6.5 and 6.6, respectively (Tables 16, 17). The mean value of the cation exchange capacity was approximately 11 $cmol \cdot kg^{-1}$, though in individual samples it varied considerably (within the range from 3.7 to 28 $cmol \cdot kg^{-1}$).

Comparison of the values of standard deviation of particular granulometric fractions, organic matter content, pH, and of the values of cation exchange capacity (CEC) (Tables 16, 17) permits the conclusion that within the fields the scatter of the values was fairly similar.

Among the physical and chemical features in fields A and B, the lowest variability, as expressed by the coefficient of variability (CV) characterized the soil reaction pH, and the highest CV was recorded for the clay fraction content - 44%. A CV value similar to that for the clay fraction content was characteristic for the organic matter content and the cation exchange capacity (CEC). Considerably lower CV values than for the clay fraction content were observed for the silt (16-19%) and sand (14-15%) fractions.

Skewness, which characterizes the degree of distribution asymmetry with relation to its mean value, was, in the case of the variables under consideration, mostly positive – for some of the variables with rather moderate symmetry, for others (mainly the soil pH and organic matter content) with considerable symmetry. The silt fraction content and, sporadically, also the clay fraction content and pH, showed a slight negative asymmetry. Kurtosis, which characterizes the relative slenderness or flatness of a distribution as compared to the normal distribution (normal distribution kurtosis equals 3), showed - for most

of the variables – values similar to the normal distribution. Relatively low slenderness of distribution (kurtosis>3) was observed for the granulometric fractions of soil for all the data from the 0-10 cm horizon of the arable fields. A considerably greater slenderness of distribution was characteristic of the soil reaction, organic matter content, and cation exchange capacity.

6.3. Results of correlation analysis

Calculation of the linear correlation of the soil features under consideration was performed at the level of significance $p<0.05$. The results of the calculation are presented in Table 18 (statistically significant correlations are shown in bold type). High and significant coefficients of correlation between the contents of particular granulometric fractions in a given horizon indicate mutual interrelationships between those variables. Negative correlation was observed between the silt and sand fractions content, and positive correlation between the silt and clay fractions. Soil reaction values (pH in KCl and pH in H_2O) were highly and positively mutually correlated, and somewhat less highly and negatively correlated with the silt fraction content and the organic matter content. Organic matter content correlated with the silt fraction content, the cation exchange capacity and the soil pH. The cation exchange capacity correlated with the sand, silt and clay fractions content, the correlation with sand being negative.

Tabela 18. Correlation between soil physical properties in 0-10 cm layers [399].

	Sand	Silt	Clay	pH KCl	pH H_2O	OM	CEC
Sand	1.00	**–0.90**	**–0.68**	0.05	0.04	–0.07	**–0.28**
Silt		1.00	**0.30**	**–0.11**	**–0.10**	**0.10**	**0.14**
Clay			1.00	0.07	0.08	–0.02	**0.40**
pH KCl				1.00	**0.98**	**0.14**	0.06
pH H_2O					1.00	**0.12**	0.05
OM						1.00	**0.45**
CEC							1.00

Correlation coefficients were determined for $p < 0.05$ and N=464. Significant correlations are written in bold type.

6.4. Results of geostatistical analysis

Measurement data from the fields were analyzed for the detection of trends in the spatial distribution of the soil features under consideration. In the case of the fields, it was found that the equation parameters show a slight decreasing trend in one direction and an increasing trend in the other, or an absence of trends. Organic matter content and cation exchange capacity also displayed no discernible trends in their data. In the case of those objects it can be assumed that the features under consideration meet the process stationarity or quasi-stationarity condition required in geostatistical analysis [122]. Moreover, the distributions of values of the soil features under study were mostly close to the normal distribution.

The spatial variability of each of the soil features studied for a given object was analyzed with the help of semivariograms. The values of nuggets, sills and spatial autocorrelation ranges were determined, and semivariogram models were fitted to empirical data, together with the determination of model fitting parameters (Table 19). The quality of fitting of semivariogram theoretical models to the emprical data was determined with the help of the determination coefficient R^2 and the sum of residual squares sum RSS, taking into consideration the values from the models and the empirical values of the semivariogram. High values of the determination coefficient (up to $R^2 > 0.85$) and low values of the residual squares sum ($RSS<10^{-6}$) found in a great majority of cases, indicate that the theoretical models can be fitted to the empirical semivariograms with a fairly high level of goodness.

Spatial correlation of the features under consideration was found in almost all of the objects. The form of the spatial correlation in the arable horizon was mostly spherical. Exponential relationship was observed only in the case of three variables. The semivariogram parameters indicate that we deal here with the nugget effect. This indicates that the variability of the features under examination is less than the minimum soil sampling separation adopted in the field measurements. Values of semivariance saturation are comparable to the values of variance determined in the classical way (Tables 16, 17). Analyzing those values we can conclude that within the fields there were no clear trends in the variation of the soil features under study. The values of semivariogram saturation were a derivative of the content of particular fractions. The highest values were observed for the sand fraction content, markedly lower for silt, and the lowest for the clay

fraction content. In the case of soil reaction (pH) and organic matter content, somewhat higher values of semivariance were observed in field A than in field B. Also the cation exchange capacity semivariance values observed for field A were considerably higher than those in field B.

Analyzing the ranges of spatial correlation of the physical and chemical properties, one can conclude that they were related to the size of the object studied. The highest values of spatial autocorrelation were observed in the arable field A where it varied from 78 to 500 m, while in field B it was from 12 to 310 m.

Table 19. Semivariogram parameters of soil properties in 0-10 cm layer for cultivated field A and B [399]

Parameter	Sand [%]	Silt [%]	Clay [%]	pH [KCl]	pH [H_2O]	OM [$m^3 \cdot m^{-3}$]	CEC [$cmol \cdot kg^{-1}$]
	Cultivated field A, layer 0-10 cm						
Model	Exp.	Spherical	Spherical	Spherical	Spherical	Spherical	Spherical
Nugget [ ]^2	27.08	28	11.24	0.07	0.08	0.107	10.5
Sill [ ]^2	54.17	38	22.24	0.09	0.1	0.12	15
Range [m]	77.9	350	450	150	150	150	500
	Cultivated field B, layer 0-10 cm						
Model	Spherical	Spherical	Exp.	Spherical	Spherical	Exp.	Spherical
Nugget [ ]^2	1.18	0.01	5.66	0.00004	0.0001	0.0161	0.33
Sill [ ]^2	28.74	17.42	11.33	0.011	0.042	0.0546	6.33
Range [m]	12.2	13.5	28.4	12	12	310	16.6

Exp. – Exponential.

6.5. Estimation and preliminary analysis of maps

The parameters and semovariogram models determined for the particular soil features, and the measurement data from the particular measurement points, were used – with the help of the kriging method – for the plotting of maps of spatial distribution of the features studied within a given object (Fig. 46, 47, 48, 49), and for the determination of the values of errors involved in the estimation. The estimation error, for all the soil features under study, did not exceed 10% of the feature under analysis. Close to the measurement points the errors were much smaller, at about 1-2%, and the greatest estimation errors occurred at the edges of the measurement grids.

Generally, it can be stated that there is an overall similarity between layers in terms of distribution of a given feature. Even if the distribution image is not exactly the same, areas can be found that are similar in terms of values and retain greater or lesser similarity of one layer to another. Maps of the content of granulometric fractions display overall similarity of distribution due to the fact

that the sum has always to be 100%, but their values vary. Where there is more sand, there has to be less silt, and the other way round. However, considering the fact that the maps have been estimated with the help of the kriging method from the measurement points, it is certainly possible to find areas where the sum of fraction content is not always equal to 100%. But the very identification of the spatial distribution of particular fraction provides so much significant information (on the range of occurrence of specific values, directions of their changes), that it can be used in taking management decisions concerning a given area.

Considerable differentiation in the spatial distribution of the content of granulometric fractions and pH values was observed in the case of the selected fields, even though their surface area was from 1 ha to 1.8 ha and one could have expected greater homogeneity of the soil in the fields (Fig. 46, 47, 48, 49). This shows the sense of taking a greater number of samples when determining the properties (features) of soil in a given field, and the necessity of determination of the spatial distribution of the features.

It should be added that the visualization of the field of values of the physical and chemical properties of soil and of the values of estimation error permits the identification of those areas in the field in which the number of sampling points should be increased (or reduced) in subsequent measurements in order for the representation of a value studied to be burdened with an error not exceeding the level assumed by the experimenter.

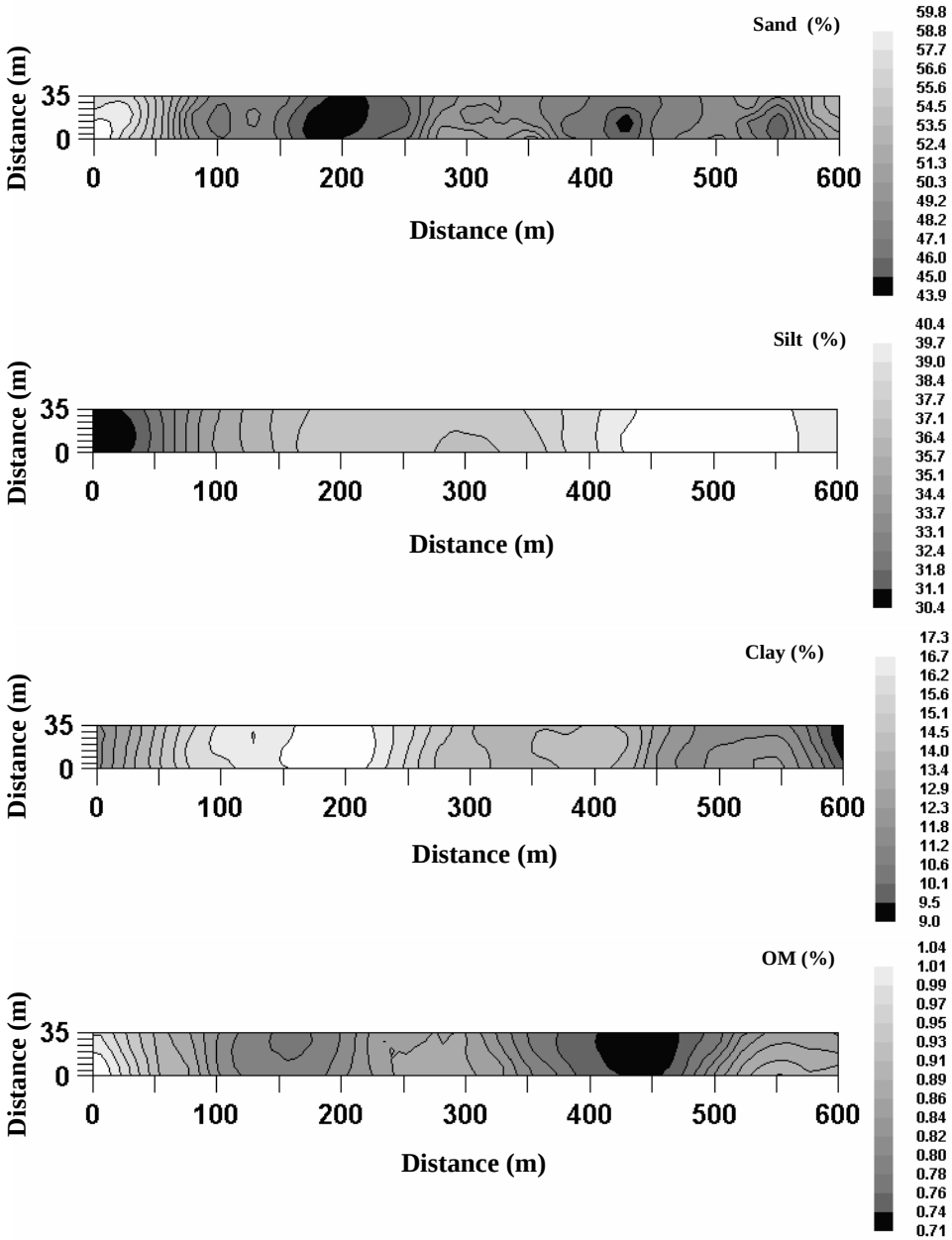

Rys. 46. Spatial distribution of sand, silt, clay and organic matter (OM) content in the cultivated field A for 0-10 cm soil layer [399]

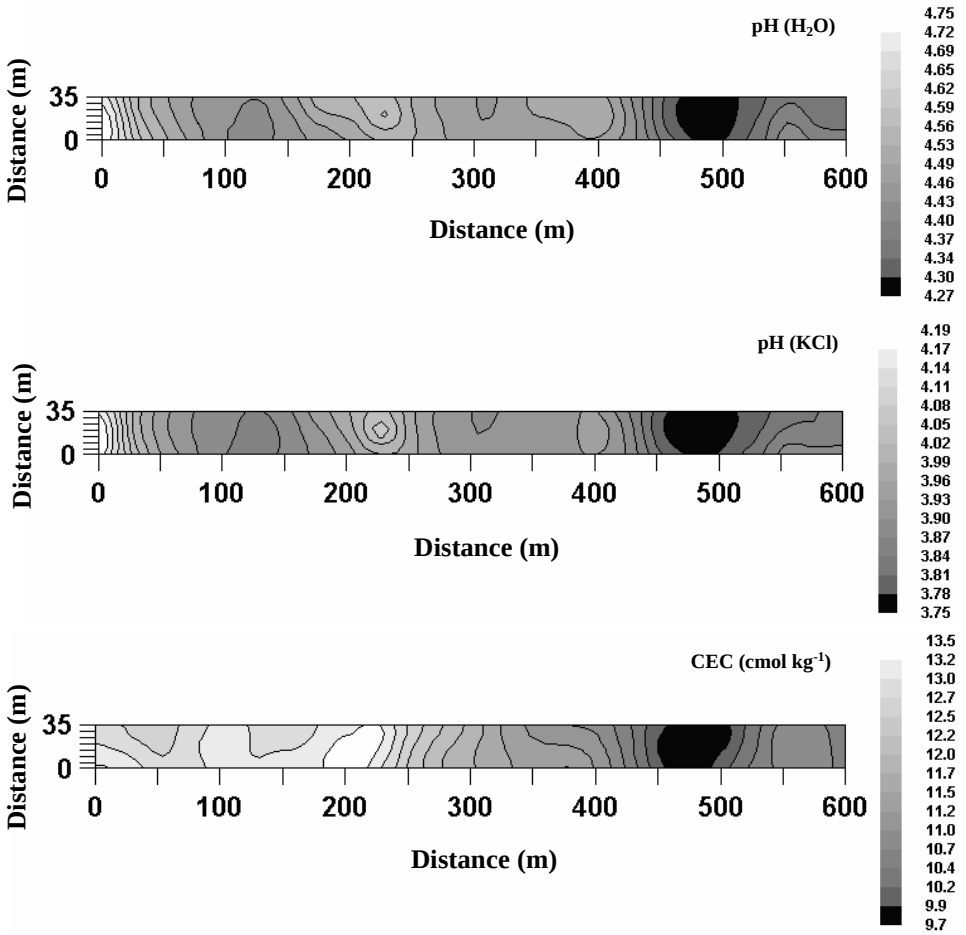

Rys. 47. Spatial distribution of pH H_2O, pH KCl and CEC in the cultivated field A for 0-10 cm soil layer [399]

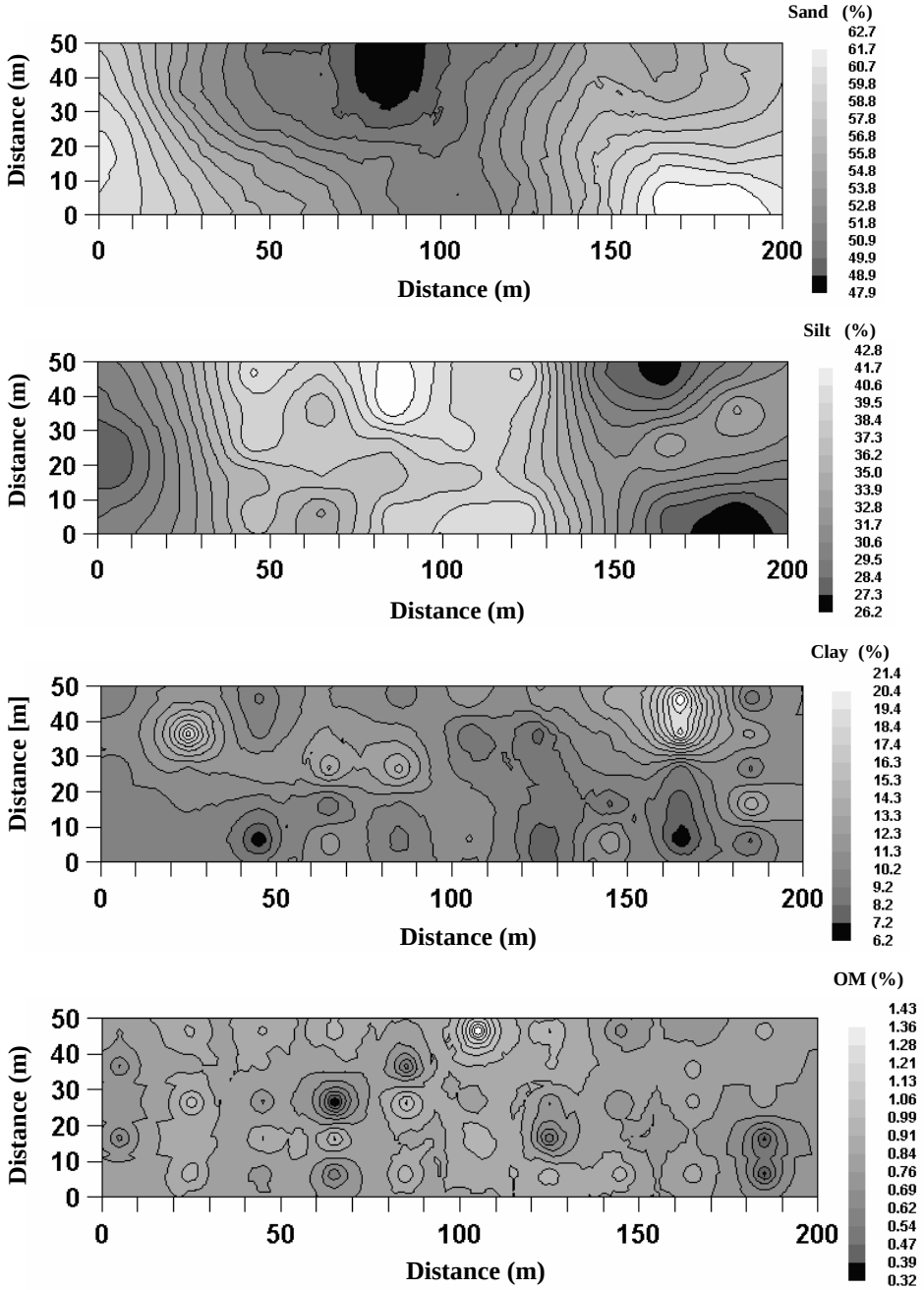

Rys. 48. Spatial distribution of sand, silt, clay and organic matter (OM) content in the cultivated field B for 0-10 cm soil layer [399]

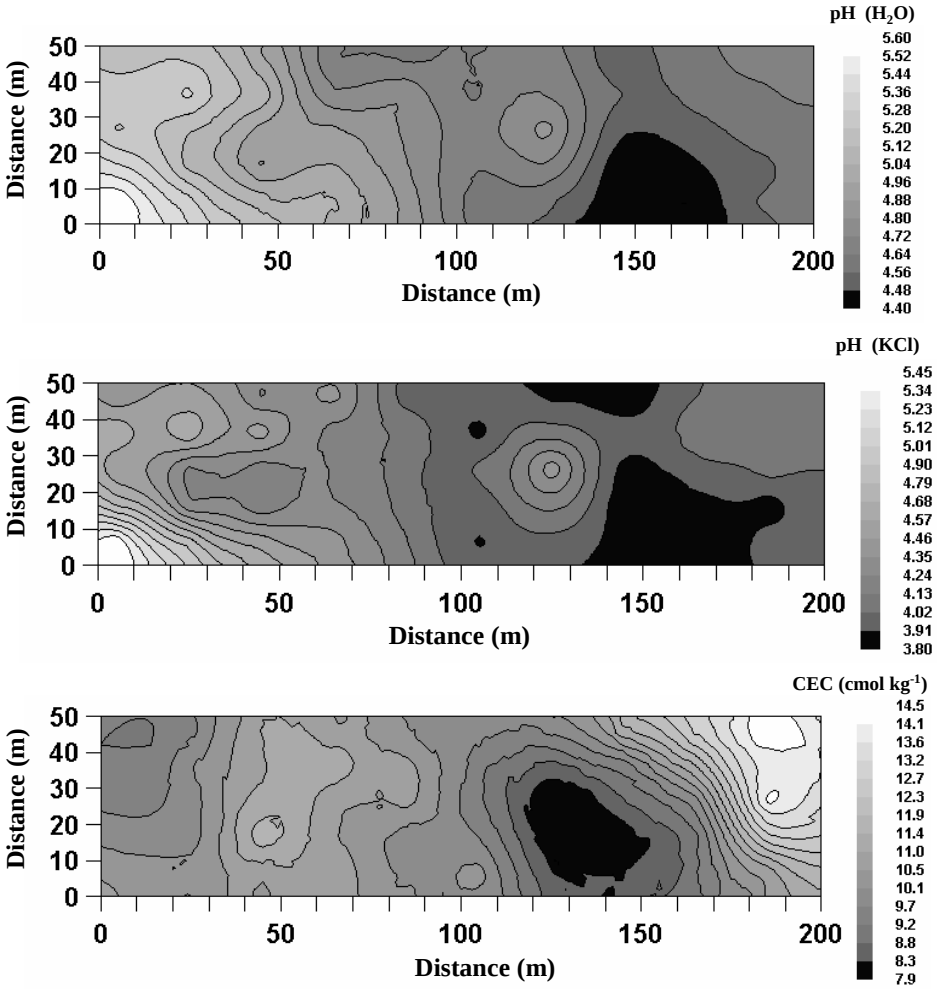

Rys. 49. Spatial distribution of pH H_2O, pH KCl and CEC in the cultivated field B for 0-10 cm soil layer [399]

6.6. Conclusion

The attempt, undertaken in this work, at determination (assessment) of the spatial variability of selected properties of soil on the scale of a field in the commune of Trzebieszów showed that there exists a distinct, though varied, variability of the values of the soil properties under consideration (content of

granulometric fractions and organic matter, soil reaction/acidity and cation exchange capacity) as well as their spatial correlation.

The granulometric composition of soil (percentage content of particular fractions), low content of organic matter, as well as – to a certain extent – the chemical properties of the soil in the fields were related with the predominant soil type of the area (sandy soils developed from loose sands, weakly loamy, overlying loam, or loamy). The average content of sand fraction was 55%, silt - 32%, clay - 13%, and organic matter - 0.8%. The soil reaction was acid or neutral (average pH about 4.4), and the average value of cation exchange capacity was 11 $cmol \cdot kg^{-1}$. However – while retaining a generally similar distribution and order of values – considerable differentiation of the features was observed, both within the larger field and in the smaller one, where due to the smaller area one could have expected a greater homogeneity of the soil.

From among the granulometric fractions, the greatest scatter of values was characteristic of the sand content, and the smallest – of clay. Scatter of the values of organic matter content was similar in both fields. Also the values of pH and cation exchange capacity had similar scatter of values in both fields.

Spatial correlation was observed for all the soil features, irrespective of which field was considered – the longer or the shorter one. The form of the spatial correlation was spherical in most of the cases, and exponential in some. The ranges of spatial correlation were mainly related to the scale of the object, but also to the type of variable.

The spatial distributions (maps) of the soil features studied, estimated on the basis of point measurements, show their differentiation within a given object (commune, cultivated field) and may constitute the basis for the identification of objects that require the application of various cultivation measures (e.g. liming or fertilization).

6.7. Soil moisture in field transects

Soil moisture was considerably differentiated along the length of the fields (Fig. 50, 51). Especially sharp changes in soil moisture was observed at the beginning ands at the end of field A, related primarily to the relief of the terrain. The beginning of the field was a slight slope, and the end – a hollow. The flat part of the field (between 100^{th} and 400^{th} meter) was characterized by uniform soil moisture content values. In the case of field B, a fairly uniform soil moisture content was observed in the first part of the field, and a considerable increase in soil moisture content in the other. The distribution of soil moisture in this field

was also related to the relief of the terrain. A slight slope was observed in the initial part of the field, then the slope angle increased in further part of the field which ended with a trough.

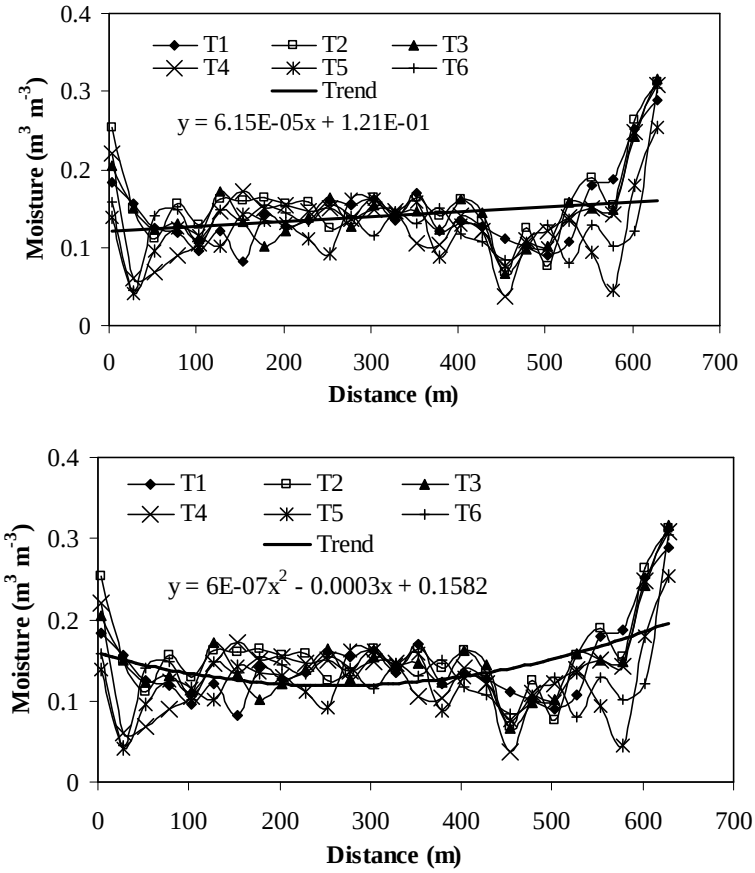

Fig. 50. Water content transects T1-T6 through field A with trend equations also shown

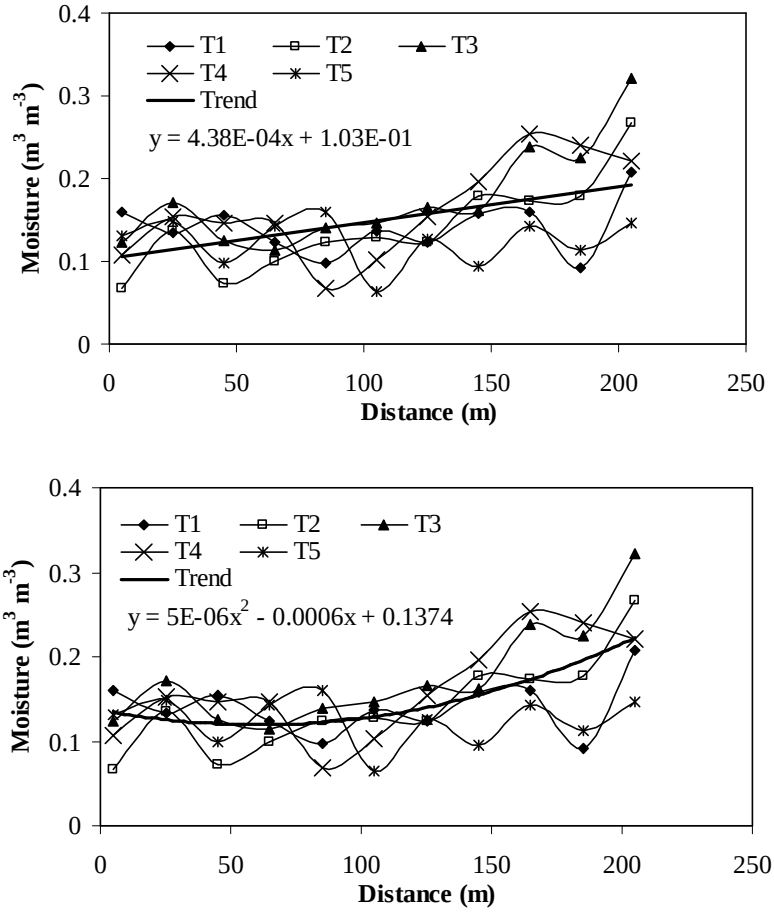

Fig. 51. Water content transects T1-T5 through field B with trend equations also shown

The presented runs of soil moisture content indicate its increase along the length of the field. The increases were examined with the help of the lines of linear and quadratic trends which were obtained from the fitting of the equation to all the data for a given field. The moisture content in field A, as compared to field B, was characterized by a lower directional index of the line (by about one order in value). The trend lines and their directional indexes indicate the existence of a small deterministic component in the soil moisture content in field A, and a much bigger one in field B. If this simple trend analysis can be the basis for the conclusion that the condition of process stationarity is fulfilled in the case of field

A, in the case of field B this condition will probably not be fulfilled. Therefore, the trends were removed from the data obtained from fields A and B in order to meet the condition of process stationarity and to find out if the trend affected the values of the semivariograms.

6.8. Basic statistics of soil moisture

The mean values of soil moisture in the two fields did not differ significantly – the difference was less than 1% (Table 20). Also similar was the scatter of soil moisture values in the two fields., as were the coefficients of variability of soil moisture – about 35%. The soil moisture distributions had right-hand skewness and were characterized by considerable slenderness – kurtosis 4-6 (skewness 0, kurtosis 3 – normal distribution [91]).

Table 20. Summary statistics of water content on field A, B, and for all data from A and B [401]

Parameters	Field A	Field B	All data from fields A and B
N – Number	156	55	211
Mean	0.140	0.149	0.143
Std. Dev.	0.049	0.052	0.050
Coef. Var.	35.1	34.6	35.0
Skewness	1.313	1.006	1.225
Kurtosis	6.097	4.366	5.549
Minimum	0.038	0.064	0.038
25th %tile	0.111	0.121	0.114
Median	0.137	0.143	0.139
75th %tile	0.156	0.162	0.158
Maximum	0.316	0.321	0.321

6.9.Semivariance

Calculations of semivariance of soil moisture were made for two fields – field A and field B. Semivariance was calculated on the basis of direct measurement data, as well as data in which the linear and quadratic trends had been removed from the original measurement data. To semivariance values determined in this way, mathematical models of semivariograms were fitted (Table 21). For comparative purposes, the classical variance was also calculated and presented. In the case of field A, the presented semivariance was estimated directly from the basic semivariance equation, while in the case of field B the standardized

semivariogram was presented. The latter semivariogram was employed bacause the scatter of semivariance values from the basic semivariance equation was extensive enough to make it difficult to fit a model of semivariogram. The standardization of semivariogram markedly improved the fitting of the model of semivariogram to the empirical data and permitted the determination of semivariogram parameters.

Table 21. Parameters and models of semivariograms for water content in fields A and B [401]

Data	Model	Nugget	Sill	Range	*Anisotropy*	
					Ratio	Angle
	Field A					
T	Exp.	0.000570	0.00180	95.3	2	48.01
DTL	Exp.	0.000671	0.00155	109.0	2	49.11
DTQ	Exp.	0.000542	0.00147	104.6	1.998	54.33
	Field B					
T	Sph.	0.37	0.87	110	1.023	109.9
DTL	Sph.	0.72	0.5	100	1	0
DTQ	Sph.	1	0.1	110	1	0

Denoted: Exp. – exponential, Sph. – spherical, T – data with trend, DTL – linear detrending, DTQ – quadratic detrending.

The existence of spatial correlation of soil moisture content was found in both objects. In field A exponential character of the spatial correlation was observed, while in field B the correlation was spherical. The values of the range of spatial correlation presented in Table 21 were similar at about 100 m, but the effective radii of spatial correlation in field A was about three-fold that of the radii in field B – this results from the definition of range for the exponential model. In both cases the nugget effect was observed. Detrending of data from field A did not cause any significant changes in the nugget values, while in the case of field B data detrending caused a significant increase in the nugget values (Table 21). The existence of nugget values in both objects under study indicates that the adopted sampling step was too large. Considering the nugget values it can be concluded that the sampling step in field A was somewhat better chosen than in field B. In field A, the semivariogram saturation parameters (sill values) decreased a little with increasing order of trend equation applied, while in field B they remained on the same level if linear trend was used, and slightly decreased with quadratic detrending. The somewhat higher semivariance in field B than the value of classical semivariance, and its decrease with increasing order of trend, indicate the existence of trend of higher order. However, due to the complexity of calculations involved in higher order detrending, no further analyses were made.

A mild anisotropy was found in the soil moisture distribution in field A, and a lack of such anisotropy in field B. Anisotropy is expressed here with the ratio of the maximum to the minimum range of semivariogram. The value of anisotropy was 2 in field A and 1 in field B. The preferential direction of anisotropy in the case of field A was about 50° and did not change with detrending. In the case if field B the direction was 109° for original data and decreased to 0° after the detrending.

6.10. Comparison of soil moisture values – measured and estimated with the kriging method

Conformance checks for soil moisture values measured directly with the TDR meter and estimated with the kriging method were performed through analysis of the determination coefficients R^2, mean values of differences in measured and estimated data, medians of absolute values of differences measured values and median of measured moisture, and root mean square of the differences of measured and estimated values (Table 22). In Table 22 bold type was used to indicate the bast conformance of measured and estimated soil moisture values.

Table 22. Summary statistics of water content measured and estimated by kriging method [401]

Data	R^2	Mean	*M.A.D.*	*R.M.S.*
			Field A	
T	**0.673**	**0.00024**	**0.0201**	**0.0286**
DTL	0.668	0.00025	0.0203	0.0289
DTQ	0.663	–0.00012	0.0208	0.0292
			Field B	
T	0.419	0.00065	0.0216	0.0397
DTL	**0.426**	**0.00057**	**0.0212**	**0.0395**
DTQ	0.414	–0.00100	0.0250	0.0408

Denoted: T – data with trend, DTL – linear detrending, DTQ – quadratic detrending, mean $\left(\frac{1}{n}\sum_{i=1}^{n} z_i\right)$, where $z_i = z_{ci} - z_{ei}$; z_{ci}, z_{ei} – calculated and measured value in point *i*, *n* – number of samples, (M.A.D. = $d_{\frac{n}{2}}$) – $d_i = \left|z_{ci} - z_{e\frac{n}{2}}\right|$ Median Absolute Deviation), ($R.M.S. = \sqrt{\frac{1}{n}\sum_{i=1}^{n} z_i^2}$) – Root Mean Square.

Considering the simple regression analysis of soil moisturee along fields A and B (Fig. 50, 51), analysis of semivariograms (Table 21) and parameters of conformance of the measured and estimated values of soil moisture (Table 22) we can assume that the results obtained on the basis of original measurement data in

field A are sufficient for representative description of the spatial correlation of soil moisture in that field and for mapping the soil moisture distribution. In the case of field B, the same is fulfilled for data after linear detrending.

6.11. Soil moisture distribution maps

Estimated maps of soil moisture distribution based on original measurement data, and on data after linear and quadratic detrending, are presented in Figures 52 and 53.

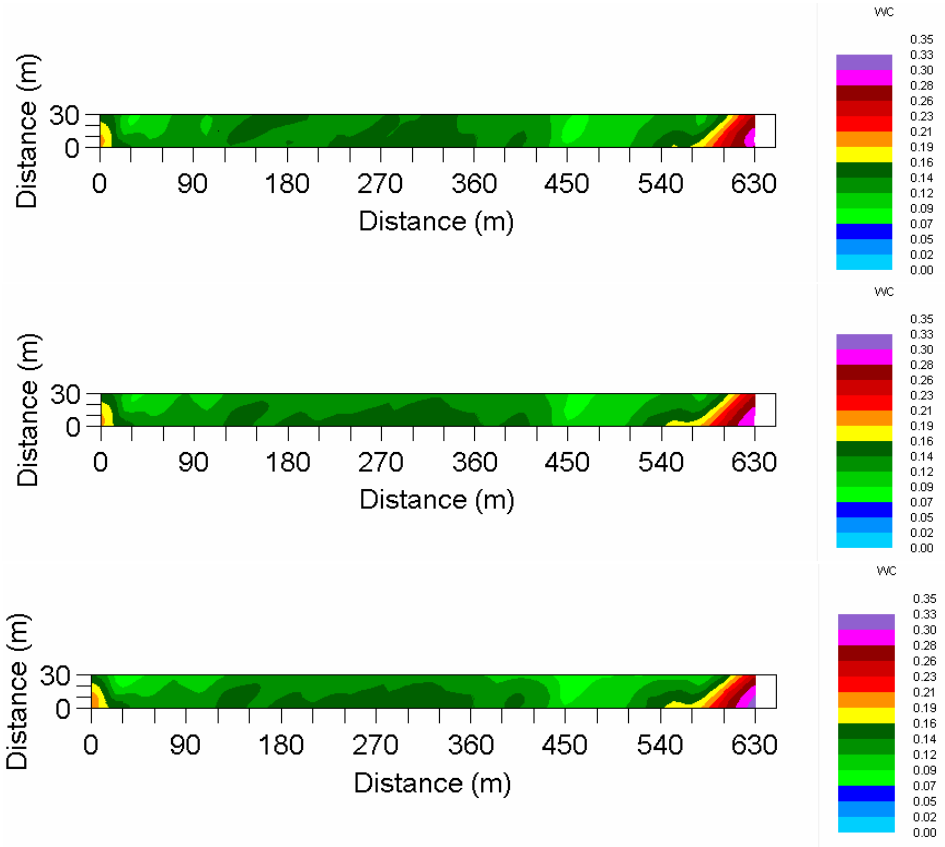

Fig. 52. Spatial distribution of water content for field A, upper figure with measured data, central figure – data with linear detrending, and lower figure – data with quadratic detrending (WC – water content (m^3 m^{-3}))

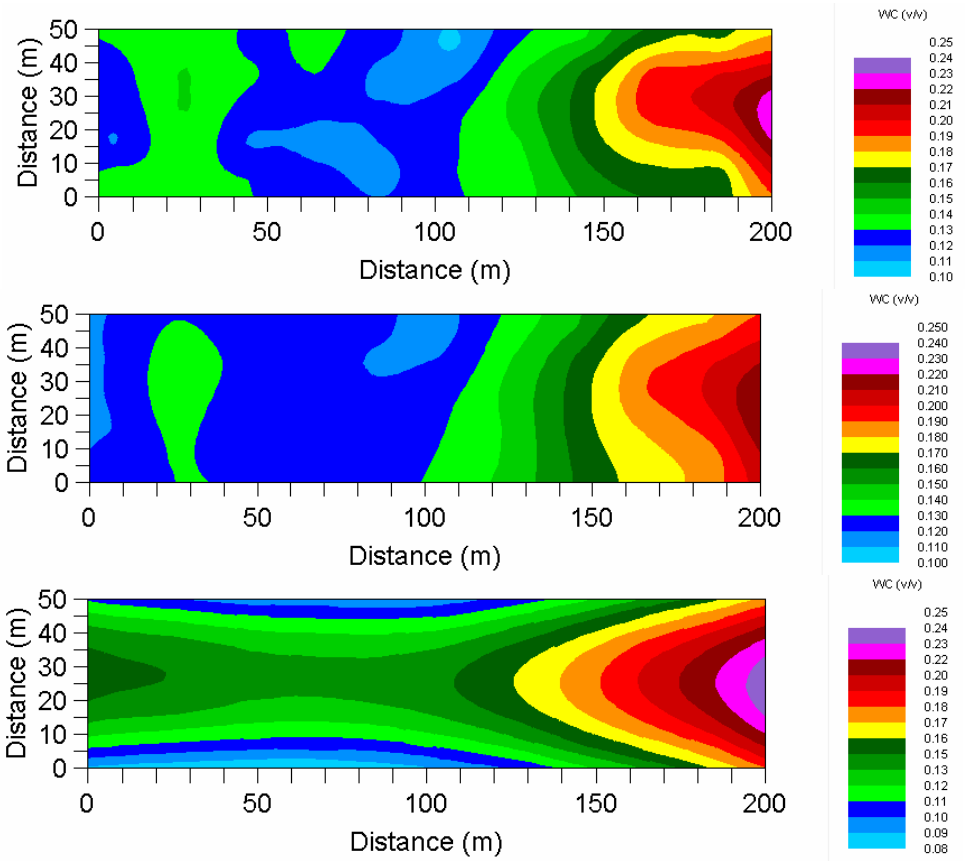

Fig. 53. Spatial distribution of water content for field B, upper figure with measured data, central figure – data with linear detrending, and lower – figure data with quadratic detrending (WC – water content (m^3 m^{-3}))

Soil moisture distributions in field A did not differ significantly. The parameters describing the conformance of measured and estimated values in that field (Table 22) confirm the above observation. Greater differences in soil moisture distributions were observed in field B. Soil moisture distributions based on measurement data were much more similar to distributions with linear detrending than to those with quadratic detrending. In this case, the parameters of conformance indicate the best data fitting for data with linear detrending.

The analyses and the parameters of conformance, their increase or decrease for particular steps in the analyses, may be provide the basis for future decisions as to whether extract the deterministic components from measurement data or not. Considering the much greater complexity of calculations involved when trends

are included in analyses, one can arrive at the conclusion that in some cases the analyses can be limited to measurement data alone, primarily in situations where linear regression shows only trace trends in the data under analysis. One should, however, keep in mind the acceptable values of estimation error.

6.12. Conclusion

Presented above are the results of analyses of the spatial variability of soil moisture content, based on measurement data obtained with the help of the TDR meter and on data from which the deterministic component, i.e. linear and quadratic trends, had been eliminated. The study was conducted on two cultivated fields, immediately after harvest. In both the objects similar variability of soil moisture was observed (coefficient of variability was about 35%). The study showed the existence of deterministic components (trends) in the soil moisture distribution in both the fields, as well as spatial correlation of the soil moisture. The character of the spatial correlation was related to the size of the object – the longer field was characterized by exponential correlation and the shorter field – spherical, the effective range of the spatial correlation being three times greater in the longer field. The estimated maps of soil moisture distribution in the longer field were similar in spite of data detrending, while in the case of the shorter field the maps were different. Conformance between measurement data and data estimated with the kriging method depended on the value of the deterministic component in the data under analysis.

7. GENERAL CONCLUSION

We have presented a new methodology for the analysis of agro-meteorological data. Wavelet transform as a time-frequency analysis method is very efficient in finding localized intermittent periodicities. Cross wavelet analysis and wavelet coherence are powerful methods for testing phase relationships between two time series. Empirical Mode Decomposition used as a data-driven sub-band filtering method allows to decompose the original time series into a number components that can be studied separately with modern power spectrum methods. The efficiency of the above approach has been confirmed using the Multitaper Method. We have shown that the heat transfer regime at the air-soil interface can be studied very accurately with these methods.

In the methodological aspect, the study showed that at the stage of recognition of the variability of soil features (especially stationary ones) a large sampling

population is required. Such a recognition will permit the determination of the necessary (optimal) number of samples for the determination of other soil features (less stationary and dynamic) – a number that will be adapted to the scale of the object and to the soil variability.

The presented study on the spatial variability of physical and chemical properties of soil have both a cognitive and a practical character. Recognition of the soil on the scale of the commune permitted the determination of the general status of the features and physical properties of the soil, determination of parameters describing their spatial variability, and mapping the spatial distribution of the features. In the case of a cultivated field, the knowledge of the spatial variability of the physical and chemical properties of soil and – contextually – of the spatial variability of crops permits the determination of the actual conditions of plant growth and crop yielding on a given object. This can constitute the basis for the formulation of agrotechnical recommendations aimed at the optimisation of tillage through the identification of areas that require e.g. additional liming, or organic or mineral fertilization.

If we know the spatial distribution of particular physical and chemical properties of soil (maps of distribution of soil features), we can employ more rational management of natural resources and energy inputs required for particular tillage operations. The ecological effects of such knowledge of spatial variability may be highly significant. First of all, we may prevent excessive accumulation of chemical components where their content in the soil is already sufficient, and thus economize on the costs of chemical fertilizers and reduce the costs of soil reclamation that would be necessary if such excessive accumulation has occurred. Moreover, known character of spatial variability should provide the basis for more accurate description of physical processes and phenomena occurring in the environment through 2D and 3D modelling of mass and energy flux within a given system under study.

It should be emphasized that the study of spatial variability of physical and chemical properties of soil constitutes the foundations of precision agriculture, currently being promoted and implemented in the most economically developed countries of the world. In Poland, studies of this type are more and more frequently developed and applied, although still predominantly in the scientific circles. Therefore, there appears a need for an integrated approach to studies of this type, so that the results can be implemented and utilized in agriculture and environmental protection as fast and as fully as possible. First of all we should make use of the results of earlier studies (already published in scientific publications and reports) and of data accumulated in data bases, although these

are not very numerous as yet. Special attention should be paid to those soil properties that are stable and do not change significantly over long periods of time, but are difficult to determine. Data concerning the physical features and properties of soils that are characterized by dynamic change are also valuable and should be collected in databases. Irrespective of whether they come from literature or originate from current data acquisition programs and studies, they may constitute material for comparisons, search for correlations among one another and with the stable features of soils, and for temporal variation analyses. Access to databases is currently difficult (sometimes impossible) and requires separate discussions and decisions. Our progress in the utilization of research results accumulated so far for purposes of precision agriculture and environmental protection will depend on how fast the scientific circles and the decision makers can solve the problem.

8. REFERENCES

1. Aboitiz, M., Labadie, J.W., Heermann, D.F., 1986. Stochastic soil moisture estimation and forecasting for irrigated fields. Water Resources Research 22, 180–190.
2. Ahmed, S., DeMarsily, G., 1987. Comparison of geostatistical methods for estimating transmisivity using data on transmisivity and specific capacity. Water Resources Research 23, 1717– 1737.
3. Albert, P.S., McShane, L.S., 1995. A generalized estimating equations approach for spatially correlated binary data: applications to the analysis of neuroimaging data. Biometrics 51, 627– 638.
4. Altese, E., Bolognani, O., Mancini, M., Troeh, P.A., 1996. Retrieving soil moisture over bare soil from ERS-1 synthetic aperture radar data: sensitivity analysis based on theoretical surface scattering model and field data. Water Resources Research 32, 653– 661.
5. 6. Anderson A. N., McBratney A. B., Crawford J. W. 1998. Applications of Fractals to Soil Science. Advances in Agronomy, (Ed. D. L. Sparks, Academic Press), 63, 2-76.
7. Anderson-Cook, C.M., Alley, M.M., Roygard, J.K.F., Khosla, R., Noble, R.B., Doolittle, J.A., 2002. Differentiating soil types using electromagnetic conductivity and crop yield maps. Soil Science Society of America Journal 66, 1570– 1652.
8. Armstrong A. C. 1986. On the fractal dimensions of some transient soil properties. J. Soil Sci., 37, 641-652.

9. Arrouays, D., Vion, I., Kicin, J.L., 1995. Spatial analysis and modeling of topsoil carbon storage in temperate forest humic loamy soils of France. Soil Science 159, 191– 198.
10. Avnir, D., Farin, D., Pfeifer, P., 1985. Surface geometric irregularity of particulate materials. The fractal approach. J. Colloid Interface Sci. 103, 112–123.
11. Baker, R., 1984. Modeling soil variability as a random field. Journal of the International Association of Mathematical Geology 16, 435–448.
12. Baranowski P., Kossowski J., Usowicz B. 1994. Spatial variability of soil water content in cultivated fields. Zesz. Probl. Post. Nauk Roln., 405, 9-19.
13. Bartoli F., Burtin G., Royer J. J., Gury M., Gomendy V., Phylippy R., Leviandier Th., Gafrej R. 1995. Spatial variability of topsoil characteristics within one silty soil type. Effects on clay migration. Geoderma, 68, 279-300.
14. Bartoli, F., Dutartre, Ph., Gomendy, V., Niquet, S., Dubuit, M., Vivier, H., 1998. Fractals and soil structure. In: Baveye, P., Parlange, J.-Y., Stewart, B.A. (Eds.), Advances in Soil Science. Fractals in Soil Science. CRC Press, Boca Raton, FL, pp. 203–232.
15. Bartoli F., Philippy R., Burtin G. 1992. Influence of organic matter aggregation in Oxisols rich in gibbsite or in goethite. I. Structures: the fractal approach. Geoderma, 54, 231-257.
16. Bartoli F., Philippy R., Doirisse M., Niquet S., Dubuit M. 1991. Structure and self-similarity in silty and sandy soils: the fractal approach. J. Soil Sci., 42, 167-185.
17. Beckett, P.H.T., Burrough, P.A., 1971. The relation between cost and utility in soil survey: IV. Comparison of the utilities of soil maps produced by different survey procedures, and to different scales. Journal of Soil Science 22, 460–480.
18. Bell, J.C., Cunningham, R.L., Havens, M.W., 1994. Soil drainage probability mapping using a soil –landscape model. Soil Science Society of America Journal 58, 464– 470.
19. Bell, J.C., Grigal, D.F., Bates, P.C., 2000. A soil– terrain model for estimating spatial patterns of soil organic carbon. In: Wilson, J.P., Gallant, J.C. (Eds.), Terrain Analysis—Principles and Applications. Wiley, New York, pp. 295– 310.
20. Bhatti, A.U., Mulla, D.J., Frazier, B.E., 1991. Estimation of soil properties and wheat yields on complex eroded hills using geostatistics and thematic mapper images. Remote Sensing of Environment 37, 181– 191.
21. Białousz S. 1966. Soil map of Poland according to FAO legend with different number of soil mapping units. Proc. Land Information System, Hannover.

22. Bierwith, P.N., 1996. Gamma-radiometrics, a remote sensing tool for understanding soils. Australian Collaborative Land Evaluation Program Newsletter 5, 12– 14.
23. Bindlish, R., Barros, A., 1996. Aggregation of digital terrain data using a modified fractal interpolation scheme. Computers and Geosciences 22, 907–917.
24. Bishop, T.F.A., McBratney, A.B., 2001. A comparison of prediction methods for the creation of field-extent soil property maps. Geoderma 103, 149–160.
25. Bishop, T.F.A., McBratney, A.B., Whelan, B.M., 2001. Measuring the quality of digital soil maps using information criteria. Geoderma 105, 93–111.
26. Bird, N.R.A., Perrier, E., Rieu, M., 2000. The water retention function for a model of soil structure with pore and solid fractal distributions. Eur. J. Soil Sci. 51, 55– 63.
27. Bogaert, P., Christakos, G., 1997. Stochastic analysis of spatiotemporal solute content measurements using a regression model. Stochastic Hydrology and Hydraulics 11, 267–295.
28. Bogaert, P., D'Or, D., 2002. Estimating soil properties from thematic soil maps: the Bayesian Maximum Entropy approach. Soil Science Society of America Journal 66, 1492– 1500.
29. Borodich, F.M., 1997. Some fractal models of fracture. J. Mech. Phys. Solids 45, 239– 259.
30. Boucneau, G., Van Meirvenne, M., Thas, O., Hofman, G., 1998. Integrating properties of soil map delineations into ordinary kriging. European Journal of Soil Science 49, 213–229.
31. Bourennane, H., King, D., Chery, P., Bruand, A., 1996. Improving the kriging of a soil variable using slope gradient as external drift. European Journal of Soil Science 47, 473–483.
32. Bourennane, H., King, D., Couturier, A., 2000. Comparison of kriging with external drift and simple linear regression for predicting soil horizon thickness with different sample densities. Geoderma 97, 255– 271.
33. Bourgault, G., 1994. Robustness of noise filtering by kriging analysis. Mathematical Geology 26, 733– 752.
34. Brus D.,J. 1993. Incorporating models of spatial variation in sampling strategies for soil. PhD Thesis, Wageningen Agricultural University, The Netherlands, 1-211.
35. Brus, D.J., De Gruijter, J.J., Marsman, B.A., Visschers, R., Bregt, A.K., 1996. The performance of spatial interpolation methods and choropleth maps to estimate properties at points: a soil survey case study. Environmetrics 7, 1–16.

36. Brus, D.J., De Gruijter, J.J., 1997. Random sampling or geostatistical modelling? Choosing between design-based and model-based sampling strategies for soil with Discussion . Geoderma 80, 1–59.
37. Buchan, G.D. 1982. Predicting bare soil temperature: I. Theory and model for the multiday mean diurnal variation. Journal of Soil Science 33:185-197.
38. Bui, E.N., Moran, C.J., 2000. Regional-scale investigation of the spatial distribution and origin of soluble salts in central north Queensland. Hydrological Processes 14, 237–250.
39. Bui, E.N., Moran, C.J., 2001. Disaggregation of polygons of surficial geology and soil maps using spatial modelling and legacy data. Geoderma 103, 79–94.
40. Burgess, T.M., Webster, R., 1980a. Optimal interpolation and isarithmic mapping of soil properties: I. The semivariogram and punctual kriging. Journal of Soil Science 31, 315– 331.
41. Burgess, T.M., Webster, R., 1980b. Optimal interpolation and isarithmic mapping of soil properties: II. Block kriging. Journal of Soil Science 31, 333– 341.
42. Burrough, P.A. 1981. Fractal dimensions of landscapes and other environmental data. Nature, 294, 240-242.
43. Burrough P. A. 1983. Multiscale sources of spatial variability in soil. I. The application of fractal concepts to tested levels of soil variation. J. Soil Sci., 34, 577-626.
44. Burrough, P.A. 1986. Principles of Geographical Information Systems for Land Resources Assessment. Oxford University Press, Oxford.
45. Burrough, P.A., 1989. Fuzzy mathematical methods for soil survey and land evaluation. Journal of Soil Science 40, 477–492.
46. Burrough, P.A., 1993. Soil variability: a late 20th century view. Soils and Fertilizers 56, 529– 562.
47. Burrough, P.A., 1993b. The technologic paradox in soil survey: new methods and techniques of data capture and handling. ITC Journal 1, 15–22.
48. Burrough, P.A., McDonnell, R.A., 1998. Principles of Geographical Information Systems. Oxford Univ. Press, Oxford.
49. Burrough, P.A., van Gaans, P.F.M., McMillan, R.A., 2000. Highresolution landform classification using fuzzy k-means. Fuzzy Sets and Systems 113, 37– 52.
50. Buscaglia H. J., Varco J. J. 2003. Comparison of Sampling Designs in the Detection of Spatial Variability of Mississippi Delta Soils. Soil Sci. Soc. Am. J., 67, 1180-1185.
51. Cahill, A.T., Ungaro, F., Parlange, M.B., Mata, M., Nielsen, D.R., 1999. Combined spatial and Kalman filter estimation of optimal soil hydraulic properties. Water Resources Research 35, 1079–1088.

52. Cain, M.L., Subler, S., Evans, J.P., Fortin, M.J., 1999. Sampling spatial and temporal variation in soil nitrogen availability. Oecologia 118, 397–404.
53. Campbell, D.J., Kinniburgh, D.G., Beckett, P.H.T., 1989. The soil solution chemistry of some Oxford shire soils: temporal and spatial variability. Journal of Soil Science 40, 321–339.
54. Campling, P., Gobin, A., Feyen, J., 2002. Logistic modeling to spatially predict the probability of soil drainage classes. Soil Science Society of America Journal 66, 1390–1401.
55. Carre, F., Girard, M.C., 2002. Quantitative mapping of soil types based on regression kriging of taxonomic distances with landform and land cover attributes. Geoderma 110, 241– 263.
56. Carvalho, L.M.T., Fonseca, L.M.G., Murtagh, F., Clevers, J.G.P.W., 2001. Digital change detection with the aid of multiresolution wavelet analysis. International Journal of Remote Sensing 22, 3871–3876.
57. Chevalier, T., Voltz, M., Blanchart, E., Chotte, J.L., Eschenbrenner, V., Mahieu, M., Albrecht, A., 2000. Spatial and temporal changes of soil C after establishment of a pasture on a long-term cultivated vertisol Martinique . Geoderma 94, 43–58.
58. Chirlin, G.R., Wood, E.F., 1982. On the relationship between kriging and state estimation. Water Resources Research 18, 432–438.
59. Christakos, G., 1990. A Bayesian/maximum-entropy view to the spatial estimation problem. Mathematical Geology 22, 763–777.
60. Christakos, G., 2000. Modern Spatiotemporal Geostatistics. Oxford Univ. Press, New York.
61. Clark, L.A., Pregibon, D., 1992. Tree-based models. In: Chambers, J.M., Hastie, T.J. (Eds.), Statistical Models. S. Wadsworth and Brooks, California, USA, pp. 377– 420.
62. Comegna, V., Basile, A., 1994. Temporal stability of spatial patterns of soil water storage in a cultivated Vesuvian soil. Geoderma 62, 299–310.
63. Comegna, V., Vitale, C., 1993. Space–time analysis of water status in a volcanic Vesuvian soil. Geoderma 60, 135–158.
64. Cook, S.E., Corner, R., Grealish, G.J., Gessler, P.E., Chartres, C.J., 1996a. A rule-based system to map soil properties. Science Society of America Journal 60, 1893–1900.
65. Cook, S.E., Corner, R., Groves, P.R., Grealish, G.J., 1996b. Use of airborne gamma radiometric data for soil mapping. Australian Journal of Soil Research 34, 183– 194.
66. Cressie, N.A.C., 1993. Statistics for Spatial Data. Wiley, New York.
67. Crestana, S., Posadas, A.N.D., 1998. 2-D and 3-D fingering in unsaturated soils investigated by fractal analysis, invasion percolation modeling and non-destructive image processing. In: Baveye, P., Parlange, J.-Y., Stewart, B.A.

(Eds.), Advances in Soil Science. Fractals in Soil Science. CRC Press, Boca Raton, FL, pp. 293– 332.
68. Crovelli, R.A., Barton, C.C., 1995. Fractals and the Pareto distribution applied to petroleum accumulation–size distributions. In: Barton, C.C., La Pointe, P.R. (Eds.), Fractals in Petroleum Geology and Earth Processes. Plenum, New York, pp. 59– 72.
69. Dale, M.B., McBratney, A.B., Russell, J.S., 1989. On the role of expert systems and numerical taxonomy in soil classification. Journal of Soil Science 40, 223– 234.
70. David, M. 1977. Geostatistical Ore Reserve Estimation. Elsevier, Scientific Publishing Co., Amsterdam, The Netherlands.
71. Davies, B.E., Gamm, S.A., 1969. Trend surface analysis applied to soil reaction values from Kent, England. Geoderma 3, 223– 231.
72. De Boer, D.H., 1997. An evaluation of fractal dimensions to quantify changes in the morphology of fluvial suspended sediment particles during baseflow conditions. Hydrol. Process. 11, 415–426.
73. De Bruin, S., Stein, A., 1998. Soil–landscape modeling using fuzzy c-means clustering of attribute data derived from a Digital Elevation Model (DEM). Geoderma 83, 17– 33.
74. De Gruijter, J.J., Bie, S.W., 1975. A discrete approach to automated mapping of multivariate systems. In: Wilford-Brickwood, J.M., Bertrand, R., van Zuylen, L. (Eds.), Automation in Cartography. Proceedings Technical Working Session, Commission III. International Cartography Association, Enschede, pp. 17– 28.
75. De Gruijter, J.J., Marsman, B.A., 1985. Transect sampling for reliable information on mapping units. In: Nielsen, D.R., Bouma, J. (Eds.), Soil Spatial Variability. Pudoc, Wageningen, pp. 150– 163.
76. De Gruijter, J.J., Walvoort, D.J.J., van Gaans, P.F.M., 1997. Continuous soil maps—a fuzzy set approach to bridge the gap between aggregation levels of process and distribution models. Geoderma 77, 169– 195.
77. Delhomme, J.P., 1978. Kriging in the hydrosciences. Advances in Water Resources 1, 251– 266.
78. de Vries, D.A., 1963. Thermal properties of soils. In W.R. van Wijk (ed.) Physics of plant environment. North-Holland, Amsterdam, 210-235.
79. De Vries, D.A. 1975. Heat transfer in soils. *In* D.A. de Vries and N.H. Afgan (ed.) Heat and Mass Transfer in the Biosphere, pp.5-28. Scripta Book Company, Washington, DC.
80. Dimitrakopoulos, R., Luo, X., 1994. Spatiotemporal modelling: covariances and ordinary kriging systems. In: Dimitrakopoulos, R. Ed, Geostatistics for the Next Century. Kluwer Academic Publishers, Dordrecht, pp. 88–93.

81. Dobermann, A., Oberthur, T., 1997. Fuzzy mapping of soil fertility— a case study on irrigated riceland in the Phlippines. Geoderma 77, 317– 339.
82. Dobos, E., Micheli, E., Baumgardner, M.F., Biehl, L., Helt, T., 2000. Use of combined digital elevation model and satellite radiometric data for regional soil mapping. Geoderma 97, 367– 391.
83. Dobos, E., Montanarella, L., Negre, T., Micheli, E., 2001. A regional scale soil mapping approach using integrated AVHRR and DEM data. International Journal of Applied Earth Observation and Geoinformation 3, 30–41.
84. Dobrzański B., Malicki A. 1950. The soils of the Krakowskie and Rzeszowskie Voivodships (in Polish). Annales UMCS, s.B, 4, 117-134.
85. Dobrzański B., Piszczek J. 1948. Map of soils of the Mielec District (in Polish). Annales UMCS, s.B, 3, 15-31.
86. Donatelli, M., Stockle, C., Constantini, E.A., Nelson, R., 2002. SOILR: a model to estimate soil moisture and temperature regimes. http://www.inea.it/isci/mdon/research/ bottom_model_soil.htm.
87. Dymond, J.R., Luckman, P.G., 1994. Direct induction of compact rule-based classifiers for resource mapping. International Journal of Geographical Information Systems 8, 357– 367.
88. Eadie W.T, Drijard D., James F.E., Roos M., Sadoulet B., 1989. Metody statystyczne w fizyce doświadczalnej. PWN. Warszawa, 63-64.
89. Edmonds, W.J., Campbell, J.B., 1984. Spatial estimates of soil temperature. Soil Science 138, 203– 208.
90. Efron, B., Tibshirani, R.J., 1993. An introduction to the bootstrap. Monographs on Statistics and Applied Probability, vol. 57. Chapman & Hall, London, UK.
91. Englund E., Sparks A. 1988. Geostatistical Environmental Assessment Software. Environmental Monitoring Systems Laboratory Office of Research and Development, U.S. Environmental Protection Agency, Las Vegas, NV 89193-3478,
92. Epinat, V., Stein, A., de Jong, S.M., Bouma, J., 2001. A wavelet characterization of high-resolution NDVI patterns for precision agriculture. ITC Journal 2, 121– 132.
93. Escoufier, Y., 1970. Echantillonage dans une population de variables ale´atoires re´ellles. Publications Institute of Statistics, University of Paris 19, 1 – 47.
94. Evans, I.S., 1972. General geomorphometry, derivatives of altitude, and descriptive statistics. In: Chorley, R.J. (Ed.), Spatial Analysis in Geomorphology. Methuen, London, pp. 17– 90.
95. Evans, I.S., 1980. An integrated system of terrain analysis and slope mapping. Zeitschrift fu¨ r Geomorphologie Supplementband 36, 274– 295.

96. Evans, I.S., 1998. What do terrain statistics really mean? In: Lane, S.N., Richards, K.S., Chandler, H. (Eds.), Land Monitoring, Modelling and Analysis. Wiley, Chichester, pp. 119– 138.
97. Fels, J.E., Matson, K.C., 1996. A cognitively-based approach for hydrogeomorphic land classification using digital terrain models. 3rd International Conference on Integrating GIS and Environmental Modeling, Santa Fe, New Mexico.
98. Filgueira, R.R., Pachepsky, Ya.A., Fournier, L.L., Sarli, G.O., Aragon, A., 1999. Comparison of fractal dimensions estimated from aggregate mass–size distribution and water retention scaling. Soil Sci. 164, 217– 223.
99. Fisher, P.F., 1994. Probable and fuzzy models of the viewshed operation. In: Worboys, M.F. Ed. , Innovations in GIS 1. Taylor and Francis, London, pp. 161–175.
100. Florinsky, I.V., 1998. Accuracy of land topographical variables derived from digital elevation models. International Journal of Geographic Information Science 12, 47–61.
101. Florinsky, I.V., Eilers, R.G., Manning, G.R., Fuller, L.G., 2002. Prediction of soil properties by digital terrain modelling. Environmental Modelling and Software 17, 295– 311.
102. Frazier, B.E., Cheng, Y., 1989. Remote sensing of soils in the eastern Palouse region with Landsat thematic mapper. Remote Sensing of the Environment 28, 317– 325.
103. Fridland, V.M., 1972. Pattern of the soil cover. Israel Program for Scientific Translations, Jerusalem.
104. Friedman, J.H., 1991. Multivariate adaptive regression splines (with discussion). Annals of Statistics 19, 1 –67.
105. Furley, P.A., 1968. Soil formation and slope development: 2. The relationship between soil formation and gradient angle in the Oxford area. Zeitschrift fu¨ r Geomorphologie 12, 25– 42.
106. Galantowicz, J.F., Entekhabi, D., Njoku, E.G., 1999. Tests of sequential data assimilation for retrieving profile soil moisture and temperature from observed L-band radio brightness. IEEE Transactions on Geoscience and Remote Sensing 37, 1860–1870.
107. Galdeano, A., Asfirane, F., Truffert, C., Egal, E., Debeglia, N., 2001. The aeromagnetic map of the French Cadomian belt. Tectonophysics 331, 99–122.
108. Gallant, J.C., Wilson, J.P., 2000. Primary topographic attributes. In: Wilson, J.P., Gallant, J.C. (Eds.), Terrain Analysis—Principles and Applications. Wiley, New York, pp. 51– 86.
109. Gamma Design Software GS+.5.3.1 Demo. 2002: Geostatistics for the environmental sciences.

110. Gessler, P.E., Moore, I.D., McKenzie, N.J., Ryan, P.J., 1995. Soil–landscape modelling and spatial prediction of soil attributes. International Journal of Geographical Information Systems 9, 421– 432.
111. Giltrap, D.J., 1977. Mathematical techniques for soil survey design. Doctor of Philosphy thesis, University of Oxford.
112. Gimenez, D., Perfect, E., Rawls, W.J., Pachepsky, Ya.A., 1997. Fractal models for predicting soil hydraulic properties: a review. Eng. Geol. 48, 161– 183.
113. Gliński J., Ostrowski J., Stępniewska Z., Stępniewski W. 1991. Bank of soil samples representing the mineral soils of Poland (in Polish). Probl. Agrofizyki, 66, 1-57.
114. Golden Software, Inc. Surfer Demo Version 8: Surface mapping system. Copyright 1993-2002.
115. Goldsztejn, P., Skrzypek, G. 2004. Wykorzystanie metod interpolacji do numerycznego kreślenia map powierzchni geologicznych na podstawie nieregularnie rozmieszczonych danych. Przegląd Geologiczny, vol. 53 nr. 3, 233-236.
116. Gołaszewski J. 2000. Analysis of spatial variability in field experiments (in Polish). Fragmenta Agronomica (XVII), 4(68), 4-14.
117. Gołaszewski J. 2000. Estimation and elimination of effects of spatial variability in field experiments (in Polish). Post. Nauk Roln., 2, 31-51.
118. Goovaerts, P., Chiang, C.N., 1993. Temporal persistence of spatial patterns for mineralizable nitrogen and selected soil properties. Soil Science Society of America Journal 57, 372–381.
119. Goovaerts, P., Journel, A.G., 1995. Integrating soil map information in modelling the spatial variation in continuous soil properties. European Journal of Soil Science 46, 397–414.
120. Goovaerts, P., 1999. Geostatistics in soil science: state-of-the-art and perspectives. Geoderma 89, 1 – 45.
121. Gopal, S., Woodcock, C., 1995. Theory and methods for accuracy assessment of thematic maps using fuzzy sets. Photogrammetric Engineering and Remote Sensing 60, 181– 188.
122. Gotway C.A., Hergert G.W. 1997. Incorporating spatial trends and anisotropy in geostatistical mapping of soil properties. Soil Sci. Soc. Am. J., 61, 298-309.
123. Goulard, M., Voltz, M., 1992. Linear coregionalization model: tools for estimation and choice of cross-variogram matrix. Mathematical Geology 24, 269–286.
124. Griffith, D.A. 1987. Spatial Autocorrelation: A Primer. Association of American Geographers, Washington, D.C., 1-86.

125. Grinsted, A, Moore, J.C. and Jevrejeva, S. 2004. Application of the cross wavelet transform and wavelet coherence to geophysical time series, Nonlinear Processes in Geophysics, 11:561-566
126. Haan C.T. 1977. Statistical Methods in Hydrology. Iowa State University Press, Ames, Iowa.
127. Haas, T.C., 1990. Kriging and automated variogram modeling within a moving window. Atmospheric Environment 24A, 1759-1769.
128. Hastie, T.J., Pregibon, D., 1992. Generalized linear models. In: Chambers, J.M., Hastie, T.J. (Eds.), Statistical Models. S. Wadsworth and Brooks, California, USA, pp. 195–248.
129. Hastie, T., Tibshirani, R., Friedman, J., 2001. The elements of statistical learning: data mining, inference and prediction. Springer Series in Statistics. Springer-Verlag, New York.
130. Henderson, R., Ragg, J.M., 1980. A reappraisal of soil mapping in an area of Southern Scotland: Part II. The usefulness of some morphological properties and of a discriminant analysis in distinguishing between the dominant taxa of four mapping units. Journal of Soil Science 31, 573–580.
131. Hengl, T., Rossiter, D.G., Husnjak, S., 2002. Mapping soil properties from an existing national soil data set using freely available ancillary data. 17th World Congress of Soil Science, Bangkok, Thailand, August 14– 21. Paper no. 1140.
132. Hengl, T., Heuvelink, G.B.M., Stein, A., 2003a. A generic framework for spatial prediction of soil variables based on regressionkriging. Geoderma (in press).
133. Hengl, T., Rossiter, D.G., Stein, A., 2003b. Soil sampling strategies for spatial prediction by correlation with auxiliary maps. Australian Journal of Soil Research (in press).
134. Heuvelink, G.B.M., Bierkens, M.F.P., 1992. Combining soil maps with interpolations from point observations to predict quantitative soil properties. Geoderma 55, 1–15.
135. Heuvelink, G.B.M., 1996. Identification of field attribute error under different models of spatial variation. International Journal of Geographical Information Science 10, 921– 935.
136. Heuvelink, G.B.M., Musters, P., Pebesma, E.J., 1997. Spatio-temporal kriging of soil water content. In: Baafi, E.Y., Schofield, N.A. Eds. , Geostatistics Wollongong ’96. Kluwer Academic Publishers, Dordrecht, pp. 1020–1030.
137. Heuvelink, G.B.M., 1998. Error Propagation in Environmental Modelling with GIS. Taylor and Francis, London.
138. Heuvelink, G.B.M., Pebesma, E.J., 1999. Spatial aggregation and soil process modelling. Geoderma 89, 47–65.

139. Heuvelink, G.B.M., Huisman, J.A., 2000. Choosing between abrupt and gradual spatial variation? In: Mowrer, H.T., Congalton, R.G. Eds. , Quantifying Spatial Uncertainty in Natural Resources: Theory and Applications for GIS and Remote Sensing. Ann Arbor Press, Chelsea, MI, pp. 111–117.
140. Heuvelink, G.B.M., Burrough, P.A., 2002. Developments in statistical approaches to spatial uncertainty and its propagation. International Journal of Geographical Information Science 16, 111–113.
141. Heuvelink, G.B.M., Webster, R., 2001. Modelling soil variation: past, present, and future. Geoderma 100, 269–301.
142. Hewitt, A.E., 1993. Predictive modelling in soil survey. Soils and Fertilizers 56, 305– 314.
143. Hoeben, R., Troch, P.A., 2000. Assimilation of active microwave observation data for soil moisture profile estimation. Water Resources Research 36, 2805–2819.
144. Hoersch, B., Braun, G., Schmidt, U., 2002. Relation between landform and vegetation in alpine regions of Wallis, Switzerland. A multiscale remote sensing and GIS approach. Computers, Environment and Urban Systems 26, 113– 139.
145. Hoosbeek, M.R., Bryant, R.B., 1992. Towards the quantitative modeling of pedogenesis—a review. Geoderma 55, 183–210.
146. Hoosbeek, M.R., Van Es, H.M., Stein, A. Eds. , 1998. Modeling Spatial and Temporal Variability as a Function of Scale. Geoderma 85, nos. 2–3.
147. Huang, H.C., Cressie, N., 1996. Spatiotemporal prediction of snow water equivalent using the Kalman filter. Computational Statistics and Data Analysis 22, 159–175.
148. Huang, N.E., Shen, Z., Long, S.R., Wu, M.L., Shih, H.H., Zheng, Q., Yen, N.C., Tung C.C., and Liu, H.H. 1998. The empirical mode decomposition and Hilbert spectrum for nonlinear and non-stationary time series analysis. Proc. Roy. Soc. London A, Vol.454, pp. 903-995.
149. Huang, N.E., Wu, M.C., Long, S.R., Long, S.S.P., Qu, W., Gloersen P., Fan, K.L. 2003. A confidence limit for the empirical mode decomposition and Hilbert spectral analysis. Proc. Roy. Soc. London A, Vol.459, pp. 2317-2345.
150. Hummatov N.G., Zheromskiy S.V., Mironenko Ye.V., Pachepskiy Ya.A., Shcherbakov R.A. 1992. Geostatistical analysis of water retention capacity spatial variability for a grey forest soil. Pochvoviedenie, 6, 52-62.
151. Hutchinson, M.F., 1998a. Interpolation of rainfall data with thin plate smoothing splines: I. Two dimensional smoothing of data with short range correlation. Journal of Geographic Information and Decision Analysis 2, 152– 167.

152. Hutchinson, M.F., 1998b. Interpolation of rainfall data with thin plate smoothing splines: II. Analysis of topographic dependence. Journal of Geographic Information and Decision Analysis 2, 168– 185.
153. Hutchinson, M.F., Gessler, P.E., 1994. Splines—more than just a smooth interpolator. Geoderma 62, 45–67.
154. Isaaks E.H., Srivastava R.M. 1989. An introduction to applied geostatistics. Oxford University Press, NY.
155. Jenny, H., 1941. Factors of Soil Formation, A System of Quantitative Pedology. McGraw-Hill, New York.
156. Journel A.G., Huijbregts C.J. 1978. Mining Geostatistics. Academic Press, New York.
157. Kantey, B.A., Williams, A.A.B., 1962. The use of soil engineering maps for road projects. Transactions of the South African Institution of Civil Engineers 4, 149–159.
158. Katz, A.J., Thompson, A.H., 1985. Fractal sandstone pores: implications for conductivity and pore formation. Phys. Rev. Lett. 54, 1325–1328.
159. Kern, J.S., 1994. Spatial patterns of soil organic carbon in the contiguous United States. Soil Science Society of America Journal 58, 439–455.
160. Kędziora A., Olejnik J. 1996. Heat balance structure in agroecosystems. In: L.Ryszkowski, N.R. French, A.Kędziora (Eds.) – Dynamics of an agricultural landscape. PWRiL, Poznań, 45-64.
161. Kim, G., Barros, A.P., 2002. Downscaling of remotely sensed soil moisture with a modified fractal interpolation method using contraction mapping and ancillary data. Remote Sensing of Environment 83, 400– 413.
162. Kimball B.A., Jackson R.D., Reginato R.J., Nakayama F.S., Idso S.B., 1976. Comparison of field-measured and calculated soil-heat fluxes. Soil Sci. Soc. Am. J., 40, 18-25.
163. King, T.V.V., Clark, R.N., Ager, C., Swayze, G.A., 1995. Remote mineral mapping using AVIRIS data at Summitville, Colorado and the adjacent San Juan Mountains, Summitville Forum ’95. Special Publication, Geological Survey, Colorado.
164. Knotters, M., Brus, D.J., Oude Voshaar, J.H., 1995. A comparison of kriging, co-kriging and kriging combined with regression for spatial interpolation of horizon depth with censored observations. Geoderma 67, 227– 246.
165. Kohonen, T., 1982. Self-organized formation of topologically correct feature maps. Biological Cybernetics 43, 59–69.
166. Komisarek J. 1994. Spatial variability of black earths and grey brown podzolic soil of the undulating bottom moraine in the Kościańska Flatland (in Polish). Roczn. AR Poznań, CCLXVIII, 205-217.

167. Kokesz, Z, Nieć, M. 1992. Metody geostatystyczne w rozpoznawaniu i dokumentowaniu złóż oraz w ochronie środowiska. Studia i Rozprawy CPPGSMiE PAN nr 19, Kraków, 1-51.
168. Korvin, G., 1992. Fractal Models in the Earth Sciences Elsevier, Amsterdam.
169. Kossowski J. 1986. An attempt at the determination of spatial variation of temperature in a cultivated field (in Polish). Zesz. Prob. Post. Nauk Rol. 315:106–128.
170. Kossowski J., Lipiec J., Tarkiewicz S. 1991. The response of spring barley yield to the degree of soil compactness related to meteorological conditions. Zesz. Probl. Post. Nauk Roln., 396, 81-87.
171. Kossowski J., Usowicz B. 2000. Characterization of soil moisture field with different sampling populations (in Polish). Acta Agrophysica, 38, 127–137.
172. Kowaliński S., Truszkowska R., Kowalkowski A., Ostrowski J. 1979. Soil environment data bank BIGLEB (in Polish). Rocz. Glebozn., 30(1), 73-84.
173. Kozak E. 1994. Methodological aspects of the determination of pre size and fractal dimension of soil minerals. Doctoral Thesis (in Polish)., Instytut Agrofizyki PAN, Lublin.
174. Kozak E., Pachepsky Y.A., Sokołowski S., Sokołowska Z., Stępniewski W. 1996. A modified number-based method for estimatig fragmentation fractal dimensions of soils. Soil Sci. Am. J., 60, 1291-1297.
175. Kozak E., Sokołowska Z., Sokołowski S., Wierzchoś J. 1995. Surface fractal dimension of soil materials from pore size distribution data. I. A comparison of two methods of determination. Polish J. Soil Sci., 28, 77-85.
176. Kravchenko A., Zhang R. 1998. Estimating the soil water retention from particle-size distributions: a fractal approach. Soil Sci., 163, 171-179.
177. Kravchenko, A.N., Bollero, G.A., Omonode, R.A., Bullock, D.G., 2002. Quantitative mapping of soil drainage classes using topo- graphical data and soil electrical conductivity. Soil Science Society of America Journal 66, 235– 243.
178. Kustas, W.P., Norman, J.M., 1996. Use of remote sensing for evapotranspiration monitoring over land surfaces. Hydrological Sciences Journal 41, 495– 516.
179. Kyriakidis, P.C., Journel, A.G., 1999. Geostatistical space–time models: a review. Mathematical Geology 31, 651–684.
180. Laba, M., Gregory, S.K., Braden, J., Ogurcak, D., Hill, E., Fegraus, E., Fiore, J., DeGloria, S.D., 2002. Conventional and fuzzy accuracy assessment of the New York gap analysis project land cover map. Remote Sensing of Environment 81, 443–455.
181. Lagacherie, P., Holmes, S., 1997. Addressing geographical data errors in a classification tree soil unit prediction. International Journal of Geographical Information Science 11, 183– 198.

182. Lagacherie, P., Voltz, M., 2000. Predicting soil properties over a region using sample information from a mapped reference area and digital elevation data: a conditional probability approach. Geoderma 97, 187–208.
183. Lagacherie, P., Robbez-Masson, J.M., Nguyen-The, N., Barthe`s, J.P., 2001. Mapping of reference area representativity using a mathematical soilscape distance. Geoderma 101, 105– 118.
184. Lane, P.W., 2002. Generalized linear models in soil science. European Journal of Soil Science 53, 241– 251.
185. Lapen, D.R., Topp, G.C., Gregorich, E.G., Hayhoe, H.N., Curnoe, W.E., 2001. Divisive field-scale associations between corn yields, management, and soil information. Soil and Tillage Research 58, 193–206.
186. Lark, R.M., 1999. Soil–landform relationships at within-field scales: an investigation using continuous classification. Geoderma 92, 141–165.
187. Lark, R.M. and Webster, R. 1999. Analysis and elucidation of soil variation using wavelets. European Journal of Soil Science, 50:185-206.
188. Lark, R.M., 2000a. A comparison of some robust estimators of the variogram for use in soil survey. European Journal of Soil Science 51, 137–157.
189. Lark, R.M., 2000b. Estimating variograms of soil properties by the method-of-moments and maximum likelihood. European Journal of Soil Science 51, 717–728.
190. Lark, R.M., 2000c. A geostatistical extension of the sectioning procedure for disaggregating soil information to the scale of functional models of soil processes. Geoderma 95, 89–112.
191. Lark, R.M., 2000. Regression analysis with spatially autocorrelated error: simulation studies and application to mapping of soil organic matter. International Journal of Geographical Information Science 14, 247– 264.
192. Lark, R.M. and Webster, R. 2001. Changes in variance and correlation of soil properties with scale and location: analysis using an adapted maximal overlap discrete wavelet transform. European Journal of Soil Science, 52:547-562.
193. Lark, R.M., Papritz, A., 2003. Fitting a linear model of coregionalization for soil properties using simulated annealing. Geoderma 115, 245– 260.
194. Lark, R.M., Kaffka, S.R., Corwin, D.L., 2003. Multiresolution analysis of data on electrical conductivity of soil using wavelets. Journal of Hydrology 272, 276– 290.
195. Lark, R.M., Milne, A.E., Addiscott, T.M., Goulding, K.W.T., Webster, C.P. and O'Flaherty, S. 2004a. Analysing spatially intermittent variation of nitrous oxide emissions from soil with wavelets and the implications for sampling. European Journal of Soil Science, 55:601-610.
196. Lark,R.M., Milne, A.E., Addiscott, T.M., Goulding, K.W.T., Webster, C.P. and O'Flaherty, S. 2004b. Scale- and location-dependent correlation of

nitrous oxide emissions with soil properties: an analysis using wavelets. European Journal of Soil Science, 55:611-627.
197. Lark,R.M., Milne, A.E., Addiscott, T.M., Goulding, K.W.T., Webster, C.P. and O'Flaherty, S. 2005. Wavelet analysis of the scale- and location-dependent correlation of modeled and measured nitrous oxide emissions from soil. European Journal of Soil Science, 56, 3-17.
198. Lark, R.M. and Webster, R. 2004d. Analysing soil variation in two dimensions with the discrete wavelet transform. 55:777-797.
199. Lascano, R.J., Baumhardt, R.L., Hicks, S.K., Landivar, J.A., 1998. Spatial and temporal distribution of surface water content in a large agricultural field. In: Robert, P.C., Rust, R.H., Larson, W.E. (Eds.), Precision Agriculture. ASA-CSSA-SSSA, Madison, WI, USA, pp. 19– 30.
200. Laslett, G.M., McBratney, A.B., Pahl, P.J., Hutchinson, M.F., 1987. Comparison of several spatial prediction methods for soil pH. Journal of Soil Science 38, 325– 341.
201. Lee, K.S., Lee, G.B., Tyler, E.J., 1988. Determination of soil characteristics from thematic mapper data of a cropped organic– inorganic soil landscape. Soil Science Society of America Journal 52, 1100– 1104.
202. Leenhardt, D., Voltz, M., Bornand, M., Webster, R., 1994. Evaluating soil maps for prediction of soil water properties. European Journal of Soil Science 45, 293–301.
203. Lees, B.G., Ritman, K., 1991. Decision-tree and rule-induction approach to integration of remotely sensed and GIS data in mapping vegetation in disturbed or hilly environments. Environmental Management 15, 823–831.
204. Liang, K.Y., Zeger, S.L., 1986. Longitudinal data analysis using generalized linear models. Biometrika 73, 13–22.
205. Lilburne, L., Hewitt, A., McIntosh, P., Lynn, I., 1998. GIS-driven models of soil properties in the high country of the south island. 10th Colloquium of the Spatial Information Research Centre, University of Otago, New Zealand, pp. 173– 180.
206. Lin, D.S., Wood, E.F., Troch, P.A., Mancini, M., Jackson, T.J., 1994. Comparison of remote sensed and model simulated soil moisture over a heterogenous watershed. Remote Sensing of the Environment 48, 159–171.
207. Lipiec J., Hakansson I., Tarkiewicz S., Kossowski J. 1991. Soil physical properties and growth of spring barley related to the degree of compactness of two soils. Soil and Tillage Res., 19, 307-317.
208. Lipiec J., Hatano R., Słowińska-Jurkiewicz A. 1998. The fractal dimension of pore distribution patterns in variously-compacted soil. Soil Tillage Res., 47, 61-66

209. Lipiec J., Usowicz B. 1997. Spatial variability of penetration resistance of soil at different compaction level. Bibliotheca Fragmenta Agronomica. t.2b, 423-426.
210. Lobell, D.B., Asner, G.P., Ortiz-Monasterio, J.I., Benning, T.L., 2003. Remote sensing of regional crop production in the Yaqui Valley, Mexico: estimates and uncertainties. Agriculture, Ecosystems and Environment 94, 205– 220.
211. Losel, G., 2003. Application of heterogeneity indices to coarsescale soil maps. Abstracts, Pedometrics 2003, International Conference of the IUSS Working Group on Pedometrics, Reading University, Reading, England, September 11– 12.
212. Lund, E.D., Colin, P.E., Christy, D., Drummond, P.E., 1999. Applying soil conductivity technology to precision agriculture. In: Robert, P.C., Rust, R.H., Larson, W.E. (Eds.), Proceedings of the Fourth International Conference on Precision Agriculture. ASA-CSSA-SSSA, Madison, WI, pp. 1089–1100.
213. MacMillan, R.A., Pettapiece, W.W., Nolan, S.C., Goddard, T.W., 2000. A generic procedure for automatically segmenting landforms into landform elements using DEMs, heuristic rules and fuzzy logic. Fuzzy Sets and Systems 113, 81–109.
214. Magnuszewski, A. 1999. GIS w geografii fizycznej. Wydawnictwo Naukowe PWN, Warszawa, 1-187.
215. Malcai, O., Lidar, D.A., Biham, O., Avnir, D., 1997. Scaling range and cutoffs in empirical fractals. Phys. Rev., E 56, 2817– 2828.
216. Malicki M. 1990. A reflectometric (TDR) meter of moisture content in soils and other capillary-porous materials. Zesz. Probl. Post. Nauk Roln., 388, 107-114.
217. Malicki, M.A., Plagge, R., Renger, M., Walczak, R.T., 1992. Application of time domain reflectometry (TDR) soil moisture miniprobe for the determination of unsaturated soil water characteristics from undisturbed soil cores. Irrigation Science 13, 65-72.
218. Malicki, M.A., Skierucha, W.M., 1989. A manually controlled TDR soil moisture meter operating with 300 ps rise-time needle pulse. Irrigation Science 10 pp. 153-163
219. Mancini, M., Hoeben, R., Troch, P.A., 1999. Multifrequency radar observations of bare surface soil moisture content: a laboratory experiment. Water Resources Research 35, 1827– 1838.
220. Mandelbrot, B., 1967. How long is the coast of Britain? Statistical self-similarity and fractal dimension. Science 156, 636–638.
221. Mandelbrot B.B. 1982. The Fractal Geometry of Nature. W.H. Freeman, London.

222. Marcinek, J. 1992. Parametryzacja środowiska glebowego w aspekcie gospodarki wodnej gleb. Problemy Agrofizyki 67, 20-53.
223. Marechal, A., 1984. Kriging seismic data in presence of faults. In: Verly, G., David, M., Journel, A.G., Marechal, A. Eds. , Geostatistics for Natural Resources Characterization, Part 1. D. Reidel, Dordrecht, pp. 271–294.
224. Matern, B., 1986. Spatial Variation. 2nd edn. Lecture Notes in Statistics, vol. 36, Springer, Berlin.
225. Matheron G. 1971. The theory of regionalized variables and its applications. Cahiers du Centre de Morphologie Mathematique, Fontainebleau, No. 5.
226. Marsman, B.A., de Gruijter, J.J., 1986. Quality of soil maps, a comparison of soil survey methods in a study area. Soil Survey papers no. 15. Netherlands Soil Survey Institute, Stiboka, Wageningen, The Netherlands.
227. Maulik, U., Bandyopadhyay, S., 2000. Genetic algorithm-based clustering technique. Pattern Recognition 33, 1455–1465.
228. McBratney, A.B., 1992. On variation, uncertainty and informatics in environmental soil management. Australian Journal of Soil Research 30, 913–935.
229. McBratney A.B., Webster R. 1983. How many observations are needed for regional estimation of soil properties. Soil Sci., 135(3), 177-183.
230. McBratney, A.B., Webster, R., 1983. Optimal interpolation and isarithmic mapping of soil properties: V. Co-regionalization and multiple sampling strategy. Journal of Soil Science 34, 137– 162.
231. McBratney, A.B., Odeh, I.O.A., Bishop, T.F.A., Dunbar, M.S., Sha-tar, T.M., 2000. An overview of pedometric techniques for use in soil survey. Geoderma 97, 293–327.
232. McBratney, A.B., Minasny, B., Cattle, S., Vervoort, R.W., 2002. From pedotransfer functions to soil inference systems. Geoderma 109, 41– 73.
233. McCullagh, P., Nelder, J.A., 1983. Generalized Linear Models. Cambridge Univ. Press, Cambridge, UK.
234. McIntosh, P.D., Lynn, I.H., Johnstone, P.D., 2000. Creating and testing a geometric soil– landscape model in dry steeplands using a very low sampling density. Australian Journal of Soil Research 38, 101–112.
235. McKenzie, N.J., Austin, M.P., 1993. A quantitative Australian approach to medium and small scale surveys based on soil stratigraphy and environmental correlation. Geoderma 57, 329–355.
236. McKenzie, N.J., Ryan, P.J., 1999. Spatial prediction of soil properties using environmental correlation. Geoderma 89, 67– 94.
237. McKenzie, N.J., Gessler, P.E., Ryan, P.J., O'Connel, D., 2000. The role of terrain analysis in soil mapping. In: Wilson, J.P., Gallant, J.C. (Eds.), Terrain Analysis—Principles and Applications. Wiley, New York, pp. 245– 265.

238. Michaelsen, J., Schimel, D.S., Friedl, M.A., Davis, F.W., Dubayah, R.C., 1994. Regression tree analysis of satellite and terrain data to guide vegetation sampling and surveys. Journal of Vegetation Science 5, 673– 686.
239. Milne, G., 1935. Some suggested units of classification and mapping particularly for East African soils. Soil Research 4, 183–198.
240. Minasny, B., McBratney, A.B., 1999. A rudimentary mechanistic model for soil production and landscape development. Geoderma 90, 3–21.
241. Minasny, B., McBratney, A.B., 2001. A rudimentary mechanistic model for soil production and landscape development: II. A two-dimensional model. Geoderma 103, 161– 179.
242. Minasny, B., McBratney, A.B., 2002. The neuro-m method for fitting neural network parametric pedotransfer functions. Soil Science Society of America Journal 66, 352–361.
243. Mohanty, B.P., Shouse, P.J., Van Genuchten, M.T., 1998. Spatio-temporal dynamics of water and heat in a field soil. Soil and Tillage Research 47, 133–143.
244. Moore, D.M., Lees, B.G., Davey, S.M., 1991. A new method for predicting vegetation distributions using decision tree analysis in a geographic information system. Environmental Management 15, 59– 71.
245. Moran, C.J., Bui, E., 2002. Spatial data mining for enhanced soil map modelling. International Journal of Geographical Information Science 16, 533– 549.
246. Moran, M.S., Inoue, Y., Barnes, E.M., 1997. Opportunities and limitations for image-based remote sensing in precision crop management. Remote Sensing of the Environment 61, 319– 346.
247. Moreno F., Usowicz B., Fernandez J.E., Andreu L. 1997. Spatial distribution of salinity and water content in the reclaimed salt-affected soils of south-western Spain. Proc Int. Conf. "Wastewater re-use in irrigated agriculture" 22-26 September 1997, vol. IV, 83-93, Valenzano (Bari), Italy.
248. Morkoc, F., Biggar, J.W., Nielsen, D.R., Rolston, D.E., 1985. Analysis of soil water content using state-space approach. Soil Science Society of America Journal 49, 798–803.
249. Morse, R.K., Thornburn, T.H., 1961. Reliability of soil maps. Proceedings of the 5th International Conference on Soil Mechanics and Foundation Engineering. I. Dunod, Paris, pp. 259–262.
250. Mucher, C.A., Steinnocher, E.T., Kressler, F.P., Heunks, C., 2000. Land cover characterization and change detection for environmental monitoring of pan-Europe. International Journal of Remote Sensing 21, 1159– 1181.
251. Munyati, C., 2000. Wetland change detection on the Kafue Flats, Zambia, by classification of a multitemporal remote sensing image dataset. International Journal of Remote Sensing 21, 1787– 1806.

252. Musierowicz A. (red.). 1961. Map of the soils of Poland in the scale of 1:300 000 (in Polish). Wyd. Geologiczne, Warszawa.
253. Myślińska E. 2001. Laboratory studies of soils (in Polish). 3rd Edition. PWN, Warszawa, str. 213,
254. Namysłowska-Wilczyńska, B.. 1993. Zmienność złóż rud miedzi na monoklinie przedsudeckiej w świetle badań geostatystycznych. Prace Naukowe Instytutu Geotechniki i Hydrotechniki Politechniki Wrocławskiej nr 64, Seria Monografie nr 21, Wrocław, 1-205.
255. New, M., Todd, M., Hulme, M., Jones, P., 2001. Precipitation measurements and trends in the twentieth century. International Journal of Climatology 21, 1922–1999.
256. Nortcliff, S., 1978. Soil variability and reconnaissance soil mapping: a statistical study in Norfolk. Journal of Soil Science 29, 403–418.
257. Noy-Meir, I., 1974. Multivariate analysis of the semiarid vegetation in south-eastern Australia: II. Vegetation catena and environmental gradients. Australian Journal of Botany 22, 115– 140.
258. Oberthur, T., Dobermann, A., Neue, H.U., 1996. How good is a reconnaisance soil map for gronomic purposes? Soil Use and Management 12, 33–43.
259. Oberthur, T., Goovaerts, P., Dobermann, A., 1999. Mapping soil texture classes using field texturing, particle size distribution and local knowledge by both conventional and geostatistical methods. European Journal of Soil Science 50, 457– 479.
260. Obukhov, A.I., Orlov, D.S., 1964. Spectral reflectivity of the major soil groups and possibility of using diffuse reflection in soil investigations. Soviet Soil Science, 174–184.
261. Odeh, I.O.A., McBratney, A.B., 2000. Using AVHRR images for spatial prediction of clay content in the lower Namoi Valley of eastern Australia. Geoderma 97, 237– 254.
262. Odeh, I.O.A., Chittleborough, D.J., McBratney, A.B., 1991. Elucidation of soil – landform interrelationships by canonical ordination analysis. Geoderma 49, 1 – 32.
263. Odeh, I.O.A., McBratney, A.B., Chittleborough, D.J., 1992. Soil pattern recognition with fuzzy-c-means: application to classification and soil – landform interrelationships. Soil Science Society of America Journal 56, 505– 516.
264. Odeh, I.O.A., McBratney, A.B., Chittleborough, D.J., 1994. Spatial prediction of soil properties from landform attributes derived from a digital elevation model. Geoderma 63, 197–214.

265. Odeh, I.O.A., McBratney, A.B., Chittleborough, D.J., 1995. Further results on prediction of soil properties from terrain attributes: heterotopic cokriging and regression-kriging. Geoderma 67, 215– 225.
266. Odeh, I.O.A., McBratney, A.B., Slater, B.K., 1997. Predicting soil properties from ancillary information: non-spatial models compared with geostatistical and combined methods. 5th International Geostatistics Congress, Wollongong, pp. 22– 27.
267. Oliver, M.A., Webster, R., 1986: Semi-variograms for modelling the spatial pattern of landform and soil properties. Earth Surface Processes and Landforms, 11, 491-504.
268. Oliver, M., Webster, R., Gerrard, J., 1989: Geostatistics in physical geography. Part I: theory. Part II: applications. Transactions Institution of British Geographers N.S., 14, 259-269, 270-286.
269. Oliver, M.A., Webster, R., Slocum, K., 2000. Filtering SPOT imagery by kriging analysis. International Journal of Remote Sensing 21, 735– 752.
270. Opsomer, J.D., Ruppert, D., Wand, M.P., Holst, U., Hossjer, O., 1999. Kriging with nonparametric variance function estimation. Biometrics 55, 704–710.
271. Ostrowski J. 1966. The South Podlasie Lowlands (in Polish). Przegl. Geogr., 38, 3, 393-406.
272. Or, D., Hanks, R.J., 1992. Spatial and temporal soil water estimation considering soil variability and evapotranspiration uncertainty. Water Resources Research 28, 803–814.
273. Owens, K.E., Reed, D.D., Londo, A.J., Maclean, A.L., Mroz, G.D., 1999. A landscape level comparison of pre-European settlement and current soil carbon content of a forested landscape in upper Michigan. Forest Ecology and Management 113, 179– 189.
274. Pace, R.K., Barry, R., 1997. Quick computations of regressions with a spatially autoregressive dependent variable. Geographical Analysis 29, 232–247.
275. Pachepsky Y.A., Korsumskaja L. P., Hajnos M. 1996. Fractal parameters of soil pore surface area under a developing crop. Fractals, 4, 97-104.
276. Pachepsky Y.A., Polubesova T.A., Hajnos M., Józefaciuk G., Sokołowska Z. 1995. Parameters of surface heterogeneity from laboratory experiments on soil degradation. Soil Sci. Soc. Am. J., 59, 410-417.
277. Pachepsky Y.A., Polubesova T.A., Hajnos M., Sokołowska Z., Józefaciuk G. 1995. Fractal parameters of pore surface area as influenced by simulated soil degradation. Soil Sci. Soc. Am. J., 59, 68-75.
278. Pachepsky, Y.A., Timlin, D.J., Rawls, W.J., 2001. Soil water retention as related to topographic variables. Soil Science Society of America Journal 65, 1787– 1795.

279. Palacios-Orueta, A., Ustin, S.L., 1998. Remote sensing of soil properties in the Santa Monica mountains I. Spectral analysis. Remote Sensing of the Environment 65, 170–183.
280. Pannatier, Y., 1993: MS-Windows programs for exploratory variography and variogram modelling in 2D. [w:] Capasso V., Girone G. & Posa D. (eds.), Statistics of Spatial Processes: Theory and Applications, Bari, Italy, sep. 27-30 1993, 165-170.
281. Pannatier Y.: Variowin 2.1. 1994. Program for Geostatistical Analysis. University Of Lousanne.
282. Papritz A.J. 1993. Estimating temporal change of soil properties. PhD thesis, Swiss Federal Institute of Technology, Zurich, 166 Pp.
283. Papritz, A., Fluhler, H., 1994. Temporal change of spatially autocorrelated soil properties: optimal estimation by cokriging. Geoderma 62, 29–43.
284. Park, S.J., Vlek, L.G., 2002. Prediction of three-dimensional soil spatial variability: a comparison of three environmental correlation techniques. Geoderma 109, 117– 140.
285. Park, S.J., McSweeney, K., Lowery, B., 2001. Identification of the spatial distribution of soils using a process-based terrain characterization. Geoderma 103, 249–272.
286. Pasierski Z. 1984. Dynamika przychodu wody do powierzchni gleby w łanach wybranych roślin uprawnych, Zesz. Probl. Post. Nauk Roln., 288, 85-101.
287. Pebesma, E.J., Duin, R.N.M., Bio, A.M.F., 2000. Spatial Interpolation of Sea Bird Densities on the Dutch Part of the North Sea. Centre for Geo-Ecological Research, Utrecht.
288. Pedrycz, W., Waletzky, J., 1997. Fuzzy clustering with partial supervision. IEEE Transactions on Systems, Man, and Cybernetics—Part B 27, 787–795.
289. Peech M. 1965. Hydrogen-ion activity. In: "Methods of Soil Analysis". Part 2, 914-926. Ed.: C.A. Black, Am. Soc. Agronomy, Inc. Publ. Madison, USA.
290. Percival, D.B., and A.T. Walden. 1993. Spectral analysis for physical applications: multitaper and conventional univariate techniques, Cambridge University Press.
291. Perfect E., Groenevelt P. H., Kay B. D., Grant C. D. 1990. Spatial variability of soil penetrometer measurements at the mesoscopic scale. Soil Tillage Res., 16, 257-291.
292. Perfect, E., Kay, B.D., Ferguson, J.A., da Silva, A.P., Denholm, K.A., 1993. Comparison of functions for characterizing the dry aggregate size distribution of tilled soil. Soil Tillage Res. 28, 123– 139.
293. Perfect, E., Kay, B.D., Rasiah, V., 1994. Unbiased estimation of the fractal dimension of soil aggregate size distributions. Soil and Tillage Research 31, 187– 198.

294. Perfect E., Kay B. D. 1995. Application of fractals in soil and tillage research: a review. Soil Tillage Res., 36, 1-20.
295. Perfect, E., 1999. Estimating soil mass fractal dimensions from water retention curves. Geoderma 88, 221–231.
296. Perrier, E., Mullon, C., Rieu, M., de Marsily, G., 1995. A computer construction of fractal soil structures. Simulation of their hydraulic and shrinkage properties. Water Resour. Res. 31, 2927– 2943.
297. Perrier, E., Bird, N., Rieu, M., 1999. Generalizing the fractal model of soil structure: the pore –solid fractal approach. Geoderma 88, 137– 164.
298. Petach, M.C., Wagenet, R.J., DeGloria, S.D., 1991. Regional water flow and pesticide leaching using simulations with spatially distributed data. Geoderma 48, 245–269.
299. Phillips, J.D., 1998. On the relations between complex systems and the factorial model of soil formation with Discussion . Geoderma 86, 1–42.
300. Phillips, J.D., 2001. The relative importance of intrinsic and extrinsic factors in pedodiversity. Annals of the Association of American Geographers 91, 609–621.
301. Pike, R.J., 1988. The geometric signature: quantifying landslide terrain types from digital elevation models. Mathematical Geology 20, 491–511.
302. Pinheiro, J.C., Bates, D.M., 2000. Mixed-Effects Models in S and S-Plus. Springer, New York.
303. Polubesova T.A., Pachepsky Y.A., Hajnos M., Józefaciuk G., Sokołowska Z. 1997. Comparison of three techniques to assess surface heterogeneity of solids in soils. Int. Agrophysics, 11, 189-198.
304. Post, D.F., Horvath, E.H., Lucas, W.M., White, S.A., Ehasz, M.J., Batchily, A.K., 1994. Relations between soil color and Landsat reflectance on semiarid rangelands. Soil Science Society of America Journal 58, 1809– 1816.
305. Quinlan, J.R., 1992. Learning with continuous classes. Proceedings of the 5th Australian Joint Conference on Artificial Intelligence, pp. 343–348.
306. Quinones, M.J., Hoekman, D.H., 2001. Biomass mapping using biophysical forest type characterization of SAR polarimetric images. Proceedings of the Third International Symposium on Retrieval of Bio- and Geophysical Parameters for SAR Data for Land Applications. University of Sheffield, Sheffield, UK.
307. Rajkai K., Ryden B.E. 1992. Measuring areal soil moisture distribution with the TDR method. Geoderma, 52, 73-85,
308. Rasiah, V., Perfect, E., Kay, B.D., 1995. Linear and nonlinear estimates of fractal dimension for soil aggregate fragmentation. Soil Sci. Soc. Am. J. 59, 83– 87.
309. Rasiah V., Alymore A. G. 1998. Characterizing the changes in soil porosity by computed tomography and fractal dimension. Soil Sci., 163, 203-211.

310. Rawls, W.J., Pachepsky, Y.A., 2002. Using field topographic descriptors to estimate soil water retention. Soil Science 167, 423– 435.
311. Rejman, J., Turski, R., Paluszek, J. 1998. Spatial and temporal variations in erodibility of loess soil. Soil and Tillage Research, 46, 61-68.
312. Renschler, C.S., Mannaerts, C., Diekkruger, B., 1999. Evaluating spatial and temporal variability in soil erosion risk-rainfall erosivity and soil loss ratios in Andalusia, Spain. Catena 34, 209–225.
313. Rieu M., Sposito G. 1991. Fractal fragmentation, soil porosity, and soil water properties. Soil Sci. Soc. Am. J., 55, 1231-1244.
314. Rieu, M., Perrier, E., 1998. Fractal models of fragmented and aggregated soils. In: Baveye, P., Parlange, J.-Y., Stewart, B.A. (Eds.), Advances in Soil Science. Fractals in Soil Science. CRC Press, Boca Raton, FL, pp. 169– 202.
315. Robertson G.P. 1987. Geostatistics in ecology: interpolating with known variance. Ecology, 68, 744-748.
316. Rockstrom, J., Barron, J., Brouwer, J., Galle, S., De Rouw, A., 1999. On-farm spatial and temporal variability of soil and water in pearl millet cultivation. Soil Science Society of America Journal 63, 1308–1319.
317. Rogowski, A.S., Wolf, J.K., 1994. Incorporating variability into soil map unit delineations. Soil Science Society of America Journal 58, 163–174.
318. Romano, N., Palladino, M., 2002. Prediction of soil water retention using soil physical data and terrain attributes. Journal of Hydrology 265, 56– 75.
319. Rosenberg, A., 2000. Philosophy of Science: A Contemporary Introduction. Routledge, London. RuleQuest Research, 2000. Cubist. RuleQuest Research, Sydney, Australia.
320. Rouhani, S., Myers, D.E., 1990. Problems in space–time kriging of geohydrological data. Mathematical Geology 22, 611–623.
321. Russo, D., 1998. Stochastic analysis of flow and transport in unsaturated heterogeneous porous formation: effects of variability in water saturation. Water Resources Research 34, 569–581.
322. Ryan, P.J., McKenzie, N.J., O'Connell, D., Loughhead, A.N., Leppert, P.M., Jacquier, D., Ashton, L., 2000. Integrating forest soils information across scales: spatial prediction of soil properties under Australian forests. Forest Ecology and Management 138, 139– 157.
323. Samra, J.S., Stahel, W.A., Kunsch, H., 1991. Modeling tree growth sensitivity to soil sodicity with spatially correlated observations. Soil Science Society of America Journal 55, 851–856.
324. Scavia, C., 1996. The effect of scale on rock fracture toughness: a fractal approach. Geotechnique 46, 683– 693.
325. Schaetzl, R.J., Barrett, L.R., Winkler, J.A., 1994. Choosing models for soil chronofunctions and fitting them to data. European Journal of Soil Science 45, 219–232.

326. Schmugge, T.J., Kustas, W.P., Ritchie, J.C., Jackson, T.J., Rango, A., 2002. Remote sensing in hydrology. Advances in Water Resources 25, 1367– 1385.
327. Schoefield R.K., Taylor A.W. 1955. The measurement of soil pH. Soil Sci. Soc. Am. Proc., 19, 164-167.
328. Schmuck A. 1965. Pluviothermal regions in Poland (in Polish). Czasop. Geogr., 36, 3, 241-244.
329. Schmuck A. 1961. Thermic regions in Poland (in Polish). Czasop. Geogr., 32, 1, 17-30.
330. Scull, P., Chadwick, O.A., Franklin, J., Okin, G., 2003a. A comparison of prediction methods to create spatially distributed soil property maps using soil survey data for an alluvial basin in the Mojave Desert California. Geoderma (in press).
331. Scull, P., Franklin, J., Chadwick, O.A., McArthur, D., 2003b. Predictive soil mapping: a review. Progress in Physical Geography 27, 171– 197.
332. Shary, P.A., 1995. Land surface in gravity points classification by a complete system of curvatures. Mathematical Geology 27, 373– 390.
333. Shary, P.A., Sharayab, L.S., Mitusov, A.V., 2002. Fundamental quantitative methods of land surface analysis. Geoderma 107 (1– 32), 1 –43.
334. Shatar, T.M., McBratney, A.B., 1999. Empirical modelling of relationships between sorghum yield and soil properties. Precision Agriculture 1, 249– 276.
335. Shepherd, K.D., Walsh, M.G., 2002. Development of reflectance spectral libraries for characterization of soil properties. Soil Science Society of America Journal 66, 988–998.
336. Simonett, D.S., 1960. Soil genesis in basalt in North Queensland. Transactions of the 7th International Congress of Soil Science, Madison, Wisconsin, pp. 238– 243.
337. Sinha, A.K., 1990. Stratigraphic mapping of sedimentary formations in southern Ontario by ground electromagnetic methods. Geophysics 55, 1148– 1157.
338. Sinowski, W., Auerswald, K., 1999. Using relief parameters in a discriminant analysis to stratify geological areas with different spatial variability of soil properties. Geoderma 89, 113–128.
339. Skidmore, A.K., Ryan, P.J., Dawes, W., Short, D., O'Loughlin, E., 1991. Use of an expert system to map forest soils from a geographical information system. International Journal of Geographical Information Science 5, 431– 445.
340. Skidmore, A.K., Watford, F., Luckananurug, P., Ryan, P.J., 1996. An operational GIS expert system for mapping forest soils. Photogrammetric Engineering and Remote Sensing 62, 501–511.

341. Skidmore, A.K., Varekamp, C., Wilson, L., Knowles, E., Delaney, J., 1997. Remote sensing of soils in a eucalypt forest environment. International Journal of Remote Sensing 18, 39–56.
342. Sławiński, C., Sobczuk, H., Stoffregen, H., Walczak, R., Wessolek, G., 2002. Effect of data resolution on soil hydraulic conductivity prediction. Journal of Plant Nutrition and Soil Science 165 (1), 45-49.
343. Sobczuk, H.A., Plagge, R., Walczak, R.T., Roth, C.H., 1992. Laboratory equipment and calculation procedure to rapidly determine hysteresis of some soil hydrophysical properties under nonsteady flow conditions. Z. Pflanzenernähr. Bodenkd. 155, 157-163.
344. Soil Survey Staff, 1993. Soil Survey Manual. Handbook No. 18. USDA, Washington, DC.
345. Sokal R.R., Oden N.L.. 1978. Spatial autocorrelation in biology. 1. Methodology. 2. Some biological implications and four applications of evolutionary and ecological interest. Biological Journal of the Linnean Society 10, 199-228.
346. Sokołowska Z. 1989. The role of surface heterogeneity in adsorption processes in soils (in Polish). Problemy Agrofizyki 58.
347. Sokołowska Z. 1989. On the role of energetic and geometric heterogeneity in sorption of water vapour by soils. Geoderma, 45, 251-265.
348. Sokołowska Z., Hajnos M., Sokołowski S. 1998. Effect of leaching of dissolved organic carbon on fractal dimension of soils. 231-239, W: Fractals and Beyond: Complexities in the Science. Novak M. M. (Ed.), World Sci. Pub. Co. Pte. Ltd., Singapore, New Jersey, London, Hong Kong.
349. Sokołowska Z., Sokołowski S. 1988. Fractal theeories of adsorption (in Polish). Problemy Agrofizyki 55.
350. Sokołowska Z., Sokołowski S. 1989. Water sorption in soils: The role of energetic and geometric heterogeneity. Int. Agrophysics, 5, 247-254.
351. Sokołowska Z., Sokołowski S. 1999. Influence of humic acid on surface fractal dimension of kaolin: analysis of mercury porosimetry and water adsorption data. Geoderma 88, 233-249.
352. Sokołowska Z., Stawiński J., Patrykiejew A., Sokołowski S. 1989. A note on fractal analysis of adsorption process by soils and soil minerals. Int. Agrophysics, 5, 3-12.
353. Sommer, M., Wehrhan, M., Zipprich, M., Castell, Z.W., Weller, U., Castell, W., Ehrich, S., Tandler, B., Selige, T., 2003. Hierarchical data fusion for mapping soil units at field scale. Geoderma 112, 179–196.
354. Souza C. F., Or D., Matsura E. E. 2004. A Variable-volume TDR probe for measuring water content in large soil volumes. Soil Sci. Soc. Am. J., 68, 25-31.

355. Stach, A. 1998. Zmienność właściwości warstwy ornej na niejednolitym litologicznie stoku morenowym. Bibliotheca Fragmenta Agronomica, 4B, 125-142.
356. Stach, A. 1999. Geostatystyczna analiza pola opadów atmosferycznych w dorzeczu Parsęty. [w:] Funkcjonowanie Geoekosystemów Zlewni Rzecznych 2, A. Kostrzewski (red.),181-193.
357. Stach, A.. 2002a. Geostatystyczna identyfikacja mechanizmów transportu roztworów w ciekach. [w:] Erozja gleb i transport rumowiska rzecznego, K. Banasik (red.), Sympozjum Naukowe, Zakopane 10-12.X.2002, 186-196.
358. Stach, A.. 2002b.: Metodyka estymacji stężeń roztworów w odpływie rzecznym. [w:] Erozja gleb i transport rumowiska rzecznego, K. Banasik (red.), Sympozjum Naukowe, Zakopane 10-12.X.2002, 174-185.
359. Stach, A., Podsiadłowski, S., 2001: Wpływ erozji eolicznej na teksturę lekkich gleb Niziny Wielkopolskiej. [w:] Geneza, litologia i stratygrafia utworów czwartorzędowych, Tom III, Seria Geografia nr 64, Wyd. Nauk. UAM, 359-379.
360. Stach, A., Tamulewicz, J., 2003: Wstępna ocena przydatności wybranych algorytmów przestrzennej estymacji miesięcznych i rocznych sum opadów na obszarze Polski. [w:] A. Kostrzewski, J. Szpikowski (red.) 2003: Funkcjonowanie geoekosystemów zlewni rzecznych, t. 3, Obieg wody – uwarunkowania i skutki w środowisku przyrodniczym, Instytut Badań Czwartorzędu i Geoekologii UAM, str. 87-111, Bogucki Wydawnictwo Naukowe, Poznań.
361. Stafford, J.V., Ambler, B., Lark, R.M., Catt, J., 1996. Mapping and interpreting the yield variation in cereal crops. Computers and Electronics in Agriculture 14, 101–119.
362. Stawiński J., Gliński J., Ostrowski J., Stępniewska Z. 1999. Map of Specific Surface Area of Arable Soils of Poland (in Polish). IA PAN Lublin – IMUZ Falenty.
363. Stein, M., 1999. Interpolation of Spatial Data. Some Theory for Kriging. Springer, New York.
364. Stein, A., Hoogerwerf, M., Bouma, J., 1988. Use of soil-map delineations to improve co- kriging of point data on moisture deficits. Geoderma 43, 163–177.
365. Stępniewska Z., Stępniewski W., Gliński J., Ostrowski J. 1996. Atlas of Redox Properties of Arable Soils of Poland (in Polish). IA PAN Lublin – IMUZ Falenty.
366. Su, Z., Troch, P.A., De Troch, F.P., 1997. Remote sensing of bare surface soil moisture using EMAC/ESAR data. International Journal of Remote Sensing 18, 2105–2124.

367. Sukop, M.C., van Dijk, G.-J., Perfect, E., van Loon, W.K.P., 2001. Percolation thresholds in 2-dimensional prefractal models of porous media. Transp. Porous Media (preprint), 1 – 22.
368. Tabbagh, A., Dabas, M., Hesse, A., Panissod, C., 2000. Soil resistivity: a non-invasive tool to map soil structure horizonation. Geoderma 97, 393–404.
369. Taylor, R., Eggleton, R.A., 2001. Regolith Geology and Geomorphology. Wiley, Chichester, UK.
370. Thomas, A.L., King, D., Dambrine, E., Couturier, A., Roque, A., 1999. Predicting soil classes with parameters derived from relief geologic materials in a sandstone region of the Vosges mountains (Northeastern France). Geoderma 90, 291–305.
371. Thomson, D.J. 1982. Spectrum estimation and harmonic analysis. *Proceedings of the IEEE*, 70:1055-1096.
372. Thompson, J.A., Bell, J.C., Butler, C.A., 1997. Quantitative soil – landscape modeling for estimating the areal extent of hydromorphic soils. Soil Science Society of America Journal 61, 971–980.
373. Thompson, J.A., Bell, J.C., Butler, C.A., 2001. Digital elevation model resolution: effects on terrain attribute calculation and quantitative soil–landscape modeling. Geoderma 100, 67–89.
374. Torrence, C. and Compo, G.P. 1998. A Practical Guide to Wavelet Analysis, Bulletin of the American Meteorological Society, 79:61-78
375. Torrence, C., Webster, P. J., 1999. Interdecadal Changes in the ENSO-Monsoon System. Journal of Climate, Vol.12, pp.2679-2690.
376. Townshend, J., Justice, C., Li, W., Gurney, C., McManus, J., 1991. Global land cover classification by remote-sensing—present capabilities and future possibilities. Remote Sensing of Environment 35, 243– 255.
377. Trangmar B.B., Yost R.S., Uehara G. 1985. Applications of geostatistics to spatial studies of soil properties. In: N.C. Brady, editor. Advances in Agronomy, Vol. 38, 45-94, Academic Press, New York.
378. Triantafilis, J., Ward, W.T., Odeh, I.O.A., McBratney, A.B., 2001. Creation and interpolation of continuous soil layer classes in the lower Namoi valley. Soil Science Society of America Journal 65, 403–413.
379. Triantafilis, J., Odeh, I.O.A., Minasny, B., McBratney, A.B., 2003. Elucidation of hydrogeological units using fuzzy k-means classification of EM34 data in the lower Namoi Valley, Australia. Environmental Modelling and Software 18, 667– 680.
380. Troeh, F.R., 1964. Landform parameters correlated to soil drainage. Soil Science Society of America Proceedings 28, 808– 812.

381. Truszkowska R. 1966. Soil Complexes with similar agricultural value (in Polish). In: Dziedzic F., Dąbrowski P. (Red.) Atlas Rolniczy Polski. Wyd. Geologiczne, Warszawa.
382. Truszkowska R. 1992. Regional Bank of Information of the Soil-Plant Environment and its Hazards (in Polish).: Bigleb-Wo. Prace Kom. PTG, 117.
383. Turcotte, D.L., 1992. Fractals and Chaos in Geology and Geophysics Cambridge Univ. Press, Cambridge.
384. Turski R., Uziak S., Zawadzki S. 1993. The Natural Environment of the Lublin Regions – Soils (in Polish). LTN, Lublin, 1-107.
385. Tyler, S.W., Wheatcraft, S.W., 1989. Application of fractal mathematics to soil water retention estimation. Soil Sci. Soc. Am. J. 53, 987– 996.
386. Tyler, S.W., Wheatcraft, S.W., 1992. Fractal scaling of soil particlesize distribution: analysis and limitations. Soil Sci. Soc. Am. J. 56, 362– 369.
387. Twidale, C.R., 1985. Old land surfaces and their implications for models of landscape evolution. Revue de Ge´omorphologie Dynamique 34, 131– 147.
388. Uehara G., Gillman.G.P. 1980. Charge characteristics of soils with variable and permanent charge minerals I. Theory. Soil Sci. Soc. Am. J., 44, 250-252.
389. Utset, A., Lopez, T., Dıaz, M., 2000. A comparison of soil maps, kriging and a combined method for spatially predicting bulk density and field capacity of ferrasols in the Havana-Matanzas Plain. Geoderma 96, 199–213.
390. Usowicz B., 1992. Statistical-physical model of thermal conductivity in soil. Polish J. Soil Sci. 25(1), 25-34.
391. Usowicz B., 1995. Evaluation of methods for soil thermal conductivity calculations. Int. Agrophysics, 9(2), 109-113.
392. Usowicz B., Baranowski P., Kossowski J. 1995. Spatial distribution of some physical quantities characterizing soil structure state in cultivated fields. Polish J. Soil Sci. 28/1, 19-27.
393. Usowicz B., Kossowski J., Baranowski P. 1996. Spatial variability of soil thermal properties in cultivated fields. Soil and Tillage Res., 39, 85-100.
394. Usowicz B., Kossowski J. 1996. Distribution of soil water content in cultivated fields based on measurement by gravimetric and reflectometric methods. Zesz. Prob. Post. Nauk Roln., 436, 157-165.
395. Usowicz B. 1998. Time and space variability of soil thermal properties in cultivated fields. Proc. 16th World Congress of Soil Science, Montpellier, France, 20-26 August 1998, CD 253-t.pdf, 1-9.
396. Usowicz, B., 1999: Zastosowanie analizy geostatystycznej i teorii fraktali w badaniach dynamiki wilgotności w profilu glebowym na polach uprawnych. Acta Agrophysica, 22, 229 – 243.
397. Usowicz, B., Rejman, J., 2000. Zmienność przestrzenna temperatury w przypowierzchniowej warstwie gleby płowej na zboczu lessowym. Acta Agrophysica, 34, 189-197.

398. Usowicz B. 2001. Assessment of the variability of selected soil features with different sampling systems and populations (in Polish). Acta Agrophysica 57, 147-158.
399. Usowicz, B., Hajnos, M., Sokołowska, Z., Józefaciuk, G., Bowanko, G., Kossowski, J., 2004. Przestrzenna zmienność fizycznych i chemicznych właściwości gleby w skali pola i gminy. Acta Agrophysica, Rozprawy i Monografie, 103, 1-90.
400. Usowicz Ł.B., Usowicz B. 2002. Spatial variability of soil particle size distribution in Poland. 17th World Congress Of Soil Science, 14-20 August 2002, Bangkok, Thailand, Symposium No.48, Paper 274, 1-10.
401. Usowicz B., Usowicz L., 2004.Point measurements of soil water content and its spatial distribution in cultivated fields. Acta Agrophysica, 111, 573-588.
402. Vachaud, G., Passerat De Silans, A., Balabanis, P., Vauclin, M., 1985. Temporal stability of spatially measured soil water probability density function. Soil Science Society of America Journal 49, 822–828.
403. Van Niekerk, H.S., Gutzmer, J., Beukes, N.J., Phillips, D., Kiviets, G.B., 1999. An 40Ar/39Ar age of supergene K–Mn oxyhydroxides in a post-Gondwana soil profile on the Highveld of South Africa. South African Journal of Science 95, 450– 454.
404. Van Es, H.M., 1993. Evaluation of temporal, spatial, and tillage-induced variability for parametrization of soil infiltration. Geoderma 60, 187–199.
405. Van Es, H.M., Ogden, C.B., Hill, R.L., Schindelbeck, R.R., Tsegaye, T., 1999. Integrated assessment of space, time, and management-related variability of soil hydraulic properties. Soil Science Society of America Journal 63, 1599–1608.
406. Van Kuilenburg, J., De Gruijter, J.J., Marsman, B.A., Bouma, J., 1982. Accuracy of spatial interpolation between point data on soil moisture supply capacity, compared with estimates from mapping units. Geoderma 27, 311–325.
407. Vauclin, M., Vieira, S.R., Vachaud, G., Nielsen, D.R., 1983. The use of cokriging with limited field soil observations. Soil Science Society of America Journal 47, 175– 184.
408. Venables,W.N., Ripley, B.D., 1994. Modern Applied Statistics with S-PLUS. Springer-Verlag, New York, USA.
409. Ventura, S.J., Irvin, B.J., 2000. Automated landform classification methods for soil – landscape studies. In: Wilson, J.P., Gallant, J.C. (Eds.), Terrain Analysis—Principles and Applications. Wiley, New York, pp. 267– 294.
410. Verboom, W.H., Pate, J.S., 2003. Relationships between cluster root-bearing taxa and laterite across landscapes in southwest Western Australia: an approach using airborne radiometric and digital elevation models. Plant and Soil 248, 321– 333.

411. Vieira S.R., Hatfield J.L., Nielsen D.R., Biggar J.W. 1983. Geostatistical theory and application to variability of some agronomical properties. Hilgardia. 51, 1-75,
412. Vold, A., Breland, T.A., Soreng, J.S., 1999. Multiresponse estimation of parameter values in models of soil carbon and nitrogen dynamics. Journal of Agriculture, Biology and Environmental Science 4, 290– 309.
413. Voltz, M., Webster, R., 1990. A comparison of kriging, cubic splines and classification for predicting soil properties from sample information. Journal of Soil Science 41, 473– 490.
414. Voltz, M., Lagacherie, P., Louchart, X., 1997. Predicting soil properties over a region using sample information from a mapped reference area. European Journal of Soil Science 48, 19– 30.
415. Wackernagel, H., 1987. Multivariate Geostatistics. Springer, Berlin. Walker, P.H., Hall, G.F., Protz, R., 1968. Relation between landform parameters and soil properties. Soil Science Society of America Proceedings 32, 101– 104.
416. Walczak R. 1994. The structure of solar radiation balance and the thermal-moisture relations of soil (in Polish). Report on Grant No. PB 1679/5/91.
417. Walczak, R., Sławiński, C., Malicki, M.A., Sobczuk, H., 1993. Measurement of water characteristics in soils using TDR technique. Water characteristics of loess soil under different treatment. Int. Agrophysics 7 (2-3), 175-182.
418. Walczak R. Usowicz B. 1994. Variability of moisture, temperature and thermal properties in bare soil and in crop field. Int. Agrophysics, 8, 161-168.
419. Walczak R., Ostrowski J., Witkowska-Walczak B., Sławiński C. 2002. Spatial characteristics of water conductivity in the surface level of Polish arable soils. Int. Agrophysics, 16, 3, 239-247.
420. Walter, C., McBratney, A.B., Douaoui, A., Minasny, B., 2001. Spatial prediction of topsoil salinity in the Chelif Valley, Algeria, using local ordinary kriging with local variograms versus whole-area variogram. Australian Journal of Soil Research 39, 259– 272.
421. Walvoort, D.J.J., de Gruijter, J.J., 2001. Compositional kriging: a spatial interpolation method for compositional data. Mathematical Geology 33, 951– 966.
422. Webster, R., 1977. Spectral analysis of gilgai soil. Australian Journal of Soil Research 15, 191–204.
423. Webster, R., 1977. Canonical correlation in pedology: how useful? Journal of Soil Science 28, 196– 221.
424. Webster R. 1985. Quantitative spatial analysis of soil in the field. Advances in Soil Sci., 3, 1-70.
425. Webster R., Burgess T.M. 1984. Sampling and bulking strategies for estimating soil properties in small regions. J. Soil Sci., 35, 127-140.

426. Webster, R. Oliver M.A. 1990. Statistical Methods in Soil and Land Resource Survey. Oxford University Press, NY, 1-316.
427. Webster, R., 2000. Is soil variation random? Geoderma 97, 149–163.
428. Webster, R., Burgess, T.M., 1980. Optimal interpolation and isarithmic mapping of soil properties, III. Changing drift and universal kriging. Journal of Soil Science 31, 505– 524.
429. Webster, R., Burrough, P.A., 1974. Multiple discriminant analysis in soil survey. Journal of Soil Science 25, 120– 134.
430. Webster, R., Oliver, M.A., 1990. Statistical Methods in Soil and Land Resource Survey. Oxford Univ. Press, Oxford.
431. Webster, R., Oliver, M.A., 2001. Geostatistics for Environmental Scientists. Wiley, Chichester.
432. Webster, R., Harrod, T.R., Staines, S.J., Hogan, D.V., 1979. Grid sampling and computer mapping of the Ivybridge area, Devon. Technical Monograph no.12, Soil Survey of England and Wales, Harpenden, Herts.
433. Wen, R., Sinding-Larsen, R., 1997. Image filtering by factorial kriging-sensitivity analysis and application to GLORIA sidescan sonar images. Mathematical Geology 21, 433– 468.
434. Wendroth, O., Pohl, W., Koszinski, S., Rogasik, H., Ritsema, C.J., Nielsen, D.R., 1999a. Spatio-temporal patterns and covariance structures of soil water status in two Northeast-German field sites. Journal of Hydrology 215, 38–58.
435. Wendroth, O., Rogasik, H., Koszinski, S., Ritsema, C.J., Dekker, L.W., Nielsen, D.R., 1999b. State-space prediction of field-scale soil water content time series in a sandy loam. Soil and Tillage Research 50, 85–93.
436. Whittle, P., 1954. On stationary processes in the plane. Biometrika 41, 434–449.
437. Wielemaker, W.G., de Bruin, S., Epema, G.F., Veldkamp, A., 2001. Significance and application of the multi-hierarchical landsystem in soil mapping. Catena 43, 15– 34.
438. Wilson, J.P., Gallant, J.C., 2000. Secondary topographic attributes. In: Wilson, J.P., Gallant, J.C. (Eds.), Terrain Analysis—Principles and Applications. Wiley, New York, pp. 87–132.
439. Wood, J., 1996. The Geomorphological Characterisation of Digital Elevation Models. PhD thesis, University of Leicester, UK. Available at: http://www.soi.city.ac.uk/~jwo/phd.
440. Wood, E.F., Lin, D.S., Mancini, M., 1993. Inter-comparisons between active and passive microwave remote sensing, and hydrological modelling for soil moisture. Advances in Space Research 13, 5167–5176.
441. Wosten, J.H.M., Bouma, J., Stoffelsen, G.H., 1985. The use of soil survey data for regional soil water simulation models. Soil Science Society of America Journal 49, 1238–1244.

442. Wosten, J.H.M., Pachepsky, Y.A., Rawls, W.J., 2001. Pedotransfer functions: bridging the gap between available basic soil data and missing soil hydraulic characteristics. Journal of Hydrology 251, 123– 150.
443. Wrigley, N., 1978. Probability surface mapping. In: Davis, J.C., Levi de Lopez, S. (Eds.), Mapas por computadora para el analisis de los recursos naturales; memorias de la reunion internacional. Univ. Nac. Auton. Mex., Inst. Geogr. Mexico City and Univ. Kans., Kans. Geol. Surv., Lawrence, Kansas, Mexico City, Mexico, pp. 39– 49.
444. Yaalon, D.H., 1975. Conceptual models in pedogenesis: can soilforming functions be solved? Geoderma 14, 189– 205.
445. Yost, R.S., Loague, K., Green, R.E., 1993. Reducing variance in soil organic carbon estimates: soil classification and geostatistical approaches. Geoderma 57, 247–262.
446. Zawadzki J., 2005. Wykorzystanie metod geostatystycznych w badaniach środowiska przyrodniczego. Politechnika Warszawska, Prace naukowe Inżynieria Środowiska –z. 49, 1-134.
447. Zeverbergen, L.W., Thorne, C.R., 1987. Quantitative analysis of land surface topography. Earth Surface Processes and Landforms 12, 47– 56.
448. Zhang, R., Yang, J., 1996. Iterative solution of a stochastic differential equation: an efficient method for simulating soil variability. Geoderma 72, 75–88.
449. Zheng, D., Hunt, E.R., Running, S.W., 1996. Comparison of available soil water capacity estimated from topography and soil series information. Landscape Ecology 11, 3 –14.
450. Zhu, A.X., 1997. A similarity model for representing soil spatial information. Geoderma 77, 217– 242.
451. Zhu, A.X., 2000. Mapping soil landscape as spatial continua: the neural network approach. Water Resources Research 36, 663– 677.
452. Zhu, A.X., Band, L.E., 1994. A knowledge-based approach to data integration for soil mapping. Canadian Journal of Remote Sensing 20, 408– 418.
453. Zhu, Z.L., Evans, D.L., 1994. US forest types and predicted percent forest cover from AVHRR data. Photogrammetric Engineering and Remote Sensing 60, 525– 533.
454. Zhu, C., Yang, X., 1998. Study of remote sensing image texture analysis and classification using wavelet. International Journal of Remote Sensing 19, 3197– 3203.
455. Zhu, A.X., Band, L.E., Dutton, B., Nimlos, T.J., 1996. Automated soil inference under fuzzy logic. Ecological Modelling 90, 123– 145.

456. Zhu, A.X., Band, L.E., Vertessy, R., Dutton, B., 1997. Derivation of soil properties using a soil land inference model (SoLIM). Soil Science Society of America Journal 61, 523– 533.
457. Zhu, A.X., Hudson, B., Burt, J., Lubich, K., Simonson, D., 2001. Soil mapping using GIS, expert knowledge, and fuzzy logic. Soil Science Society of America Journal 65, 1463–1472.

Addresses of the Authors:
Bogusław Usowicz
Instytut Agrofizyki im. Bohdana Dobrzańskiego PAN
ul. Doświadczalna 4, 20-290 Lublin
e-mail: Usowicz@demeter.ipan.lublin.pl
http://www.ipan.lublin.pl/~usowicz/

Jerzy Bogdan Usowicz
Centrum Astronomii, Uniwersytet Mikołaja Kopernika
ul. Gagarina 11, 87-100 Toruń
e-mail: ju@astro.uni.torun.pl

Spatial and temporal variation of selected physical and chemical properties of soil

Bogusław Usowicz, Jerzy Bogdan Usowicz

EDITED BY
BOGUSŁAW USOWICZ, RYSZARD T. WALCZAK

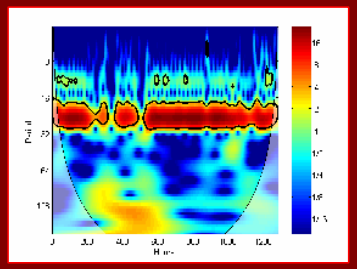

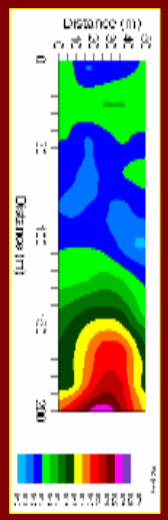

Institute of Agrophysics
Polish Academy of Sciences

Centre of Excellence for Applied
Physics in Sustainable Agriculture
AGROPHYSICS

EU 5th Framework Program
QLAM-2001-00428

Institute of Agrophysics
of the Polish Academy of Sciences
ul. Doświadczalna 4. 20-290 Lublin. Poland

Centre of Excellence for Applied Physics
in Sustainable Agriculture AGROPHYSICS
ul. Doświadczalna 4, 20-290 Lublin, Poland